Spring 2008

Study of Gas Diffusion Layers in direct methanol fuel cells (DMFC)

Jason Morgan
University of New Hampshire, Durham

STUDY OF GAS DIFFUSION LAYERS IN DIRECT METHANOL FUEL CELLS (DMFC)

BY:

JASON MORGAN
B.S. UNH, 2002

THESIS

Submitted to the University of New Hampshire
in partial fulfillment of
the requirements for the Degree of

Master of Science
in
Chemical Engineering

May 2008

This thesis has been examined and approved.

Virendra K. Mathur

Thesis Director, Virendra K. Mathur, Professor of Chemical Engineering

Stephen S. T. Fan

Stephen S. T. Fan, Professor of Chemical Engineering

Gupta

Nivedita Gupta, Assistant Professor of Chemical Engineering

April 23, 2008

Date

DEDICATION

Dedicated to my mother Elizabeth and my father Michael.

ACKNOWLEDGEMENTS

I would like to thank Dr. Mathur very much for his continuous support and dedication in helping me to finish this work. It would not have been possible without his hard work and encouragement throughout all of my education.

I also thank Dr. S.S.T. Fan, Dr. N. Gupta, Dr. P. Vasudevan, Dr. D. Barkey, John Newell and Nancy Littlefield for all their help and support throughout my education.

I would also like to thank Michael Johnston for his help with the design and construction of the PEM/DM fuel cell apparatus and Rob Cinq-Mars for his help with the electrical work and computer programming.

I am grateful to the following individuals without whom I would not have been able to complete this work: Ralph Draper, Department of Engineering, UNH Manchester; Dawn Meredith, Associate Professor and Chair of the Department of Physics, UNH; William Grant, Project Manager, Ballard Material Products; and Donald Connors, Sr. Engineer Product Development, Ballard Material Products.

I would also like to express my gratitude to the corporations who sponsored my research, provided expensive materials free of charge and helped me to begin my career. I am also grateful for the stipend provided to me by the Department of Chemical Engineering throughout my education.

Finally I would like to thank my parents without whose support, both financially and emotionally, I would have never been able to complete this work.

TABLE OF CONTENTS

LIST OF TABLES

LIST OF FIGURES

NOMENCLATURE

Symbol	Description	Units
α_C	Transfer coefficient	-
η	Efficiency	-
δ	Diffusion distance	meters
C_B	Bulk Concentration	mol
C_S	Surface Concentration	mol
D	Diffusion Coefficient	m^2/s
E	Cell potential	V
F	Faradays Constant	96485 C/mol
ΔG	Molar Gibbs Free Energy	kJ/mol
ΔH	Molar Enthalpy	kJ/mol
I_0	Current exchange density	A/cm^2
i_L	Limiting current density	A/cm^2
N	Number of electrons	-
R	Gas Constant	8.314 J/mol-K
R_i	Internal Resistance	Ohm
ΔS	Molar Entropy	kJ/mol
T	Temperature	K

Acronym	
AFC	Alkaline Fuel Cell
DC	Direct Current
DMFC	Direct Methanol Fuel Cell
EW	Equivalent Weight
GDL	Gas Diffusion Layer
MEA	Membrane Electrode Assembly
MCFC	Molten Carbonate Fuel Cell
MPL	Micro Porous Layer
NASA	North American Space Association
PAFC	Phosphoric Acid Fuel Cell
PEMFC	Proton Exchange Membrane Fuel Cell
SOFC	Solid Oxide Fuel Cell
UNH	University of New Hampshire

ABSTRACT

STUDY OF GAS DIFFUSION LAYERS IN DIRECT METHANOL FUEL CELLS (DMFC)

By

Jason Morgan

University of New Hampshire, May 2008

An automated single-cell fuel cell system has been designed and fabricated in this work. The apparatus is capable of operating on both hydrogen and methanol fuels, and can control the mass flow rates and humidity of the inlet gases, and temperature and pressure of the cell with a LabVIEW program. A series of experiments are conducted to determine the optimum cell operating temperature (75°C), methanol concentration (4 molar), methanol flow rate (3 mL/min) and catalyst loading on Gas Diffusion Layers (GDLs) (~2.5 mg/cm^2). A new anode GDL is fabricated by optimizing the hydrophobicity in the substrate and microporous layer (MPL), as well as the MPL loading. The key factors for improved cathode performance are found to be thickness and basis weight. One of the end results of this work is a new GDL system, which is manufactured continuously at low cost, providing improved cell performance compared to a commercial standard.

CHAPTER I

INTRODUCTION

1.1 – Background Information

Today's society is highly dependent on fossil fuels for transportation, electricity generation and heat during the long winter months. Currently, burning or combusting these fuels produces the necessary energy in the form of heat. This heat produces steam to use in turbines to produce the electricity that powers our homes. Burning of fossil fuels is an effective way to produce energy; however, there are some major drawbacks with this process. Combustion is usually at high temperatures, is an inefficient process, tends to be noisy and produces pollutants such as SOx (sulfur oxides), NOx (nitrogen oxides) and COx (carbon oxides). These chemical compounds are polluting our atmosphere, contributing to global warming and producing acid rain, which adversely affects our environment. It is imperative, therefore, that we find a better way to produce the energy on which our society has become so dependent.

There are currently many different possible solutions to this energy problem. Solar or wind power is a clean renewable energy source that would be an excellent possibility for future considerations. However, to generate the

amount of energy required the cost is simply too high, both economically and spatially. In addition, the peak power demands tend to be in the evening, when there is no sun for solar power, and wind power is unpredictable. Nuclear power, although promising, is viewed as a scary proposition on which to depend. Hydroelectric power is useful where available, but is simply not abundant enough to meet all of our power requirements and it is not portable. The most promising alternative to combusting fossil fuels is currently a fuel cell system.

A fuel cell is an electrochemical device that directly produces electricity through an electrochemical reaction of hydrogen and oxygen combining to form water. The operation of the device is similar in principle to a battery, but it never needs to be recharged. The cell will operate as long as both reactants (H_2/O_2) are present. Fuel cells allow us to generate electricity directly and cleanly with the most prominent by-product being pure water.

Fuel cells are sometimes thought of as a new technology, although Sir William Grove invented them almost 170 years ago. In 1839, Grove developed what he called a "gaseous voltaic battery". He knew that when you passed a current through water you were able to generate hydrogen and oxygen gas. He set up an experiment to see if the reaction could be reversed as well. He placed platinum strips into tubes that were filled with hydrogen and oxygen gas. He then submerged the tubes into a dilute sulfuric acid solution and observed that he could in fact generate a current. Unfortunately, he was unable to generate large amounts of power. He did realize that there was an important three-phase boundary (hydrogen/oxygen (gas), sulfuric acid electrolyte (liquid) and platinum

electrode (solid)) and that using hydrogen, instead of coal or wood, may greatly improve the potential of energy production [1].

1.2 - Types of Fuel Cells

Today there are numerous types of fuel cells, which are classified by the type of electrolyte that is used in the cell. The cell proposed by Grove is most closely related to the Phosphoric Acid Fuel Cell (PAFC). In addition there is also the Molten Carbonate Fuel Cell (MCFC), Solid Oxide Fuel Cell (SOFC), Alkaline Fuel Cell (AFC), Polymer Electrolyte Membrane Fuel Cell (PEMFC) and the Direct Methanol Fuel Cell (DMFC).

MCFCs and SOFCs are high temperature (600-1000°C) fuel cells, which are most promising as stationary power generation systems. They use molten carbonate melts (Li_2CO_3/K_2CO_3) and Yttrium Stabilized Zirconia (YSZ), respectively, as their electrolytes [2]. The greatest advantage of these fuel cells is that they are not damaged by the presence of carbon monoxide (CO). The catalyst in other fuel cell systems are poisoned by the presence of small amounts of CO, but MCFCs and SOFCs can use the CO (as well as natural gas or other hydrocarbons) directly as fuel without any reforming. These cells are very useful as industrial or stationary power sources because the need for reforming stations or gas purifiers is eliminated. The exceedingly high operating temperatures and start-up times make them unsuitable for portable power applications, such as automobiles.

The development of the AFC was pursued by F.T. Bacon in the late 1940s and was later chosen by NASA as the power supply for space missions in the 1960s. In modern systems, they operate at fairly low temperature and pressure (90°C, 4 bars) and use potassium hydroxide (KOH) as the liquid electrolyte. The most difficult problem with an AFC is that its electrolyte reacts with carbon dioxide (CO_2) to form potassium carbonate (K_2CO_3), which greatly reduces performance and therefore requires an ultra-clean supply of hydrogen for optimum operation. This need for a clean supply of hydrogen makes it unsuitable for portable power applications as the storage and transportation of hydrogen is a problem.

PEMFCs and DMFCs are very similar in that they both use a solid polymer electrolyte, rather than bulky liquid electrolytes as used in PAFCs or AFCs. They also operate at low temperatures and pressures unlike the MCFCs and SOFCs. This makes them most suitable for use in small portable appliances, such as laptops, personal digital assistants (PDAs) or cell phones. The difference between the PEMFC and the DMFC is the nature of the fuel that is fed to the cell. PEMFCs require the direct feed of hydrogen and oxygen/air to react generating the current. The DMFCs require a direct feed of methanol (MeOH) and oxygen/air. The PEMFCs produce only clean water, as a by-product, but they have to deal with the commercial problems of storage and transportation of hydrogen. The DMFCs use liquid methanol, which is much more convenient (higher energy density) for storage and transportation. However, it is also toxic even in very small doses and extremely flammable, which raises many issues for

its use in commercial products. The ability to easily transport and store methanol, as well as manufacture it from numerous sources cheaply, is why the DMFC looks more promising than the PEMFC for small portable applications.

Unfortunately, the performance of the DMFC does not currently compare to that of the PEMFC. Several authors [1, 2] have presented detailed analysis for all of these different types of fuel cells and their operating conditions. This study is primarily concerned with DMFCs, although a fundamental understanding of PEMFCs and how they operate is helpful. A brief history of the development of DMFCs, as well as a look at the major pitfalls associated with methanol fuel is also discussed.

1.3 - Direct Fuel Cells

As early as 1894 researchers realized the importance of finding a direct fuel to improve the practicality of fuel cells. Many researchers tried to use coal directly in a fuel cell system as a way to reduce the amount of energy lost from normal combustion of coal. Researchers such as Jacques, Ostwald, Haber and Bruner [1] investigated the possibility of using coal directly to produce an electrochemical reaction. Jacques was actually successful in creating such an apparatus and speculated that improvements to his method would run trains with higher speeds, less polluted air in cities, quieter engines and cheaper electricity [1]. Although his method could not be vastly improved upon, the concept and benefits for the direct methanol fuel cell system are very optimistic.

In the late 1950s and early 1960s the desire to have a direct fuel cell system was enhanced. Researchers from Shell and ESSO experimented with

aqueous acidic electrolytes. Alkaline electrolytes were examined around the same time by researchers from Allis-Chalmers. Unfortunately, they were unable to make much progress and the development work was dropped again. In 1992, however, scientists at the Jet Propulsion Laboratory made a major breakthrough. They discovered that methanol could be used directly with the solid polymer electrolyte membrane fuel cell, which is now known as a DMFC. They were able to feed the methanol directly to the anode as opposed to having to feed it through the electrolyte as they did with the acidic/alkaline electrolytes. They used the Nafion® membrane manufactured by Dupont along with Pt-Ru catalysts and were able to generate an adequate current output. The major problem with this system was, and still is, methanol crossover, which is the passing of methanol through the membrane directly from the anode to the cathode without reacting and producing power.

Another major problem with the DMFC is the use of methanol as a fuel itself. It is a liquid, is easily manufactured, and can be transported and stored easily. However, it is also highly combustible, toxic and burns clear. Particularly the inhalation of methanol is very dangerous, which worries many people who dream of having cars that run off of methanol. Exposure of just 200 ppm for 8 hours or more can be fatal for people. Also ingestion of methanol, even as little as 25 mL can be fatal [2]. In addition to these health risks, methanol burns completely clear, so if a fire starts there is no visible evidence of it. Therefore it is very important that every safety precaution is taken if we are to pursue using methanol as a fuel for the general public. Vapor barriers and other safety

mechanisms need to be applied to all commercial products to prevent any accidental or intentional hazards associated with methanol.

Many scientists suggest the possible use of ethanol as the feed for a direct fuel cell system. Ethanol is not nearly as toxic as methanol, is a liquid at room temperature, is easily manufactured and it is similar to methanol molecularly, with an adequate amount of hydrogen. However, it is difficult to oxidize ethanol completely and the power output from fuel cells using ethanol as a fuel has been minimal. Thus, the fuel efficiency is much lower, it is much more expensive per kW and with poor kinetics the reaction proceeds too slowly for good cell performance. Overall, it is not considered to be a good choice as a fuel for direct fuel cells.

1.4 - Major Problems and Scientific Remediation Methods

Currently the major problems with the DMFC are fuel crossover, slow anode kinetics, and 2-phase flow in the anode diffusion layer. Many groups [3-6] are currently examining new membranes that can prevent methanol crossover when the cell is operated under a wide array of temperatures. Others [7-9] are researching cheaper and more effective catalysts to improve the slow anode kinetics. The work is important, but there has been very little progress achieved towards developing easily produced and inexpensive membranes or catalysts that perform as well as or better than the market available materials (Nafion®, Pt/Pt-Ru). It is also important to work on an often-overlooked cell component, the gas diffusion layer or GDL.

The GDL is typically a carbon paper or cloth that needs to control the flow of reactants to the catalyst, remove excess water produced by the cell and conduct the produced electricity to the current collectors. Wang et al. [10-13] have suggested methods for improving the anode/cathode GDLs for DMFCs, helping to limit methanol crossover, allowing the use of highly concentrated methanol and managing the CO_2 gas in the anode flow channels. This work is perhaps the most important, because it allows the use of well-understood materials (Nafion®, Pt-Ru/C), which are already commercially produced, rather than relying on the future development of efficient, new polymeric materials or catalysts that then need to be mass-produced at a reasonable cost.

At the University of New Hampshire (UNH) there is currently a program in operation to examine both PEMFCs with hydrogen and oxygen/air feed as well as DMFCs with methanol and oxygen/air feeds. There are two experimental systems that are designed and built in-house for the purpose of evaluation and optimization of cell materials, particularly GDLs. Both systems consist of a 5 cm^2, single cell, typically using Nafion® membranes, with Pt or Pt-Ru catalyst. The DMFC apparatus also has computerized data acquisition software and computer controlled mass flow controllers and temperature/pressure monitoring.

The work under this thesis includes the design and construction of the 2^{nd} generation DMFC/PEMFC system at UNH and the optimization of operating parameters for this system. In addition, new anode and cathode GDL materials are developed for improved performance in DMFC applications. The GDLs are improved by the addition of an optimized microporous layer (MPL), which can

more effectively control the flow of methanol to the catalyst layer. One of the end results of this work is a GDL system that can be used with commercially available membranes with high methanol concentrations, with limited methanol crossover. This can help with the development of cheaper and more cost effective fuel cell systems, which will lower the overall cost and make DMFCs more viable. This project is primarily funded privately by the fuel cell industry.

CHAPTER II

LITERATURE REVIEW

This chapter is divided into three sections for the convenience of the readers. The first section discusses the basics of the operation of a fuel cell primarily focusing on the DMFC. The second section deals with the various components of a PEMFC/DMFC such as the membrane, gas diffusion layer, catalysts and bipolar plates. The final section examines the mass transport in these fuel cells, including water management and methanol crossover effects.

2.1 - Operation of the Fuel Cell

A PEMFC or DMFC operates in a manner similar to a battery. A schematic of the basic fuel cell structure is provided in Figure 2.1. There are aluminum alloy end plates, shown in black in Figure 2.1, which serve as the outer casings of the fuel cell. Just inside of the end plates are plastic or Teflon insulating layers (shown in light blue) and copper current collectors (shown in red). Against the current collectors are poco graphite blocks (shown in gray), which typically have serpentine flow fields machined into them. These blocks serve as gas flow channels as well as electron conductors.

There are two sides, the anode (fuel) and the cathode (oxidant), of a fuel cell and there is a gas diffusion layer on each side. Between each GDL, shown in dark blue, there is a catalyst layer, shown in green, and a polymer electrolyte membrane (PEM), shown in purple, is sandwiched by the two catalyst layers, as shown in Figure 2.1. The fuel, either hydrogen or methanol, is fed to the anode side, while the cathode side is supplied with an oxidant, either oxygen or air. At the anode the fuel, say hydrogen, reacts with the catalyst present to disassociate the hydrogen into protons and electrons. In the case of methanol, the fuel is first split into hydrogen and CO_2 and then the hydrogen proceeds to disassociate into electrons and protons. The protons then pass through the ion conducting membrane (polymer electrolyte) and react with the oxygen/air at the cathode to form water. The electrons travel through the external circuit, generating a current, which is used to power whatever load is connected to the fuel cell.

In the case of a PEM cell, the half-cell reactions are given as follows:

Anode:

$$H_2 \rightarrow 2\,H^+ + 2\,e^-$$

Cathode:

$$\tfrac{1}{2}\,O_2 + 2\,H^+ + 2\,e^- \rightarrow H_2O$$

The overall reaction:

$$H_2 + \tfrac{1}{2}\,O_2 \rightarrow H_2O$$

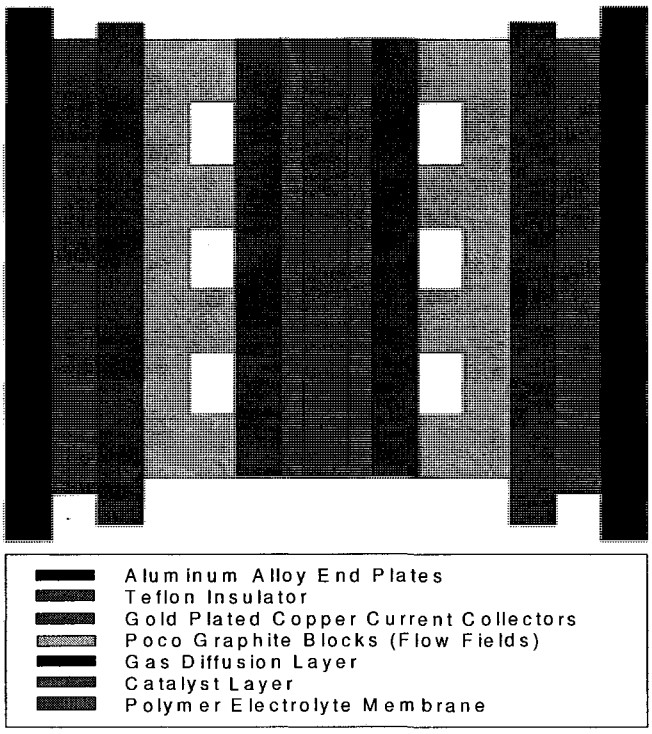

Figure 2.1 – Schematic of a PEM Fuel Cell

This is a simple reaction, which can generate about 1.23V under theoretical (perfect) conditions with no waste product, other than pure water. There have been many technological advances since the inception of a modern fuel cell in the 1960s [14-16]. Although the fuel cell is an effective method for power production, the voltage produced is so low that you need very large cells or multiple cells in series (known as a "stack") to produce a significant amount of power.

The major problems with the hydrogen-powered fuel cell are the transportation and storage of hydrogen and its relatively low energy density (68,000 Btu per ft^3). Hydrogen is a gas at room temperature and therefore must be either compressed in a tank, or cryogenically stored in liquid form, to operate

a fuel cell. Compressed hydrogen is relatively dangerous to keep as a fuel for non-commercial applications due to explosion and fire risks, as was seen with the Hindenburg disaster. For these reasons, it is more practical to examine the Direct Methanol Fuel Cell (DMFC) for portable power applications.

For a DMFC the appropriate half-cell equations are given as follows:

Anode:

$$CH_3OH + H_2O \rightarrow 6H^+ + 6e^- + CO_2$$

Cathode:

$$1\frac{1}{2}\, O_2 + 6H^+ + 6e^- \rightarrow 3H_2O$$

The overall reaction:

$$CH_3OH + 1\frac{1}{2}\, O_2 \rightarrow 2H_2O + CO_2$$

As one can see from these reactions, methanol is a very attractive fuel choice because it generates six electrons for every mole of methanol, giving it a relatively high energy density of 488,000 Btu per ft^3. Comparing the six electrons that are generated from methanol with the two from hydrogen and considering that methanol is a liquid fuel at ambient conditions, it is clearly a better choice for portable power applications. One downside to using methanol for a fuel is the production of CO_2 as a waste. However, only one mole of CO_2 is produced for every 6 electrons generated, so the amount is still minor when compared to the amount of CO_2 generated from the combustion of fossil fuels. Small amounts of CO may also be formed due to incomplete oxidation of carbon, which may act as a catalyst poison and as a pollutant. This can also be considered minor and, with

proper catalysts, it should be possible to selectively oxidize the CO to CO_2 to minimize this problem.

Currently, fuel cells are being developed for use in cellular telephones, PDAs, laptops, and other portable devices using both hydrogen and methanol, as well as formic acid [17]. These micro-fuel cells could create a better, cleaner world. We would no longer need batteries, and the amount of hazardous waste they generate, but rather a cartridge of fuel that can be easily replaced or refilled. We would not need to transport huge amounts of electricity to our homes, just to recharge our batteries every few days. Although they are very promising, there are still some major obstacles to overcome, particularly with DMFCs. Problems such as methanol crossover, poor catalysts, catalyst poisoning, water management and others that will be discussed later in this chapter need to be resolved.

A single cell PEM or DM fuel cell, as shown in Figure 2.1, is basically comprised of the following:

- A membrane electrode assembly (MEA), which consists of two gas diffusion layers, two catalyst layers, and an electrolyte membrane. Gas diffusion layers are placed on either side of a membrane and between them is a catalyst layer coated either on the GDL or the membrane itself.
- On either side of the MEA there is a graphite block attached to a copper plate, known as a current collector. These graphite blocks have flow

patterns (or fields) carved into them to allow the fuel / oxygen maximum exposure time to the catalyst coated GDL or membrane for the reactions. For all of the experiments done at UNH a serpentine flow pattern is used, as shown in Figure 4.2.

- Auxiliary equipment is used to monitor temperature, pressure, flow rates, gas humidification and other process variables.

The following sections will discuss the literature review for these basic components of a single cell DMFC and their effect on the cell performance.

2.2 - Components and Materials

2.2.1 - Membrane Electrode Assembly (MEA)

The MEA is the heart of the fuel cell operation. It can be broken into its three main components, which are: the polymer electrolyte membrane, the gas diffusion layers (GDLs) and the catalyst coatings. Each of these parts is examined individually as they are the most important components of the PEM/DM fuel cell. Generally, the MEA is made by sandwiching the membrane between two catalyst layers and two GDLs, as shown in Figure 2.1. The catalysts are either placed on each side of the membrane [7] or coated onto the GDLs themselves. The catalyst, typically Pt on carbon, is usually combined with water, ionomer solution and an alcohol to form an ink solution, which is either painted or sprayed onto these surfaces. It has been reported that the spraying method is more uniform and therefore more effective. However, many facilities

continue to paint the catalyst onto the GDL for cost and process simplification [18]. For methanol, a new technique for preparing MEAs has been proposed by Frey et al. [19] by a layer-upon-layer fabrication process, which may further improve uniformity and performance.

2.2.2 - Polymer Electrolyte Membrane (PEM):

The membrane is often considered to be the heart of the PEM or DM fuel cell. It needs to allow protons to move freely, while preventing electrons from passing through. It must not allow the fuel or oxidant to crossover and must also act as an insulator between the electrodes. This is particularly important in DMFCs, where methanol crossover is currently the biggest factor associated with low performance. To be useful the membrane must be chemically and thermally stable, not breaking down during use and be mechanically durable to resist any structural damage or deformation.

Prior to the 1970s, the most common membrane used in PEMFC applications was the polystyrene sulfonic acid (PSSA) membranes [14]. Although these membranes were inexpensive and had relatively high ionic conductivities, they had a low tensile modulus and were easily degraded in the oxidizing environment of the fuel cell. The performance of these membranes was also limited due to fuel crossover, reducing the external flow of electrons during the cell operation.

In the early 1970s there was a significant advance in membrane technology when DuPont invented Nafion®. Nafion® is a perfluorosulfonic acid membrane which offers nearly twice the ionic conductivity of previous

membranes with more thermal and mechanical durability. This membrane is used in current fuel cells, although its high cost and environmental disposal hazards keep researchers looking for other alternatives. Other companies have followed in DuPont's footsteps and produced their own perflorinated polymer electrolyte membranes that are commercially available, such as: Asahi Chemicals Co. (Aciplex), Asahi Glass Co. (Flemin), Dow [6] and W.L. Gore and Associates, Inc. (PRIMEA) [20].

All of these membranes are structurally based on polyethylene. When this base structure is changed such that the C-H bonds are broken and hydrogen atoms replaced with F atoms, we are left with a polytetrafloroethylene (PTFE), which is given the trade name Teflon®. Teflon® is useful because it is highly resistant to chemical attacks because of the strong C-F bonds. It is also considered one of the most stable substances in the world and prevents most anything from binding to it, including water. To make this material conductive to protons, a sulphonic acid group is attached by the process of sulphonation. These groups are also highly hydrophilic (attract water) and with the hydrophobic (repels water) Teflon® base, pockets of water are created inside the membrane. The methods by which these sulphonic acid groups are added differ with the base membrane structure, but regardless of the technique used, the SO_3^- group is strongly attached while the H^+ ion is weakly attached to the membrane. These H^+ ions (protons) are able to easily move from one location to another, thus conducting protons through an otherwise electrically resistant material [1].

Problems with these types of membranes are generally cost and environmental disposal. Nafion® currently retails for approximately $500 [21] per square meter, making it one of the most expensive parts of the fuel cell. In methanol systems these membranes also allow a significant portion of the methanol to crossover, leading to poor efficiencies [22]. Commonly when a membrane separates two solutions of different concentrations, there is some flow of a component from the higher concentration to the low concentration side. In methanol systems there is a small concentration (typically ~3%) of methanol at the anode, but no methanol present at the cathode, thus there is diffusional flow. In addition to this, methanol is pulled through the membrane by the water molecules by electro-osmotic drag. This means that as water moves through the membrane, it drags methanol with it across the membrane to the cathode side unreacted. It is necessary to eliminate this crossover flow because the methanol that passes through the membrane does not produce electrons at the anode and thereby decreases the overall cell performance.

Currently either thicker or structurally enhanced membranes are used to decrease the amount of methanol crossover. Gamburzev et. al. [15] examined the performance of Nafion® membranes with respect to thickness and equivalent weight (EW). It was reported that thinner membranes had much better proton conductivities; however, membranes that were too thin often led to thermal or mechanical degradation and system failure. It was also found that membranes with a lower EW performed better than those with a higher EW, even if the membrane itself was thicker [15]. Nafion® membranes are characterized relative

to their equivalent weights and thickness. For example Nafion® 115 is a membrane of EW of 1100 and a thickness of .005 inches [1]. For current DMFC systems it is important to have a relatively thicker membrane with a lower EW, such as Nafion® 117, to get the best performance.

There are other less common membranes, which are also being used as low cost and environmentally friendly alternatives. Some of these alternatives include: polyether ether ketone (PEEK) [3], polyvinyl alcohol (PVA) [4], acid doped polybenzimidazole (PBI) [5] and polyphosphazene [23]. The benefits of these alternatives are low-cost, environmental friendliness, chemical stability and reduced methanol crossover. The major disadvantage is the relatively low proton conductivity compared to Nafion®, decreasing the overall performance of the cell. Chen et al. have experimented with a resin/polystyrene sulfonate (PSS) composite membrane [24]. The resin is a cross-linked polystyrene sulfonate ion exchange resin, which is easily blended with the PSS to create a composite membrane that is highly conductive and has relatively low cost. It is also more environmentally friendly, structurally and chemically stable. This membrane may also prove to be highly successful in decreasing methanol crossover because of the cross-linked network.

One way to improve cell performance is raising the cell temperature. However, most of the membranes, especially Nafion®, break down at relatively low temperatures (less than 100ºC). Park et al. [25] examined nanocomposite membranes based on 3-glycidoxyproplytrimethoxysilane (GPTS), silicotungstic acid and α-zirconium phosphate hydrate for proton conductivity. They found that

the proton conductivity was sufficiently high and the membranes were stable at temperatures above 100ºC. Jalani et al. [26] examined nanocomposite membranes, using Nafion® as a base, for performance in the 90ºC -120ºC temperature range. They found that all the nanocomposites had higher water sorption than normal Nafion® in their specified temperature range. Adjemian et al. [27] examined modified perflouorsulfonic acid silicon oxide composite membranes in the temperature range of 80ºC-140ºC. They found that the modified membranes performed better than conventional membranes at these high temperatures and that they were physically more robust and not subject to degradation. Hogarth et al. [28] developed solid acid membranes, which performed well in the 100ºC-130ºC range. All of these advances indicate that higher temperature operation may be possible, leading to better overall efficiency.

The ionic conductivity of different proton exchange membranes was determined using AC impedance spectroscopy, as reported by Beattie et al. [29]. They found that EW and water content alone were not good indicators of proton conductivity, but rather a mixture of those plus the H_2O/SO_3^- ratio gave the best indication of how well a membrane conducted ions. Okada et al. [30] studied ionic and water transport characteristics for Nafion® membranes. The open-ended coaxial probe method was used by Anantaraman et al. [31] to study the membrane conductivities. Barragan et al. [22] examined the methanol crossover rate for Nafion® membranes with and without the presence of an electrolyte (KCl)

in the solution. Fransesco et al. [32] developed an analytical way to calculate the membrane resistance.

Although the focus of this study is not on the polymer electrolyte membrane, it is essential that we fully understand the advantages and disadvantages of each of the membranes. It is important to understand that thinner membranes with lower EWs will lead to higher proton conductivity, at the expense of methanol crossover. Proper water management must be maintained for the cell to function properly. Further advances in membrane must be made to minimize the amount of methanol crossover, while keeping proton conductivity high, and to lower the cost and make them more environmentally friendly.

2.2.3 - Gas Diffusion Layer (GDL):

The gas diffusion layer (GDL) is one of the most important parts of the membrane electrode assembly. Every MEA is composed of a membrane sandwiched between two gas diffusion layers. Between the membrane and each of the gas diffusion layers is a thin catalyst layer. The catalyst layer can be applied either on the gas diffusion layer or directly on either side of the membrane. We will first focus on the gas diffusion layers and then will turn our focus to the catalyst layers.

Gas diffusion layers are generally made of porous carbon paper or cloth/fabric. The carbon base gives it relatively good electrical conductivity between the catalyst layer and the current collecting plates. In general, the gas diffusion layers are roughly 100-400μm thick and highly porous to allow the gas

to diffuse through to the catalyst. Thinner diffusion layers are generally better as they have minimal electrical resistance and allow the fuel and oxidants (CH_3OH/H2, O_2/Air) to easily pass through [2].

The gas diffusion layers are often wet-proofed with a hydrophobic material such as Teflon® (PTFE). The hydrophobic material allows excess water to be rejected from the cell, preventing the cell from flooding. Flooding occurs when an excess of water is present at the GDL surface, which prevents the gas from successfully reaching the catalyst layer. When flooding occurs, the cell performance drops drastically. Park et al. [33] studied the effect of PTFE contents in the gas diffusion layer and found that the incorporation of a micro layer was crucial to proper water management. They were able to conclude that reduced thickness and larger pore diameter in the GDL are the best for water management and consequently cell performance. Giorgi et al. [34] also investigated the effect of PTFE contents in the diffusion layer and came to the conclusion that minimizing the content was best, but not limiting it to zero as then the GDL floods, yielding no performance. Water management is one of the most important functions of the gas diffusion layer, as too little water causes poor proton conductivity of the membrane and excess water causes the cell to flood.

Often times the gas diffusion layer is coated with a thin layer of Nafion® solution. This solution affects the gas permeability, catalytic activity and ionic resistance of the GDL. Sasikumar et al. [35] reported that as the platinum loading decreased the optimum Nafion® loading increased, showing an inverse relationship. Lee et al. [36] also studied the effects of Nafion® impregnation and

concluded that there was a sharp increase of catalyst activity with a moderate Nafion® loading (1.3mg/cm^2) and then a gradual increase as the loading was raised to a maximum of 1.9 mg/cm^2.

Some of the major physical properties that affect the performance of the gas diffusion layers in the cell are the gas permeability and the pore size diameter. Prasanna et al. [37] reported the optimum pore size diameter to be roughly 25-40μm, anything larger than that led to excessive flooding of the cell. Kong et al. [38] used mercury intrusion porosimetry and AC impedance analyses to show that an increase in pore size distribution led to a reduction in cell performance loss due to mass-transport limitations. It was also confirmed that if the pore size was too large, the cell was easily flooded and performance dropped drastically. Chu et al. [39] also studied the effects of porosity change on performance and developed a theoretical mathematical model, which showed that as the porosity increased, the current density also increased. However, the GDL would be more prone to flooding, leading to lower power generation. The thickness and Teflon® content of the GDL have a larger impact on GDL performance than just the porosity.

There are numerous types of commercially available GDLs that have been studied and compared for PEM fuel cell performance. The different GDLs are characterized by their thickness, gas permeability and electrical conductivity. As previously mentioned, thinner GDLs tend to have higher gas permeability and electrical conductivity, which make them preferable. However, very thin GDLs cannot adequately provide good electrical contact between the current collecting

plates and the catalyst layer. There is an optimum thickness for a GDL and it is dependent on the type of material used. Researchers [40, 41] have compared different types of carbon fiber and carbon paper GDLs in PEMFCs. One of the most common types of fabric GDL is the ELAT (E-TEK), which has been studied and results reported by Qi et al. [42]. The study of paper GDLs such as Toray and Kureha was conducted and results were reported by Giorgi et al. [34] and Passalacqua et al. [43], respectively. Toray paper remains one of the most commonly used GDL because of its high performance. Moreira et al. [44] studied the paper and cloth GDLs and found that the paper performance was better at low current densities, but fabric GDLs performed better at high current densities because of improved water management.

Single layered GDLs were originally used in PEM fuel cells. These were wet proofed with PTFE or some other similar coating and worked relatively well. Later these GDLs have been modified to include another separate hydrophobic layer, which helps manage the water in the cell more effectively. Song et al. [45] used a layer of PTFE and carbon film cast on the surface of the GDL using an alcoholic suspension. Glora et al. [46] used carbon aero gels to form a porous substrate layer. Both these methods worked to decrease the contact resistance between the electrode and the membrane/plates. The aero gel method only produced a minimal amount of power, however. The problem is believed to lie with poor catalyst layer preparation, although that was not confirmed. Both of these methods confirm that an additional layer applied to the GDLs helps to minimize resistance and thereby improves performance.

Another concept approach to forming a multi-layer GDL is through the use of a microporous sublayer (MPL). This has been tested by Qi and Kaufman [47] and has shown promising results. When this MPL is present, the paper appears to act only as a mechanical support to the sublayer. Different sublayers of varying thicknesses which contained anywhere from 25-45% PTFE were examined. It was found that the presence of the sublayer seems to reduce mass transport problems and give better performance. They were able to operate a four-cell stack at a current density of 145 mA/cm^2 with un-humidified gases. Wang et al. [12, 13] have attempted to use MPLs with the gas diffusion layer to control CO_2 gas management and methanol crossover effects. They have models that show that thick GDLs may act as a barrier to methanol transport and allow the use of highly concentrated methanol solutions, even with thin membranes with high ionic conductivity. The results of these studies of multi-layered GDLs are promising and may lead to further advances in the near future.

For the DMFC, the problem of flooding within the cell is a major factor because the fuel is a methanol/water mixture. The concept of a multi-layered GDL to prevent flooding and use of a cross-linked polymer membrane to prevent methanol crossover could go a long way in improving the cell technology. Understanding how small changes in the electrodes (GDL and catalyst layer) will affect the cell performance is critical. Water management is of vital importance to keep the membrane hydrated enough for proton conduction, but limit flooding. This is a very delicate balance, which must be controlled properly by the GDLs.

2.2.4 -Catalyst Layer:

The catalyst layer is located between the gas diffusion layer and the membrane as shown in Figure 2.1. It is often called the active layer and it must remain close to the membrane, as the reactions only take place on the catalysts. The catalyst slurry, called ink, is composed of a metal catalyst on mostly carbon support suspended in H_2O, alcohol (typically propanol) and Nafion® solution. This catalytic ink is then spread on either the gas diffusion layer or on the membrane itself. Shin et al. [48] examined the effect of using the ink either as a solution or as a colloid. They found the colloidal method led to larger reaction area and therefore an increase in cell performance.

Typically the catalyst is Pt or Pt-Ru on some type of support, usually carbon. Liu et al. [49] studied the effect of the carbon support for the catalyst and found that the supported catalyst had much higher activity and generally performed well. However, it seemed to lead to higher methanol crossover effects in DMFC applications possibly because of carbon corrosion and Pt dissolution damaging the membrane. Tian et al. [50] studied the effect of Pt catalyst preparation conditions and found that cell performance was enhanced when the Pt was deposited on heat-treated carbon black. Maruyama and Abe [51] did a similar study and found that performance was increased as much as 6 times by using activated carbon rather than just carbon black.

If CO is present, in the fuel (if there is a reformer) or formed as a product during methanol breakdown, it can poison the catalyst, decreasing reaction rates and therefore the performance of the cell. Toad et al. [8] tried to improve

performance by creating Pt alloys with Fe, Ni and Co and found that there was a slight increase in performance. Gupta et al. [9] developed heat-treated iron based catalysts, which showed no performance degradation when exposed to methanol for over 24 hours. Generally in the case of DMFCs the catalyst used on the anode is Pt-Ru on carbon in a 50:50 atomic ratio. There are several studies underway for the development of CO-tolerant catalysts.

The catalyst loading can have a great impact on the overall performance of a cell. It may seem that an increase in catalyst amount would lead to an increase in reaction rate and therefore an increase in performance. In general this is true, as the catalyst amount increases, the cell performance increases. However, when the loading gets too high the pores of the gas diffusion layer clog and the fuel/oxidant can no longer reach all of the catalyst sites. This decrease in mass transfer rates leads to a much lower cell performance. Gasteiger et al. [52] studied the effect of catalyst loading and found that PEM fuel cells performed even with anode Pt loadings as low as 0.05 mg/cm^2 on the anode. On the cathode side the performance was greatly reduced if the Pt loadings dropped below 0.2 mg/cm^2. Antoine et al. [53] studied the effect of particle size and distribution on reaction rates in PEM fuel cells. They found that on the cathode side the slow kinetics had a larger impact than diffusion resistance, while on the anode side both kinetics and diffusion rates were hindered with increased particle size.

Several authors have attempted to study and model the kinetics that take place in a fuel cell [54, 55, 56]. Generally it is understood that the kinetics on the

anode side of a PEM cell (hydrogen oxidation on Pt) occurs very rapidly, while at the cathode (oxygen reduction on Pt) the kinetics are very poor and thus efficiency limiting. In DM fuel cells the anode kinetics are very slow as methanol must break into hydrogen and CO_2 and then the hydrogen must react with platinum to form a proton and an electron to drive the reaction. Grgur et al. [57] studied the effect of methanol oxidation rates on Pt-Ru catalysts by itself and in the presence of CO. It was found that the CO would bond to the Ru sites and deactivate the catalysts leading to very poor performance with a potential as low as 0.15V.

Pozio et al. [58] derived a semi-empirical equation to model the hydrogen oxidation rates on Pt, Pt-Ru and Pt-Mo catalysts on carbon support. It was found that there was a strong kinetic limitation on the Pt-Ru and Pt-Mo catalysts as opposed to the rates provided by the Pt alone. This indicates that even with the improved conversion of methanol to hydrogen with bi-metallic catalysts, the overall kinetics will decrease and thus the performance of the cell will be lower than that of hydrogen alone. Ye et al. [59] made an interesting discovery when they found that by interrupting the oxygen supply to a DM fuel cell there was an accumulation of hydrogen at the anode, which led to an increase in power when the oxygen feed, was resumed. This allowed the DMFC to behave like a hydrogen cell because of the accumulation of hydrogen feed at the anode [59].

Several authors have developed a model to optimize the catalyst layer in a fuel cell [60, 61]. Generally, it is found that the cell is most dependent on the layer thickness and the Pt loading. The optimal results occur when the layer is

as thin as possible with a maximum Pt loading. This supports the conclusion that when applying catalyst ink it is ideal to spray the catalyst as opposed to painting it. Also many authors have tried to further decrease the catalyst layer thickness by using electrochemical deposition [62, 63, 64]. Usually these methods improve the overall performance by increasing the amount of Pt in a very thin catalyst layer.

2.2.5 - Bipolar Plates and Flow Fields

Bipolar plates are currently another very expensive part of a fuel cell system. Their primary function is to allow one side to act as a cathode and the other side as an anode simultaneously. That allows multiple cells to be connected in a stack, while limiting the number of plates that are needed. The plates must be made of a good conductive, both thermal and electrical, material such as graphite or stainless steel [2]. The reason why these plates are so expensive is because they are currently machined carefully for gas flow and you need multiple pieces for a cell stack. Zhang et al. [65] studied the effect of graphite particles and particle size on bipolar plate performance. They found that flake graphite particles outperform spherical graphite particles and that in both cases as the particle size decreased, electrical and thermal conductivity were reduced, although strength was enhanced.

Arico et al. [66] have examined the effect of flow field design on DMFC performance and concluded that serpentine flow patterns show lower methanol crossover and fuel utilization than interdigitated flow patterns. Yang and Zhao

[67] did a similar study comparing serpentine flow fields to parallel flow fields and also concluded that parallel flow fields tend to be blocked by CO_2 gas bubbles, while serpentine flow fields did not. Jung et al. [68] also examined various combinations of flow field designs and concluded that a parallel flow on the anode combined with a serpentine flow on the cathode led to the best performance in their system. They concluded that the serpentine flow path was too long to adequately remove CO_2 bubbles on the anode side, while on the cathode side the high pressure drop from the serpentine channels help to exclude water and improve mass transfer.

Along the same lines Yang et al. [69] examined the formation of CO_2 gas bubbles in flow fields and determined that higher methanol flow rates reduced the size and number of bubbles in the flow channels and that cell orientation had a large effect on performance, especially at low temperatures. They also examined the pressure drop in the anode flow field [70] and found that it always increased with increased methanol flow rate, however the performance deteriorated at very high or very low flow rates. Also they concluded that the pressure drop was almost independent of current density at sufficiently high methanol flow rates and that temperature and methanol concentration had little to no effect on pressure drop.

2.3 – Mass Transport and Water Management

Water management, as we have seen in the membrane and GDL sections, plays a crucial role in the operation of a fuel cell. There must be a

proper balance between keeping the membrane hydrated, for protons to flow, and keeping the GDL from flooding, leading to mass transport limitations. This section examines the mathematical models and in-situ studies that have been reported on water management and transport phenomena and their impact on the design and operation of a fuel cell.

There have been numerous mathematical models [71-75] to describe the effects of flooding in a PEM fuel cell system. Yan et al. [76] took these base models and developed a model that describes both heat transfer and water management in a PEM system. Others, such as Tuber et al. [77], developed transparent PEM cells to visualize the cathode flooding and determine how to stop it. Satija et al. [78] designed an in situ neutron imaging technique, which allows researchers to determine exactly where water is building up in the cell and under what conditions. Nguyen et al. [79] suggest a water management strategy, using inderdigitated flow field system on fuel cell stacks, which led to twice the power density of conventional stack systems.

The system design for a DMFC is similar to that of a PEMFC. However, in a PEMFC water management is primarily focused on the cathode side, where flooding occurs. In a DMFC, water management is important on both the anode and cathode because of the issue of methanol crossover as well as the formation of CO_2 on the anode side. Jiang and Menheng [80] developed a two-phase one-dimensional flow model for both heat and water management in a DMFC. Wang [10] examined two-phase flow and mass transport in a DMFC in depth, while developing a comprehensive three-dimensional model [81]. Others [69]

developed a transparent DMFC system to study the formation and transportation of CO_2 in the anode of a DMFC.

Water transport and mass transfer limitations present a significant barrier to improving DMFC performance. Improvements in CO_2 management on the anode side will greatly improve performance by allowing MeOH to reach the catalyst site quickly. Water transport through the membrane leads to higher MeOH crossover rates because of electro-osmotic drag effects. Lu et al. [11] proposed a method of using an MPL on the cathode side of the DMFC to build up hydraulic pressure and limit the water transport through a Nafion® membrane. This method greatly reduced MeOH crossover and improved performance. It also showed that new membranes were not required for DMFCs if the water/gas management was designed properly. Work towards improving the anode GDL will play a crucial role in the development and eventual implementation of DMFC as a power source.

CHAPTER III

THEORY OF FUEL CELL OPERATION

This chapter is divided into three sub-sections. The first section discusses the theoretical fuel cell potential and efficiency. The second section deals with different overpotentials of the cell and their causes. The final section examines different parameters that affect the overpotentials and ways for possible cell performance improvement.

3.1 - Theoretical Potential of a Fuel Cell

As has been previously discussed in Chapter 2, a fuel cell operates on the basis of two simultaneous electrochemical reactions occurring at the anode and cathode electrodes. The basic reactions for hydrogen fuel are:

At the Anode:

$$H_2 \rightarrow 2\,H^+ + 2\,e^- \qquad (1)$$

At the Cathode:

$$\tfrac{1}{2}\,O_2 + 2\,H^+ + 2\,e^- \rightarrow H_2O \qquad (2)$$

Overall:

$$H_2 + \tfrac{1}{2}\,O_2 \rightarrow H_2O \qquad (3)$$

Although these reactions may have some intermediate steps and/or have some unwanted products, it is essentially an accurate description of the internal operation of the fuel cell.

It is clear that the overall reaction is simply the combustion of hydrogen. This means that the energy released from the combustion of hydrogen must be the same as the theoretical potential energy that can be generated in the cell. Since the fuel cell operates because of chemical reactions, not all of the energy can be directly converted into electricity, because a portion must involve a change in entropy. The amount of energy that can possibly be produced is given by the change in enthalpy minus the change in entropy, which is the same as the Gibbs free energy governed by the following equation:

$$\Delta G = \Delta H - T \cdot \Delta S \tag{4}$$

where ΔG is the change in Gibbs free energy, ΔH is the change in enthalpy, T is the temperature in Kelvin and ΔS is the change in entropy.

If we assume the cell operates at 25°C, then the ΔH for hydrogen is -286 kJ per mole and the $T\Delta S$ is -48.68 kJ per mole, which means that the Gibbs free energy (or total amount of energy that can be converted to electricity) is -237 kJ per mole [1].

The standard potential (or open circuit voltage) can be determined with the following equation:

$$E = \frac{-\Delta G}{n \cdot F} \tag{5}$$

where n is the number of electrons present (with H_2, n=2 because there are two electrons present for every one mole) and F is Faraday's constant (96,485 Coulombs per electron-mol). Since all the values are known in this case, we can find the theoretical fuel cell potential (using hydrogen and oxygen) to be:

$$E = (237{,}340\ J \cdot mol^{-1}) / (2 * 96{,}485\ C \cdot mol^{-1}) = 1.23\ V \quad (6)$$

This shows that at 25°C the theoretical hydrogen fuel cell potential is 1.23 V. The same analysis can be applied to a direct methanol fuel cell (DMFC), which undergoes the following reactions:

At the Anode:

$$CH_3OH + H_2O \rightarrow CO_2 + 6\ H^+ + 6\ e^- \quad (7)$$

At the Cathode:

$$1\frac{1}{2}\ O_2 + 6\ H^+ + 6\ e^- \rightarrow 3\ H_2O \quad (8)$$

Overall:

$$CH_3OH + 1\frac{1}{2}\ O_2 \rightarrow 2\ H_2O + CO_2 \quad (9)$$

From these reactions the change in Gibbs free energy is found to be 698.2 kJ per mol and since there are 6 electrons per mole of CH_3OH, the theoretical fuel cell potential for the DMFC is found to be 1.21 V.

Although understanding and computing the maximum theoretical potential is a useful tool, it is perhaps more advantageous to look towards the maximum theoretical efficiency of a fuel cell. There are 2 different ways to examine the theoretical efficiency [1]. The first method is to simply compare the ratio of maximum electrical energy produced to the amount of energy input. We know

the maximum electrical energy output is the Gibbs free energy and the amount of energy input is the heating value (enthalpy) of the fuel. Therefore, the theoretical efficiency of a hydrogen fuel cell can be calculated from:

$$\eta = \frac{\Delta G}{\Delta H} \tag{10}$$

This shows that when ΔG and ΔH are –237 and –286, respectively, the maximum possible efficiency of a PEMFC is only 83%.

The other method of determining the efficiency of the fuel cell is to take the ratio of the potentials. By dividing ΔG and ΔH each by nF we can find the maximum potential for both the actual and the perfect cell, if we were to ignore change in entropy. We find that based on ΔG, the maximum potential is 1.23 V and based on ΔH, it is 1.482 V. Therefore, the maximum efficiency of the cell would be equal to the ratio of these two potentials or:

$$\eta = \frac{\frac{\Delta G}{n \cdot F}}{\frac{\Delta H}{n \cdot F}} \tag{11}$$

As previously shown, the theoretical efficiency of a hydrogen fuel cell is found to be 83%. Similarly for a DMFC system, the theoretical maximum efficiency is again $\Delta G/\Delta H$ as given by equation 10. Since ΔG for the oxidation of methanol is known to be -698 kJ per mole and ΔH is -727 kJ per mole, the theoretical efficiency for DMFC system is 96%.

3.2 - Overpotentials and Their Causes

In the operation of a hydrogen fuel cell there are 3 major types of overpotentials that decrease the theoretical voltage of a cell. The first overpotential is known as activation overpotential and it typically occurs at very low current densities of 0-0.1 A/cm^2. The second major overpotential is known as ohmic losses and it usually occurs over a wide range of medium current densities from 0.1-1 A/cm^2. Another major overpotential is known as mass transport or concentration losses and it causes a major voltage drop-off in the high current density range above 1 A/cm^2. Each of these overpotentials is illustrated in Figure 3.1 and their causes are discussed in detail in the following pages.

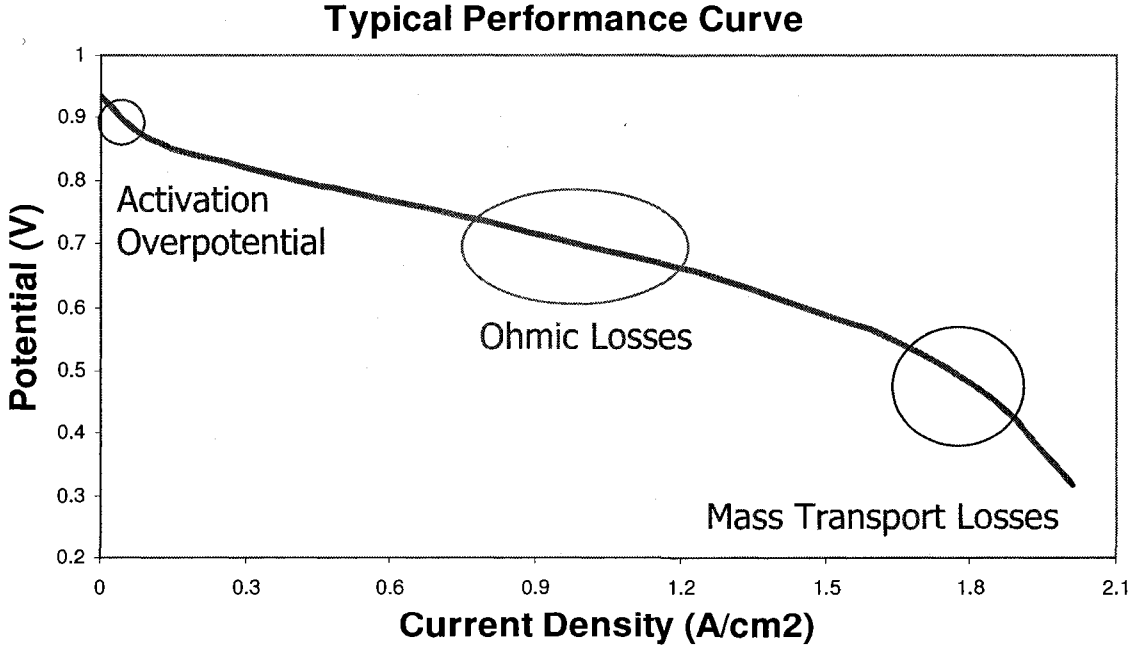

Figure 3.1 – Illustration of the Three Major Overpotentials

When the cell is initially put into operation, a certain amount of potential is required to start the electrochemical reactions. This portion of the potential is "lost" and is commonly known as activation potential, shown with the red circle in Figure 3.1. This overpotential represents the size of the activation energy that is required when the reactions proceed at the rate necessary for the desired current. It is important to note that at higher current densities the activation losses are much lower than at low current densities. The losses occur at both the anode and cathode and the expressions for these can be derived from the Butler-Volmer equation. For the cathode the activation overpotential is given by:

$$E_{rC} - E_C = \frac{R \cdot T}{\alpha_C \cdot F} \cdot \ln\left[\frac{i}{i_{0C}}\right] \tag{12}$$

where, $E_{r,c} - E_C$ is the overpotential (the difference between the reference and the cell), R is the universal gas constant, T is the temperature in Kelvin, α_c is the cathodic transfer coefficient, F is Faraday's constant, i is the current density and i_{0C} is the exchange current density on the cathode side.

For the anode the activation overpotential is given by:

$$E_C - E_{rA} = \frac{R \cdot T}{\alpha_A \cdot F} \cdot \ln\left[\frac{i}{i_{0A}}\right] \tag{13}$$

where, $E_C - E_{rA}$ is the overpotential (the difference between the reference and the cell), R is the universal gas constant, T is the temperature in Kelvin, α_A is the anodic transfer coefficient, F is Faraday's constant, i is the current density and i_{0A} is the exchange current density on the anode side.

These equations can be represented by the Tafel [2] equation by using the properties of the natural log function as follows:

$$\Delta V_{act} = A + B \cdot \ln(i) \tag{14}$$

where

$$A = \frac{-R \cdot T}{\alpha \cdot F} \cdot \ln(i_0) \qquad B = \frac{R \cdot T}{\alpha \cdot F} \tag{15}$$

and ΔV_{act} is the difference between the cell voltage and the reference as given in Equations 12 and 13 for the cathode and anode, respectively.

Since the reversible potential of the hydrogen oxidation ($E_{r,a}$) is zero by definition [1], the overall cell potential (only accounting for activation polarization losses) would be:

$$E_{cell} = E_r - \frac{R \cdot T}{\alpha_C \cdot F} \cdot \ln\left[\frac{i}{i_{0C}}\right] - \frac{R \cdot T}{\alpha_A \cdot F} \cdot \ln\left[\frac{i}{i_{0A}}\right] \tag{16}$$

where, E_r is the theoretical cell potential, the second term is the activation loss from the cathode side and the final term is the activation loss from the anode side as given in Equations 12 and 13, respectively.

Since the anode reaction proceeds much more rapidly, the exchange current density for the anode is significantly larger than that of the cathode and therefore its activation polarization can be neglected. Therefore, the last term drops out and the cell potential is given by:

$$E_{cell} = E_r - \frac{R \cdot T}{\alpha_C \cdot F} \cdot \ln\left[\frac{i}{i_{0C}}\right] \tag{17}$$

Thus, the cathode exchange current density, i_{0C}, is the single largest factor in determining the activation overpotential. As i_0 increases, the overpotential decreases, thus improving the performance of the cell. The transfer coefficient (α) is typically around 1 for oxygen reduction on Pt [1].

Ohmic losses are caused by any resistance to the flow of ions or electrons through the fuel cell system. These losses typically cause the linear voltage drop that is seen at the middle current density range. It is governed by Ohm's law, which states:

$$\Delta V = i \cdot R_i \tag{18}$$

where, i is the current density and R_i is the total internal resistance of the cell. The R_i value for a typical fuel cell is usually somewhere in the range of 0.1-0.2 Ω cm^2. Usually the largest resistance is found in the electrolyte, although resistance in the bipolar plates may also be important [1].

Mass transport or concentration losses (polarization) are caused by rapid consumption of a reactant at the electrodes, which leads to concentration gradients. This usually occurs in the high current density range, as there is not enough reactant present on the catalyst surface for the current demands. This overpotential is governed by the Nernst equation:

$$\Delta V = \frac{R \cdot T}{n \cdot F} \cdot \ln\left[\frac{C_B}{C_S}\right] \tag{19}$$

where, C_B and C_S are the concentrations of the reactants in the bulk and at the surface, respectively. By using Fick's law and manipulating it by knowing that at

steady state the rate at which the reactants are consumed is equal to the diffusion flux [2], one is able to find the relationship between C_s and i as follows:

$$i = \frac{n \cdot F \cdot D \cdot (C_B - C_S)}{\delta} \tag{20}$$

where, D is the diffusion coefficient of the reacting species and δ is the diffusion distance. When the reactant is consumed faster than it can diffuse to the catalyst surface, the cell can no longer perform and the current density is known as the limiting current density (i_L) and can be represented by the following equation:

$$i_L = \frac{n \cdot F \cdot D \cdot C_B}{\delta} \tag{21}$$

By manipulating Equations 19, 20 and 21 one can find that the relationship between the overpotential and the limiting current density as:

$$\Delta V = \frac{R \cdot T}{n \cdot F} \cdot \ln\left[\frac{i_L}{i_L - i}\right] \tag{22}$$

This equation shows that as the current density, i, approaches the limiting current density there will be a large drop in cell potential. In actuality we rarely reach the limiting current density because of non-uniform surface conditions [2].

Internal losses or crossover losses, although minor in hydrogen fuel cells, can play a major role in DMFCs. Internal losses are caused when electrons manage to cross from the anode to the cathode without going through the external load. This is not typically found in Nafion® membranes (typically used in hydrogen cells), but can be common in some specialty membranes, which are designed to reduce methanol crossover. This has the effect of lowering the

overall efficiency of the fuel cell, as some of the electrons formed are not contributing to the current flow. Fuel crossover has a similar effect to internal losses; however, it results from reactants passing through the membrane. This not only means that some of the reactant is being wasted, but also it "depolarizes" the cathode, thus reducing the cell's potential. This is a major concern as methanol crossover is reported as high as 30-40% when using Nafion® membranes [82].

3.3 - Improving Performance

Many parameters affect these overpotentials in a cell and can be controlled to improve the overall efficiency. It appears from Equation 12 that as the temperature increases, the activation overpotential will also increase. In practice this is not the case because as the temperature increases the exchange current density also increases by a large amount, which offsets any adverse effect of temperature. Ohmic losses are independent of temperature. Methanol crossover may increase with higher temperatures as gaseous methanol can more easily pass through the membrane due to dilation of pores. Internal losses, however, are not affected by temperature. Concentration polarization increases slightly with an increase in temperature. The effect is minimal, however, compared to the relative concentration of reactants. Overall, there is an improvement with an increase in temperature as the kinetics improve and activation losses are decreased more than the relative increase in methanol crossover or concentration polarization [2].

Pressurizing the system, on the cathode side, tends to decrease the concentration polarization by increasing the concentration at the surface. When pressurizing the anode side, there may be a slight increase in fuel crossover, which may adversely affect the system. Overall, it is found that increasing the pressure moderately (20-50 psi) on the cathode side improves the cell performance by reducing the concentration polarization and increasing the current exchange density [2].

Improving the effectiveness of the gas diffusion layer will greatly improve the performance of the system and help to decrease voltage losses. Improving the porosity and the gas permeability can help to decrease the concentration polarization drastically. Increasing the electrical conductivity can greatly reduce the internal losses of the cell. Increasing the roughness of the GDL will also improve exchange current density by increasing the real area while holding the nominal area constant.

Finally, improving the electrolyte and catalyst will greatly reduce losses and increase efficiency. Ideally the electrolyte should be as thin as possible to help reduce internal losses. Currently, this is not possible as there is more methanol crossover with very thin membranes and thus worse performance. As new membranes are developed to reduce the amount of crossover, it will be possible to have thinner membranes, which will also decrease the internal resistance and improve the efficiency of the cell. The catalyst could be improved by increasing the surface area or improving the effectiveness, which would help to reduce concentration polarization at high current densities.

Other major ways to improve the performance of a fuel cell would be to prevent water from building up or flooding the cell. Also find a way to prevent the nitrogen present in air from blocking oxygen from reaching the catalyst. Both of these may lead to large diffusion problems and greatly reduce cell performance, especially in the high current density region.

CHAPTER IV

APPARATUS AND EXPERIMENTAL PROCEDURE

This chapter is presented in three sections. The first section describes the apparatus that has been used for all the experiments done in this study, including all materials, such as membranes, GDLs and catalysts. The second section deals with all of the computer programs, electrical diagrams and data acquisition components. The final section pertains to the experimental procedure used to prepare and evaluate MEAs and the operation of the fuel cell system.

4.1 - Apparatus and Materials

The PEM fuel cell system used in this study is an in-house design and is made to handle both hydrogen and methanol feed to the anode and air or oxygen to the cathode [59]. The system is composed of a single cell (5 cm^2), 3 thermocouples, 2 mass flow controllers, 11 solenoid valves, 2 pressure transducers, 2 pressure gauges, a humidification system, a DC electronic load, a power supply and data acquisition software and hardware. A magnetic stirrer, vacuum drier, heating plates and a hot press are used in the pre-treatment of membranes and MEA preparation.

4.1.1 - Fuel Cell System:

The fuel cell hardware consists of a single cell made of a pair of Poco Graphite grade AXF-5Q blocks (see item B in Figure 4.1). Each block is 3" by 3", made of poco graphite and machined with serpentine flow pattern for the methanol and air feed to the cell. They form a part of the 5 cm^2 cell and function as both electron conductors and liquid/gas diffusion channels. The assembled cell is shown in Figure 4.1. The carbon blocks with their serpentine flow channels are shown separated in Figure 4.2.

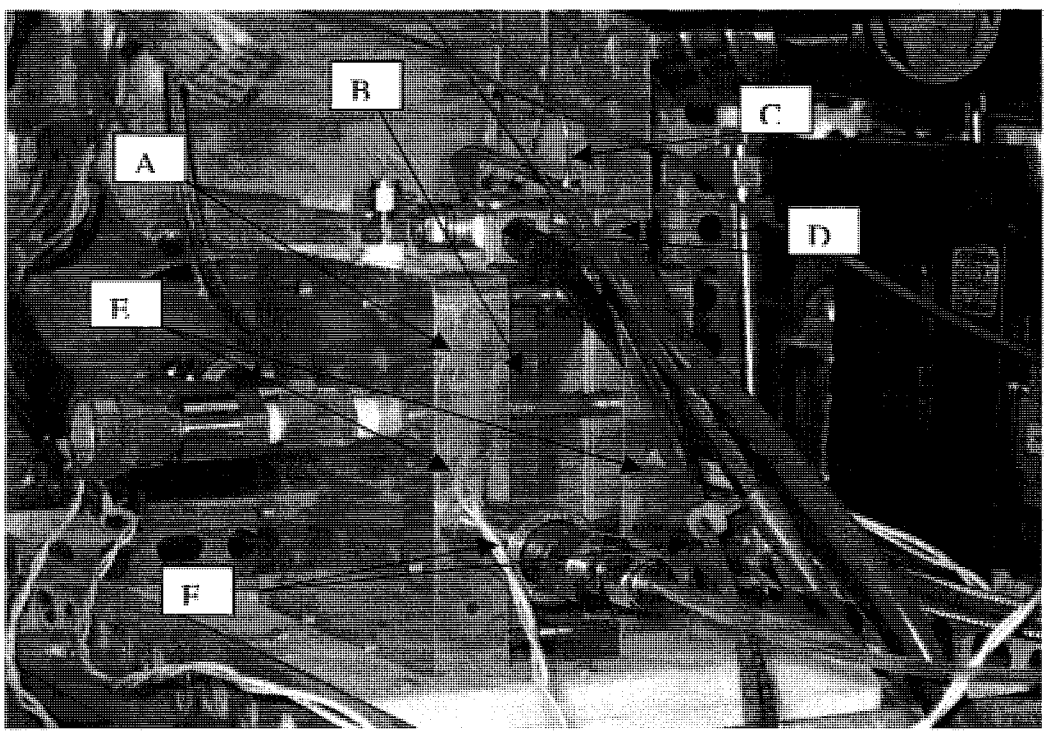

A) Aluminum alloy end plate
B) Poco graphite blocks
C) Thermocouple
D) Gold plated copper current collectors with wire to electronic load
E) Cartridge heaters
F) Liquid/Gas outlet (quick connects, inlet are similar and located on the other side)

Figure 4.1 - Assembled Single Cell System

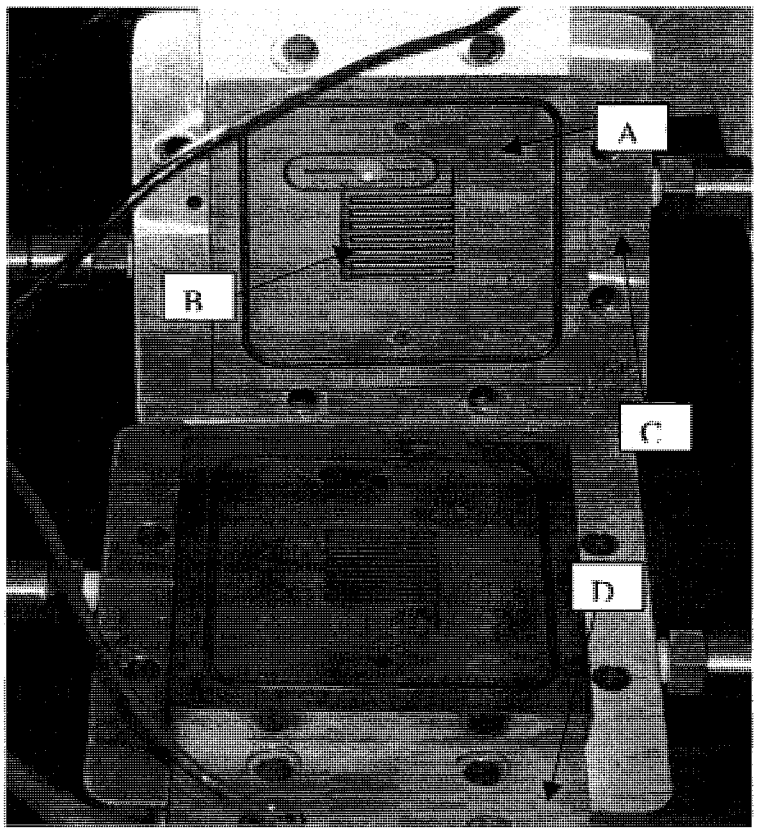

A) Poco graphite block
B) Serpentine flow pattern
C) Aluminum alloy end plate
D) Gold plated copper current collector

Figure 4.2 - Single Cell System Components

The aluminum alloy end plates, A and C as shown in Figures 4.1 and 4.2 respectively, are fitted with Swagelok© quick connect fittings and help to hold the assembly together. A thin layer of Teflon© tape is placed on the inside of the aluminum alloy plates to insulate them from the gold plated copper current collecting plates, shown as D in both Figures 4.1 and 4.2. These plates collect the current from the cell and transport it to the electronic load. The whole system is bolted together with 8 bolts in an octagonal pattern (tightened in a star pattern

for uniform pressure distribution). Cartridge heaters (shown as E in Figure 4.1) are used in conjunction with a thermocouple (shown as C in Figure 4.1) to monitor and maintain cell temperature. Liquid/gas input and output lines are connected to the end plates with Swagelok© quick connect fittings, shown as F in Figure 4.1.

4.1.2 - Humidification System

There are two humidification systems in the apparatus, one for hydrogen and the other for oxygen/air, consisting of one (12" tall, 2" diameter) stainless steel bottle with two (4" tall, 2" diameter) refilling bottles, used for PEMFC application. Inlet gas is fed to the anode or cathode through the bottom of the larger humidification bottle and bubbles through the water, becoming saturated. There is a thermocouple in each of the large bottles and a heating tape wrapped around the outside to heat the bottles to the desired temperature. Each of the two smaller bottles is set up in parallel and ensures that the water level remains constant at all times. A switch at the front of the testing apparatus opens two solenoid valves simultaneously to refill the bottles. When these valves are opened, the sight glass tubes allow the user to check the liquid level in the bottles. The main advantage of this system is that it allows the user to check the liquid level or refill the bottles while the system is operating, allowing for long-term cell operation.

4.1.3 - Cell Temperature Control

The cell temperature is carefully controlled with two cartridge heaters and a type J thermocouple. The thermocouple feeds the temperature information into a LabVIEW© program and controls it with a PID loop. The desired cell temperature information is fed to the program and the PID loop automatically turns the cell heaters on and off as necessary, maintaining the temperature within 2°C at all times.

4.1.4 - Mass Flow Controllers

For the system to be operated as a PEMFC, two Omega FMA5400/5500 mass flow controllers are used to monitor the feed rate of the gases. The hydrogen controller is factory-calibrated for flow rates up to 1000 mL/min while the air/oxygen flow controller is calibrated for flow rates up to 2000 mL/min. The desired flow rates are input into the LabVIEW© program and the computer sets the mass flow controllers to the right settings automatically.

4.1.5 - Pressure Gauges

Two Tescom pressure gauges (0-100 psi) are installed in the outlet of the system, allowing the application of backpressure to the system. Each of the gauges is manually controlled; however, there are also 2 pressure transducers that allow the computer to monitor the pressure of the system at all times. This is useful in case of a leak or other malfunction during unsupervised operation. This design allows the system to operate without supervision for lifetime testing of MEAs.

4.1.6 - Syringe Pump

In the case of DMFC operation, a Sage Instruments model 355-syringe pump is used to feed methanol to the system. It allows flow rates ranging from 0.0080 mL/min to 80 mL/min to the system. All the flow rates are controlled manually and the syringe needs to be removed and refilled as necessary. This is the only portion of the fuel cell system that cannot be conducted automatically, as of now.

As discussed above, the fuel cell system is equipped with temperature, mass flow, humidity and pressure controls. A schematic of the fuel cell apparatus is provided in Figure 4.3. Nitrogen gas is used to purge the system and all of the solenoid valves are fail-safe to automatically shut off reactant flow gases in case of system failure. Hydrogen, oxygen and air are all fed to the system from pressurized gas cylinders. The solenoid valves are controlled through switches on the LabVIEW© front panel, allowing the user to turn on and off gas flow and humidification at will. The gas lines are equipped with 50-micron filters to remove any particulate matter. The mass flow controllers have check valves to prevent any gas backflow to the system, which could lead to erroneous flow rates.

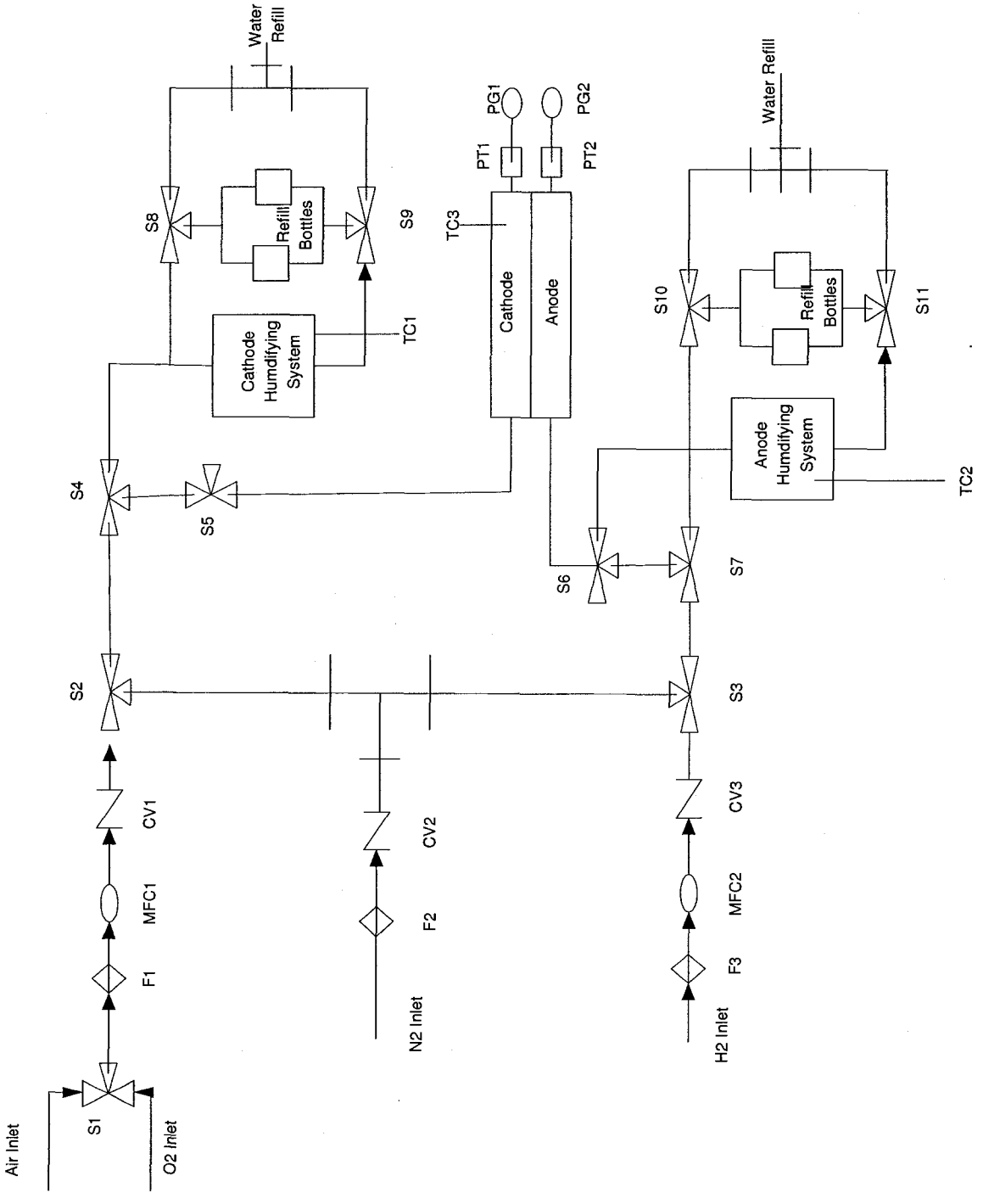

Figure 4.3 - Fuel Cell System Flow Chart

4.2 - Computer Programming

The PEM fuel cell system used in this study is also programmed in-house using the LabVIEW© programming language. This section discusses the user-interface of the program and then block diagram of the program. The hardware used for this program includes 1 SC-2345 connector block with 8 SCC-RLY01, 4 SCC-FT01, 3 SCC-TC02 and 1 SCC-AI07 modules. These components are connected via a computer with a NI PCI-6071E data acquisition card. Power is supplied to the system from a Radioshack© 3A, 13.8 VDC power supply and controlled through a fuse box designed to cutoff power to the system quickly in case of an emergency.

4.2.1 - LabVIEW© User Interface

All thermocouples, solenoid valves, mass flow controllers and pressure transducers are controlled and monitored with a LabVIEW© program file. The front panel (user interface) of the computer program is shown in Figure 4.4. The switches in the top left of the interface (section A) turn on and off the three heaters in the system. The oxygen and hydrogen switches control the heating tape on the humidification bottles, while the fuel cell switch controls the cartridge heaters in the aluminum alloy end plates. These switches can be activated manually or control through the PID loop (described later) by the computer.

The switches in the lower left of the interface (Section B in Figure 4.4) control the eleven solenoid valves located in the system. The first switch (O_2/air split) controls the solenoid S_1, as shown in Figure 4.3. This switch controls whether air or oxygen is being fed to the system. When this switch is activated

the computer automatically adjusts the gas correction factor in the mass flow controller settings based on whether air or O_2 is being fed. The second switch (H_2/N_2 safe) controls solenoid S_3, as shown in Figure 4.3. This switch defaults with nitrogen flowing through the system, but when activated allows H_2 to pass through the system to the cell for PEMFC testing. The third switch (O_2/N_2 safe) controls solenoid S_2, as shown in the Figure 4.3. It defaults allowing nitrogen through the system but when activated allows either air or O_2 (depending on S_1, as shown in Figure 4.3) to flow through the system to the cell. The fourth switch (H_2 bypass) controls solenoids S_4 and S_5, as shown in Figure 4.3. The default position allows the H_2 to bypass the humidification system, but when energized the gas is forced through the humidification system where it is saturated with water vapors to the desired degree.

The final switch controls solenoids S_6 and S_7 as shown in Figure 4.3. The default position allows the oxygen to bypass the humidification system, but when energized it forces the gas through the humidifier where it is saturated with water vapors at a particular temperature.

The controls in the top middle section of the user interface (Section C) monitor and control both the PID (propagation, integration, derivation) control loops. The top three controls (labeled as 1) regulate the temperature set point. This helps the PID loop to regulate the temperature as desired for each section. Both the thermometers and numeric indicators (labeled as 2) allow the user to see the real-time temperature of each component. The section labeled O_2 is the temperature of the oxygen humidification system, H_2 is the temperature of the

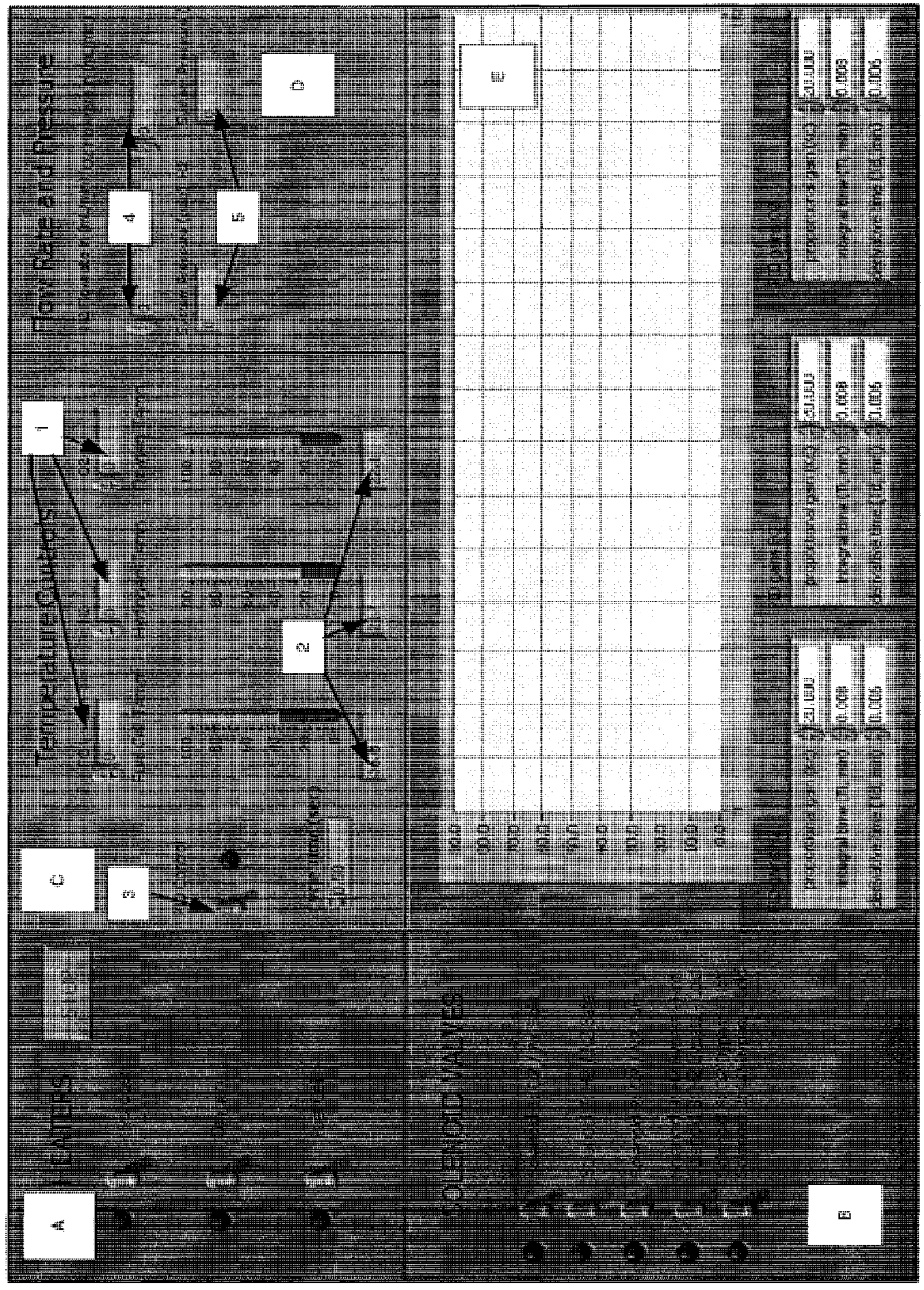

Figure 4.4 - User-Interface of LabVIEW© Program

hydrogen humidification system and FC is the temperature of the cell. Finally the switch located in the lower left of this section (labeled as 3) controls the PID loop. When it is off all temperatures are manually controlled and the set point temperatures are not used. When it is activated the computer automatically turns the heaters on and off (shown by the switches in Section A) to maintain a constant temperature within 2°C.

The controls shown at the top right section of the user interface (Section D) control the mass flow meters and the pressure transducers. The top two controls (labeled as 4) allow the user to set the desired mass flow rate. The H_2 mass flow controller is calibrated for hydrogen and thus will automatically set the flow rate for the desired output. The O_2 mass flow controller is calibrated for oxygen, but will automatically adjust for air flow rate if the O_2/air switch is activated in section B (S_1 in the schematic). The bottom two numeric indicators (labeled as 5) give readings from the pressure transducers in the system. Although the backpressure is controlled manually with pressure gauges, the program can monitor for any change in case of leaks and can record the pressure to the output file for long-term cell evaluation.

Finally the controls in the bottom right section (Section E) allow us to control the PID loop control settings to ensure the system reaches the set point quickly on start-up and is able to maintain the temperature for the duration of the trial. Each of the three temperature systems can be changed independently as necessary, although for these experiments it is not necessary to change the

default settings. The graph allows the user to see the temperature of each component for the last 3 minutes to quickly diagnose any problems.

4.2.2 - LabVIEW© Block Diagram

A block diagram of the computer program is provided in Figures 4.5a and 4.5b. The program is divided into 7 sections labeled A-G. The program consists of 3 "while" loops, 3 "conditional" loops, and numerous individual Virtual Instruments (VIs), which are discussed in detail below.

The first section (Section A of Figure 4.5a) of the program is designed to reset all of the variables and switches. It is very important to ensure that if the program restarts for any reason all the valves will default safe and all of the heaters will shut down.

This can prevent serious damage to the equipment as well as potential hazards associated with a reactant leak. This initialization step is very important in any computer program and especially so in one that controls a system such as this one.

The next section of the program (Section B of Figure 4.5a) allows the computer to determine if the switches are in the on or off position. The computer stores this information in an array and then sends that information to the SCC-2345 block. The SCC-2345 block then activates the solenoid valves or heaters as necessary. The third portion of the program (Section C of Figure 4.5a) is designed to shut down the program if the stop button is pressed. The program is placed inside a "while" loop, which allows it to run continuously until an error occurs or the stop button is

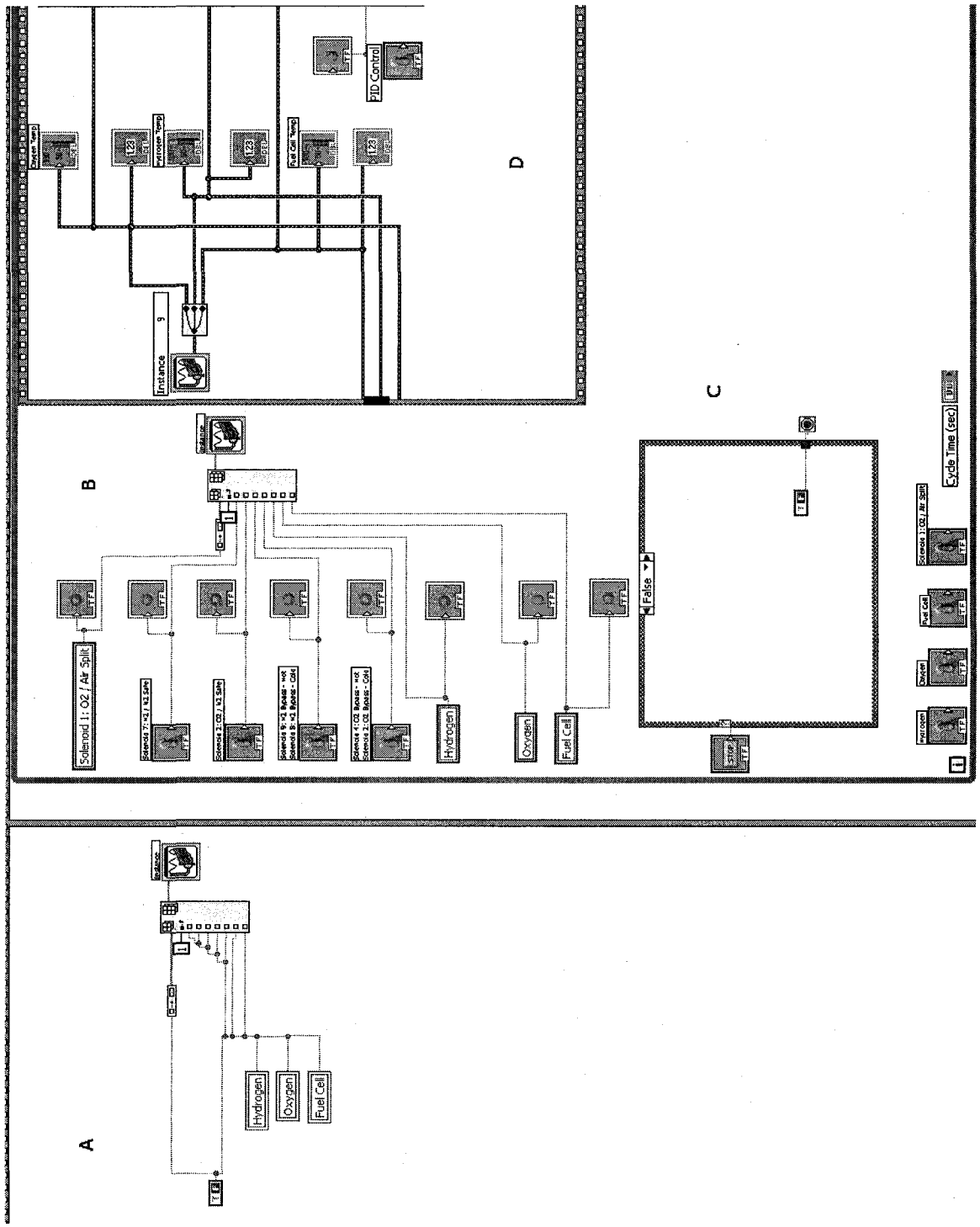

Figure 4.5a - Block Diagram of LabVIEW© Program

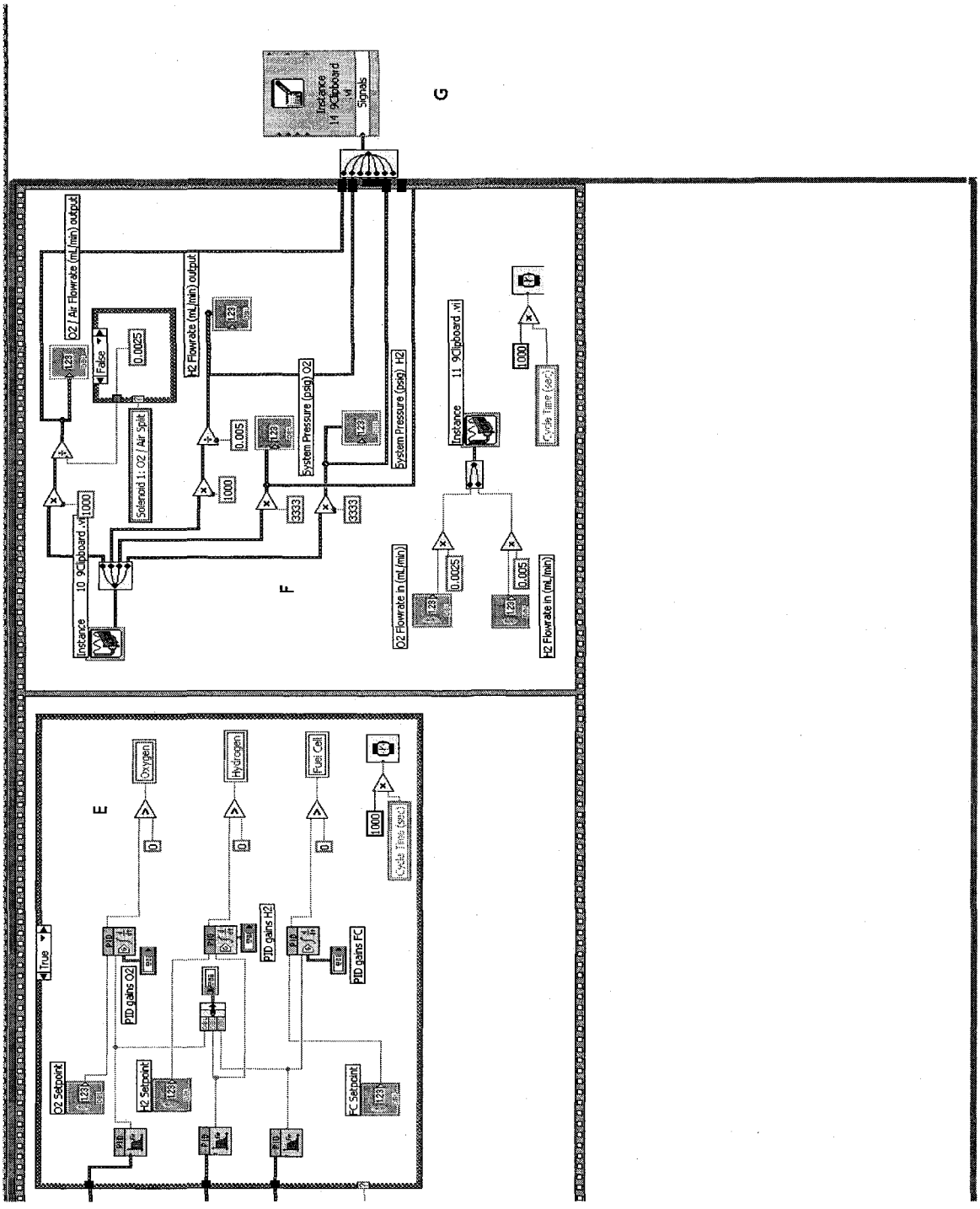

Figure 4.5b - Block Diagram of LabVIEW© Program

pressed. Once the stop button is pressed the program will stop and it will prompt the user to save their data.

The fourth portion of the program (Section D of Figure 4.5a) acquires the temperature readings from the thermocouples and displays them in the numerical indicators on the user-interface (labeled as 2 on section C of Figure 4.4). Each of these three signals is then sent into part 5 of the program (Section E of Figure 4.5b), which is the PID loop. The program will check to see if the PID switch is enabled (labeled as 3 on section C of Figure 4.4), and if it is not, the computer bypasses the loop, if it is then it proceeds as follows. Each signal is sent to its own control loop, along with the desired set point temperatures and the PID gains as input by the user (Section E of Figure 4.4). The computer program will then automatically operate the heaters as necessary to maintain the desired temperatures. This section also manages the graph (Section E of Figure 4.4) that shows the temperature of each of the three components over a period of approximately 5 minutes (or longer if set by the user). This allows the user to see if the components have reached the set point temperatures or to check to be sure there have been no spikes in temperature.

The sixth section of the program (Section F of Figure 4.5b) handles the mass flow meters and the pressure transducers. The upper section inputs the desired mass flow rate for both hydrogen and oxygen/air. It then adjusts the oxygen mass flow meter as necessary in case air is being fed. Then it changes the desired input value to the proper corresponding voltage, which is then sent to the mass flow controller causing it to allow the desired flow. The signal from the

pressure transducers is received just below the mass flow controllers and it simply reads the voltage and converts it to the proper pressure in psig and displays it to the user-interface.

The final section of the program (Section G of Figure 4.5b) only activates once the stop button has been pressed. The program is constantly sending all of the performance variables (pressure, temperature, mass flow rates) to a single file every minute during the run. When the stop button is hit, the program allows the user to name the file appropriately and then allows the user to examine the performance for any problems during a run. This is extremely useful in cases where the system is operating without supervision as it allows the user to see if there are any discrepancies during the experiment, which could lead to erroneous results.

CHAPTER V

RESULTS AND DISCUSSION

The first objective of this work has been to design, construct, and operate a PEM/DM fuel cell system. This apparatus improves on the original PEM system that was developed at the University of New Hampshire [40] as it allows both hydrogen and methanol feeds. The new apparatus is also fully automated such that it is capable of performing lifetime MEA evaluation, which requires long hours of continuous, unsupervised operation.

The work done under this study includes the building and data validation for this DMFC apparatus, the optimization of operating cell conditions for methanol feed with particular reference to gas diffusion layers (GDLs), the development of an anode GDL incorporating a microporous layer (MPL) and the study of the effect of ex-situ GDL parameters on DMFC performance. The chapter is presented in four sections focusing on the various aspects of this work. The work presented under the last two sections has been funded by Ballard Material Products (Lowell, MA) to develop a competitive GDL material specifically for use in a DMFC. They supplied us with their three best performing PEM GDLs (labeled randomly as F through H in Table 5.2), which are studied and then modified for DMFC applications. Their performance is compared against

well known commercially available GDLs under similar experimental conditions.

The first section pertains to cell performance using both hydrogen and methanol, individually as the fuel to validate our results against published work. This work is done to ensure that the apparatus is fully functional and that the results are comparable to literature values. The second section discusses the effects of various operating parameters, such as cell temperature, methanol concentration and flow rate, etc on DMFC performance using various commercially available GDLs. The third section deals with the development of a modified anode GDL, focusing on the incorporation of a microporous layer on the anode, for the specific use in a DMFC. The final section discusses the work done for the development of a DMFC MEA using a combination of GDLs. The anode consists of the modified GDL (as described in Section 5.3) and the cathode includes various unmodified GDLs. It is believed that a combination of these varied GDLs will provide improved performance in DMFC applications. The optimized MEA is then benchmarked against similar MEAs made with various commercial GDLs.

In this study, the cell potential (V) is plotted on the primary y-axis against the current density (A/cm^2) on the x-axis. In addition, the power density (W/cm^2) is plotted on the secondary y-axis against the current density. Catalysts used in the experiments are purchased from Alfa Aesar: 20% Pt-C black for the cathode electrode and 50:50 Pt-Ru for the anode electrode, unless otherwise specified. A 15-wt % Nafion® solution purchased from Ion Power Inc. is used for the Nafion® loading on the GDL as described in Section 2.2.3.

The catalyst is hand-painted onto the GDLs and then sandwiched, with Nafion® 117 membrane in between, to form an MEA for all experiments through section 5.2.4. From section 5.2.5 onward, a commercially available catalyst coated membrane (CCM), consisting of 4 mg Pt-Ru on the anode side and 4 mg Pt on the cathode side of a Nafion® 117 membrane, is used in all experiments. This change is necessitated by the inconsistent loadings that are obtained through the hand painting method. The methanol is fed to the cell at room temperature when entering the heated cell, which may lead to some temperature variations within the cell. These variations may slightly affect the cell performance. The general operating parameters, as listed in Table 5.1, are used for all experiments, unless otherwise specified.

Table 5.1 – General Experimental Parameters for this Study

Operating Parameter	Material Used
Membrane	Nafion® 117
Catalyst Anode	4 mg/cm^2 Pt-Ru/C (50:50)
Catalyst Cathode	0.4 mg/cm^2 20% Pt/C
MeOH Flow Rate	3 mL/min
MeOH Concentration	4 Molar
Air Flow Rate	2x Stoich (Appendix C)

5.1 – Calibration and Validation of PEMFC/DMFC System

Determining that the PEMFC/DMFC system is operating properly is a challenging task. The system is first checked for leaks and all of the instruments are calibrated. The performance curves generated for the system are then compared against performance curves under similar conditions that are reported in literature, to ensure that our system is working properly. Since this is the

second PEMFC system assembled at the University of New Hampshire, the performance data of the GDL samples tested on the new apparatus are compared against data obtained for similar GDLs tested earlier [40] on the first apparatus. Multiple polarization curves are obtained, using either hydrogen or methanol as fuel, to validate the results generated from this apparatus. Error bars have been added to these validation plots to indicate the approximate error associated with this testing (~7-11%). During the course of this study, nine different commercially available GDLs have been used. They are available under well-known trade names; such as Ballard, E-tek, Lydall, SGL, Techniweave and Toray, but for proprietary reasons they are randomly labeled A through I. Table 5.2 provides the basic characteristics of each of these GDL materials including: material type (paper or fabric), typical thickness (μm) and basis weight (g/cm^2).

Table 5.2 – GDLs Evaluated in this Study

GDL Nomenclature	Material	Thickness (μm) / Basis Weight (g/m^2)
GDL A	Paper	385 / 55.1
GDL B	Fabric	390 / 210
GDL C	Paper	330 / 123
GDL D	Fabric	250 / 125
GDL E	Fabric	260 / 200
GDL F (Ballard)	Paper	158 / 62
GDL G (Ballard)	Paper	238 / 88
GDL H (Ballard)	Paper	196 / 60
GDL I	Paper	315 / 140

5.1.1 – Performance Validation of PEMFC/DMFC System using Hydrogen Fuel

The first set of experimental data is taken using fabric GDL B with a 1.5-mg/cm^2 Pt loading on both electrodes (Figure 5.1). Experiments are also conducted using paper GDL F (supplied by Ballard) with a 1.82-mg/cm^2 Pt loading hand painted on both electrodes. GDL B is selected, as it is a known brand and previously well studied fabric, while GDL F is used to establish a comparative baseline for the Ballard material. The power density outputs from these two GDLs are compared with results obtained earlier [40] using fabric GDL B with 2.0-mg/cm^2 catalyst loading (0.4- mg/cm^2 Pt loading) as shown in Figure 5.1. The cell performance using GDL B is found to be about 10% lower than reported previously.

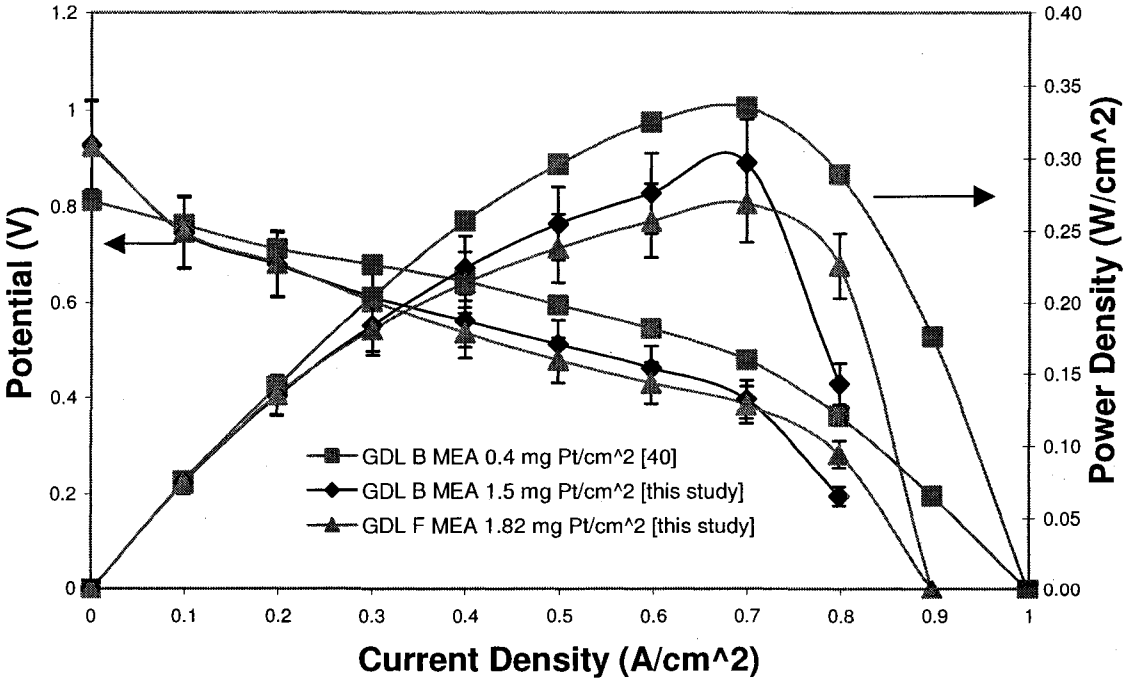

Figure 5.1 - Cell Performance Curves for Validation of PEMFC/DMFC System at High Temperature using Hydrogen as Fuel
75°C, 3x Air Stoich, 2x H2 Stoich, Ambient Pressure

The published data are reported at 60°C, while both tests in this study are performed at 75°C. GDL F (paper), with a 1.82-mg/cm^2 Pt loading, performs 30% below the published data for GDL B, 0.4-mg/cm^2 Pt loading. These results are also 12% below the results from the PEMFC/DMFC apparatus using GDL B, 1.5-mg/cm^2 Pt loading.

The higher catalyst loading may limit the mass transfer in the high current density range and probably causes some reduced performance. This decrease in performance may be offset by any increase in performance expected due to the increased kinetics at the higher temperature. The higher catalyst loading is due to an error in calculation; however, the results are still presented to show that the results are similar to what are seen previously. These results show that the apparatus built for this study provides reasonable data for both fabric and paper GDLs using hydrogen as a fuel, even with a variety of catalyst loadings, temperature and GDL materials.

Continuing our work on the validation of test performance for the new system, paper GDLs A and F are each used as both the anode and cathode in separate experiments and compared with previously reported results. GDL A is selected to compare its results with the previously reported results, while GDL F is used for establishing a comparative base for the Ballard supplied GDL. The results are compared with published data [40] obtained using GDL A, as shown in Figure 5.2. The MEA used in the published work has a catalyst loading of 0.4 mg/cm^2 Pt on each electrode and reaches a maximum power output of 0.255 W/cm^2. Our test MEA, also using GDL A, has a Pt loading of 0.32 mg/cm^2 on each

electrode and reaches a maximum power output of 0.228 W/cm^2, a 10% difference. There is also a sharp decline in the performance of our MEA at 0.6 A/cm^2 indicative of mass transport loss. This may be partly due to the 20% lower catalyst loading, which limits the ability of the catalyst to break down the oxygen and can lead to mass transport losses.

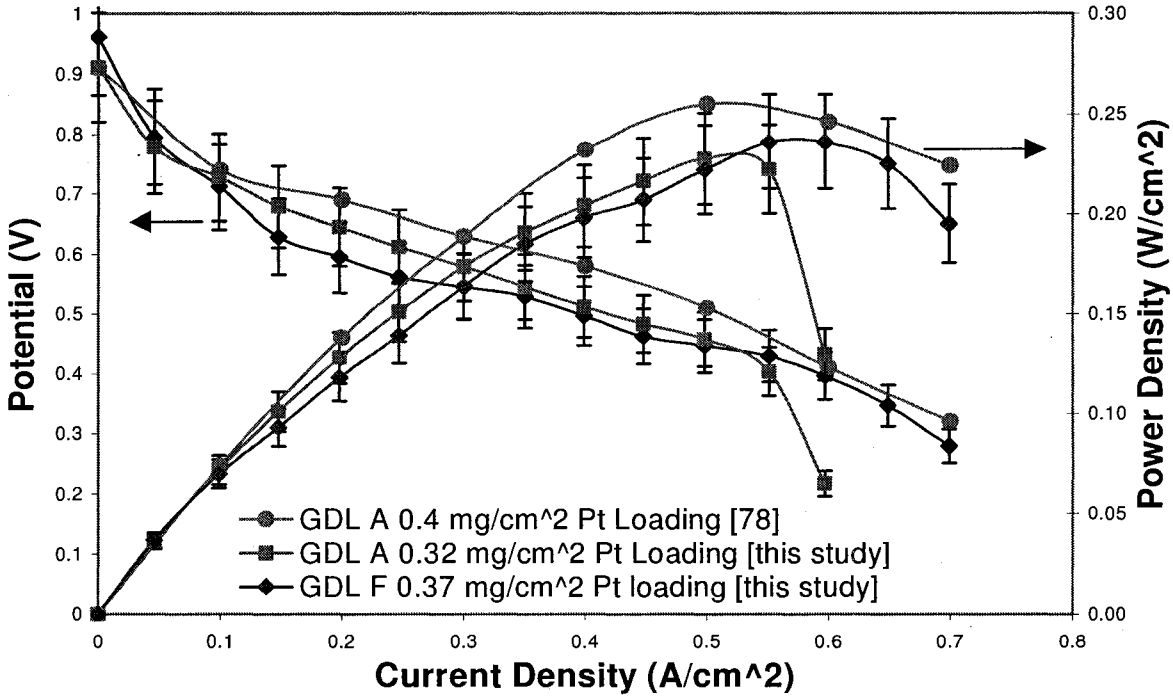

Figure 5.2 - Cell Performance Curves for Validation of PEMFC/DMFC System at Low Temperature using Hydrogen as Fuel
65°C, 3x Air Stoich, 2x H2 Stoich, Ambient Pressure

GDL F, at a 0.37 mg/cm^2 Pt loading, reached a maximum power output of 0.236 W/cm^2, a 7% increase over GDL A (from this study). There is also a noticeable decline in performance at 0.7 A/cm^2, similar to the drop at 0.6 A/cm^2 seen with GDL A. This performance is much closer to the values reported in the literature and supports the belief that the lower catalyst loading is the reason for the decreased performance of GDL A. Figure 5.2 also shows that GDL A and

GDL F are comparable papers, whose performances are similar for hydrogen as a fuel. This also satisfactorily validates the performance of our newly built PEMFC/DMFC system.

5.1.2 – Performance Validation of PEMFC/DMFC System using Methanol Fuel

The validation data for the system are taken at a cell temperature of 70°C, 40 psi-air backpressure, and at 2 mL/min flow rate of 2M MeOH solution. GDL A (paper) is used for both the anode and cathode GDLs with Nafion® 115 as an electrolyte. The anode has a Pt-Ru loading of 1.63 mg/cm^2 and the cathode has a Pt loading of 0.4 mg/cm^2. The experimental data are compared against published results [83] as shown in Figure 5.3. Our results show a maximum power density of 0.054 W/cm^2 at 0.15 A/cm^2. The results from the published source, using GDL A, show maximum power densities of 0.065 and 0.044 W/cm^2 at 75°C and 60°C, respectively. Our experiments are conducted at a temperature of 70°C.

It can be seen that our results are within 10% of the published data [83] at the interpolated temperature of 70°C. Our results show a decline in performance at 0.15 A/cm2, similar to what is seen in the published results at 60°C, but the cell achieves a higher maximum power density. The Pt-Ru loading is most likely lower on our anode GDL; typically the anode has a loading of approximately 4 mg/cm^2 Pt-Ru as reported for the commercially available CCMs. This is believed to be the reason for the decrease in power output compared to the results of the published data at 75°C, as well as the sharp decrease in performance at 0.15

A/cm^2 that does not occur until 0.25A/cm^2 in the published work. These results are sufficient to validate the performance of our DMFC system.

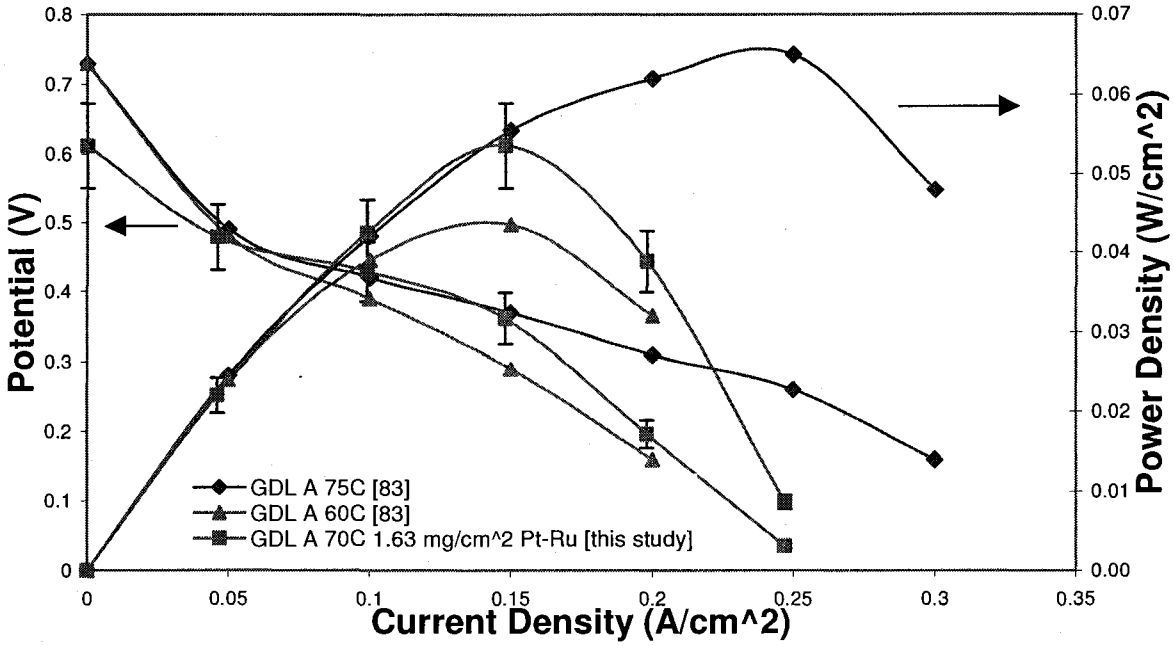

Figure 5.3 - Cell Performance Curves for Validation of PEMFC/DMFC System using Methanol as Fuel
2 mL/min 2M MeOH, Nafion® 117, 0 psig

5.2 – Effect of Operating Parameters on DFMC Performance

This investigation is about the development and evaluation of GDLs for a methanol operated fuel cell system. All of the subsequent experiments have been conducted using the previously described apparatus as a DMFC system. This section focuses on the effect of different experimental operating parameters on DMFC performance. These data provide us with an optimized set of operating parameters, which may be held constant in subsequent work. It is important to note that these optimized variables are specific to the type of membranes and GDLs used, the catalyst loading, the flow field design, as well as other operating parameters and cell characteristics.

5.2.1 - Temperature Effects on DMFC performance

This work is performed using GDL B (fabric) because it is known to perform well and is commercially available. Dry air with a backpressure of 40 psig and a 2-mL/min-flow rate of 4M MeOH solution at ambient temperature is fed to the cell. The anode and cathode catalyst loadings are held constant at 0.33-mg/cm^2 Pt-Ru and 0.4-mg/cm^2 Pt, respectively. The cell temperature is successively increased from 40°C to 85°C, as shown in Figure 5.4.

The data show that the power output first increases with an increase in temperature and eventually reaches a maximum. Any further increase in temperature leads to a decrease in performance and power generation. There are several reasons for this behavior. The relatively slow anode kinetics increase rapidly as temperatures increase, as governed by the Arrhenius equation, and thus the performance is improved. The results show that from 40°C to 60°C the MeOH reacts very slowly, limiting the power density to 0.038 W/cm^2. As the temperature further increases from 60°C to 80°C the reaction kinetics increase rapidly and performance increases until reaching a maximum power output of 0.060 W/cm^2.

The electro-osmotic drag is the number of water molecules that pass through the membrane along with the protons and has been shown to increase with temperature [82, 84]. This leads to an increase in MeOH crossover through the membrane, as the water molecules tend to pull methanol with them as they pass through the membrane [84]. The results show that beyond 80°C the power density drops 33% from 0.060 W/cm^2 to 0.040 W/cm^2. At temperatures above

80°C, it appears that the benefit of increased anode kinetics is offset by the increase in methanol crossover due to electro-osmotic drag, resulting in poor performance. This is seen from the very similar performance curves of the cell at both 70°C and 85°C, which almost lie perfectly on top of one another.

Although the optimum temperature from this study is found to be 80°C, concerns about membrane degradation at such a temperature outweigh the slight benefit in performance. For this reason all further experiments are carried out at 75°C, to maximize the increased anode kinetics without the risk of irreversibly damaging the membrane.

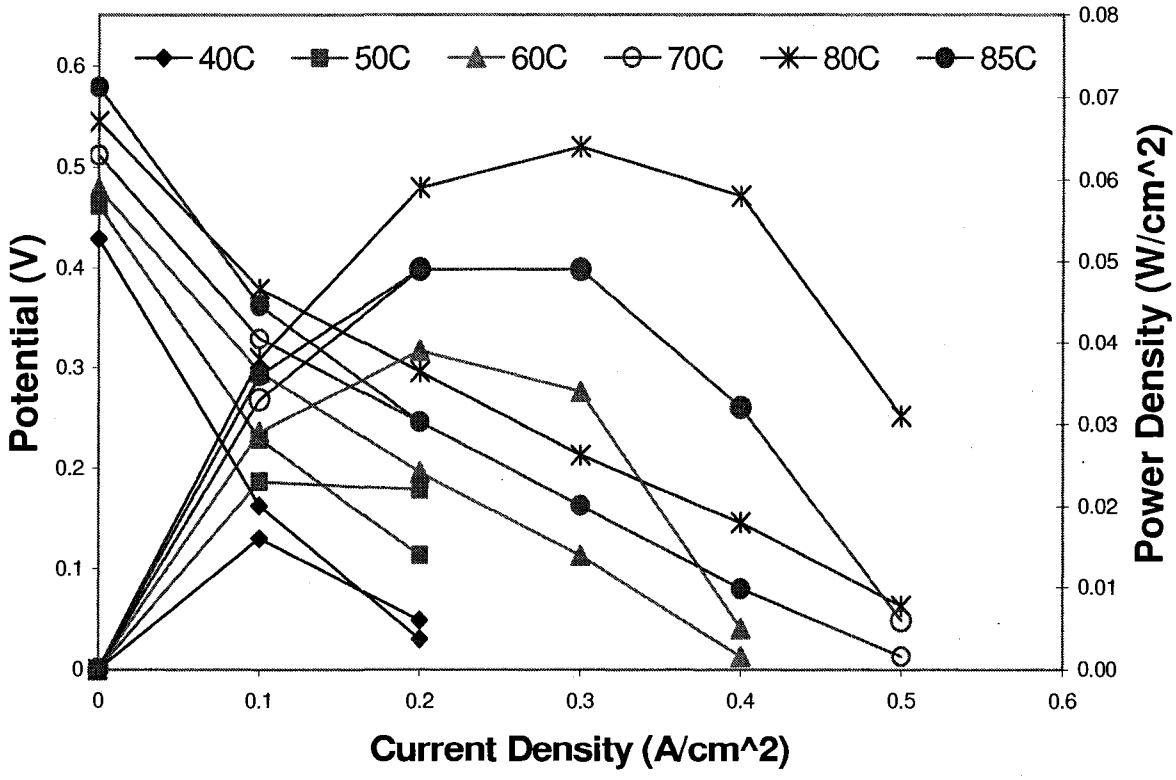

Figure 5.4 – Temperature Effects on DMFC Performance
GDL B, 40 psi, 2 mL/min 4M MeOH, 0.33mg/cm^2 Pt-Ru anode, 0.4mg/cm^2 Pt cathode

5.2.2 - Effect of Anode Catalyst Loading on Cell Performance using Fabric GDL B

We examine the effect of catalyst loading on fabric GDL B because it is commercially available and known to perform well, as explained in Section 5.2.1. These data are taken at a temperature of 75°C, 40 psi air backpressure, using a 4 molar MeOH solution at a feed rate of 2 mL/min. All of the MEAs are prepared using the same fabric GDL B, with metal loadings ranging from 0.519-mg/cm^2 to 3.8 mg/cm^2 Pt-Ru, hand-painted on the anode electrode. Similarly a constant metal loading of 0.4-mg/cm^2 Pt is hand-painted onto the cathode electrode. The Nafion® loading, as described in Section 2.2.1, is held constant around 2.5-mg/cm^2 for all of the MEAs. The results, presented in Figure 5.5, show that the 2.42-mg/cm^2 Pt-Ru loading is the optimum, achieving a maximum power density of about 0.100 W/cm^2. The cell performance with 0.5-mg/cm2 and 3.8-mg/cm2 catalyst loadings is very similar providing power outputs of 0.063 and 0.061 mW/cm^2, respectively.

The 1.45-mg/cm^2 performance is very poor, reaching only a maximum power density of 0.044 mW/cm^2, possibly due to a defective MEA. The poor results for both the 0.5-mg/cm^2 and 3.8-mg/cm^2 Pt loadings are as expected for several reasons. At lower Pt-Ru loadings, there are less catalyst sites, which lower the already slow anode kinetics and give a poor cell performance. At higher Pt-Ru loadings there can be GDL pore blockage, which prevents adequate liquid/gas diffusion to take place, leading to poor mass transport and

thus reducing the cell performance. It can be concluded that the optimum catalyst loading on GDL B (fabric), is about 2.5-mg/cm^2.

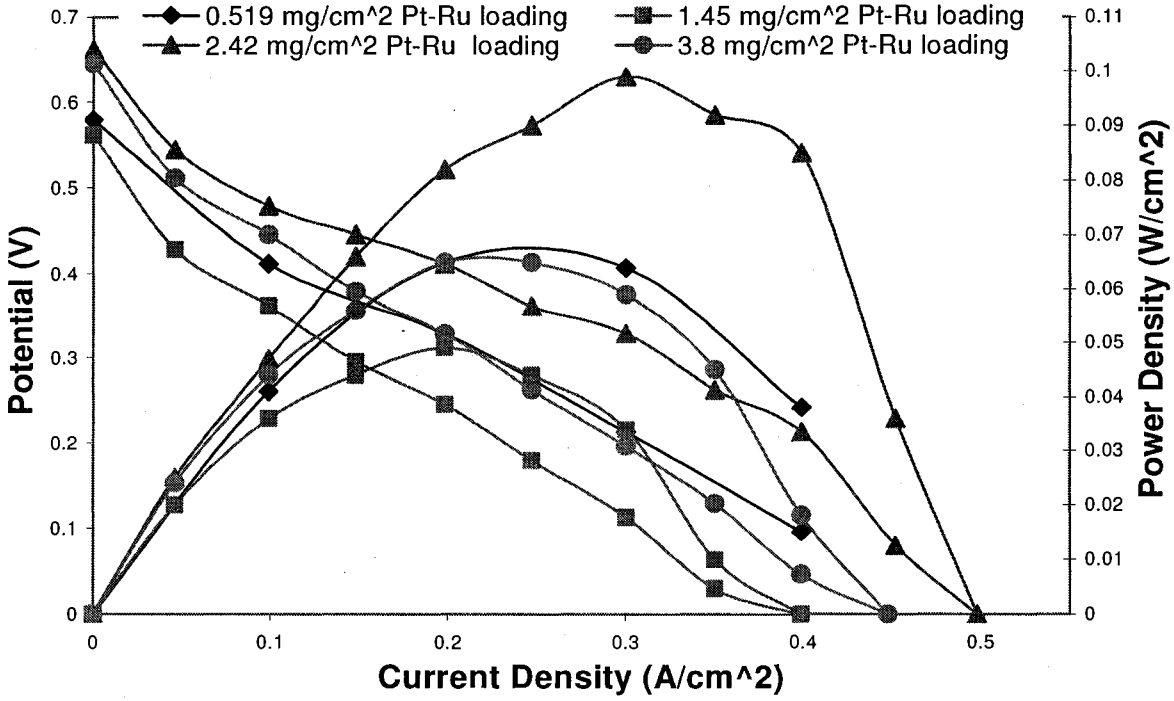

Figure 5.5 – Effect of Anode Metal Catalyst Loading on GDL B (fabric)
75°C, 40 psi, 2 mL/min 4M MeOH, Cathode: 0.4 mg/cm^2

5.2.3 - Effect of Anode Catalyst Loading on Cell Performance using Paper GDL C

It is important to also examine the effect of catalyst loading on cell performance using paper GDLs. GDL C is used for this purpose because it is commercially available. All MEAs are prepared using GDL C (paper) with target anode catalyst loadings ranging from 0.5 to 2.5-mg/cm^2 Pt with cathode catalyst loading held constant at 0.4-mg/cm^2. The results, presented in Figure 5.6, show that this GDL gives poor cell performance with methanol under the catalyst loadings tested. There does seem to be a trend, as the catalyst loading

increases cell performance increases, with maximum power outputs of 0.022, 0.029 and 0.039 W/cm^2 for loadings of 0.6, 1.85 and 2.1-mg/cm^2, respectively. Comparing these results to the results obtained with GDL B (fabric), it is clear that GDL C has excessive losses in both the ohmic and mass transport regions, as described in Section 3.2. This indicates that GDL C does not adequately manage the water formation in the cell (mass transport) and provides high resistance to electrical current (ohmic) to be useful in DMFC applications.

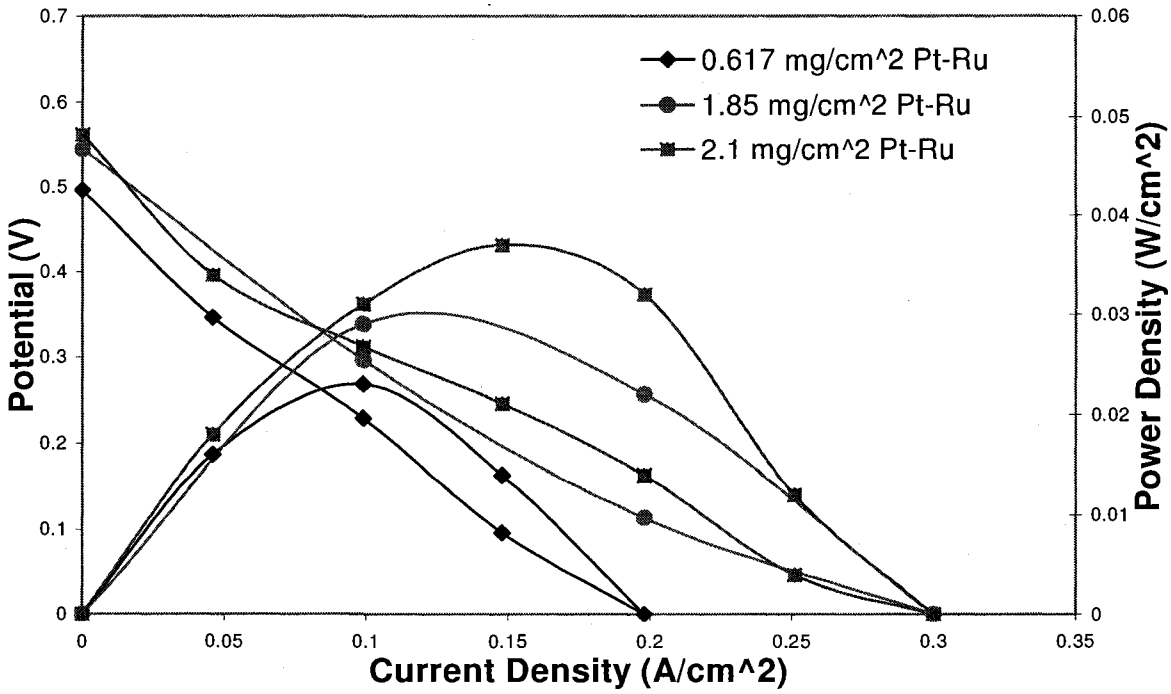

Figure 5.6 – Effect of Anode Metal Catalyst Loading on GDL C (paper)
75°C, 40 psi, 2 mL/min 4M MeOH, Cathode: 0.4 mg/cm^2 Pt

5.2.4 - Effect of Catalyst Loading on Cell Performance using Various GDLs

There are many different types of GDLs that are currently being used for DMFCs. This section compares three commercially available GDLs, two fabrics and one paper, under similar catalyst loadings. This evaluation is conducted at a

temperature of 75°C, 40-psi air backpressure, using a feed rate of 2 mL/min 4M MeOH solution, with Nafion® 117 as the membrane. Figure 5.7a compares the cell performance curves for GDL B (fabric), GDL C (paper) and GDL D (fabric) with anode catalyst loadings of approximately 0.5-mg/cm^2 Pt-Ru with cathode catalyst loadings held constant at 0.4-mg/cm^2 Pt. The results show that GDL D (fabric) gives the best performance, yielding a power density of 0.082 W/cm^2 at 0.4 A/cm^2. GDL B (fabric) gives a maximum power density of 0.061 W/cm^2 at 0.25 A/cm^2, a 25% decrease from GDL D, while GDL C (paper) provides a maximum power density of 0.02 W/cm^2 at 0.1 A/cm^2, one third of the performance of GDL B and one fourth that of GDL D. GDL D also shows superior performance in the high current density range (>0.3 A/cm^2) indicating superior mass transport and improved electrical conductivity.

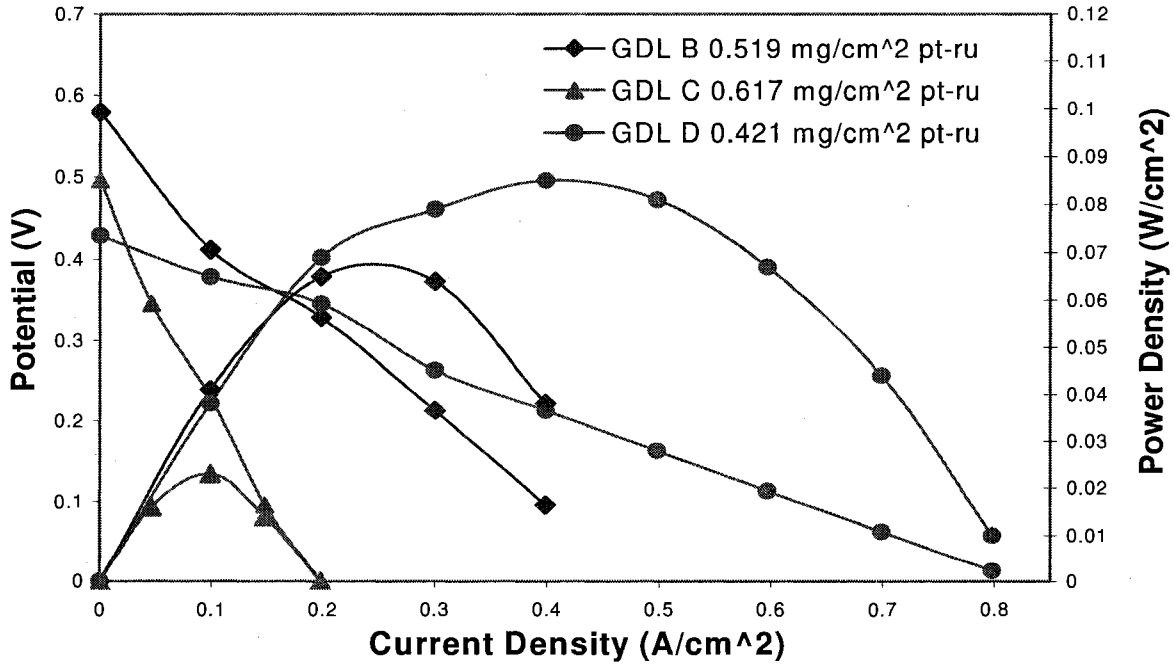

Figure 5.7a – Cell Performance Comparison with Various GDLs with Low Anode Metal Catalyst Loadings

75°C, 40 psi, 2 mL/min 4M MeOH, Cathode: 0.4 mg/cm^2 Pt

Continuing with our evaluation of three different commercial GDLs under similar catalyst loadings, Figure 5.7b compares the cell performance curves for GDL B (fabric), GDL C (paper) and GDL D (fabric) with anode catalyst loadings of approximately 1.5-mg/cm^2. The results show that GDL B and GDL D both give a maximum power density of about 0.049 W/cm^2, while the GDL C gives a maximum power density of about half of that at 0.029 W/cm^2. Although this is an improvement from the 0.5 mg/cm^2 Pt-Ru catalyst loadings, GDL C (paper) is still far behind both GDLs B and D (fabrics). It is important to note that GDL B, although reaching roughly the same maximum power density as GDL D, continues to perform well up to current densities of 0.3 A/cm^2, while the performance of GDL D collapses due to mass transport losses at about 0.2 A/cm^2. From these results we can conclude that GDLs B and D have rather comparable DMFC performance at this particular catalyst loading. At lower catalyst loadings (0.5 mg/cm^2) GDL D seems to outperform GDL B with the reverse true at higher catalyst loadings (1.5 mg/cm^2).

Although the optimum catalyst loading is found to be 2.5 mg/cm^2 Pt-Ru, as shown in Section 5.2.2, limited supply of GDLs and catalyst did not allow for comparison between the three GDLs at this loading. At both of these lower catalyst loadings, GDLs B and D have approximately the same maximum power density and GDL C performs well below that level. We can conclude that this performance trend will be similar under the optimum catalyst loading of 2.5 mg/cm^2. Since we are only looking for the comparative base and not optimum performance, the additional tests are not essential for this study.

Reproducing the same catalyst loading for each sample is very challenging task. Although the optimum value is found to be approximately 2.5 mg/cm^2, it is difficult to get loadings within even 15% of this target consistently. For this reason, all subsequent experiments use catalyst-coated membranes (CCMs), which are commercially available and are expected to carry more uniform catalyst loadings. The reported loadings on the anode and cathode sides of a Nafion® 117 membrane are 4 mg/cm^2 Pt-Ru and 4 mg/cm^2 Pt, respectively.

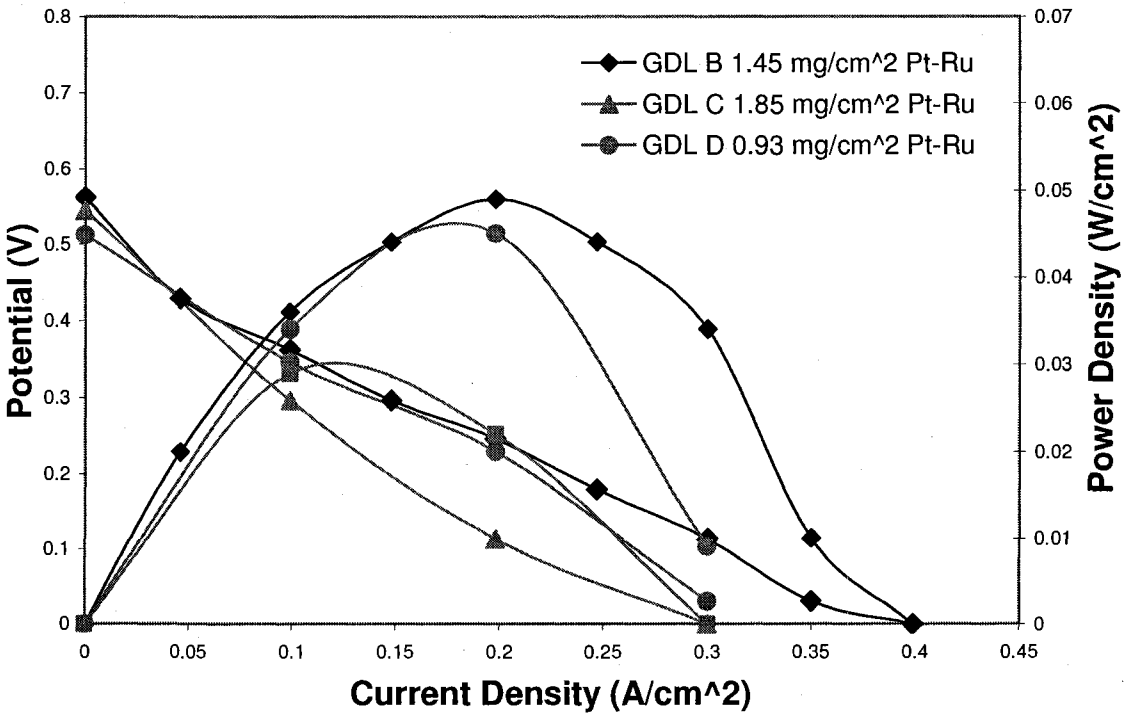

Figure 5.7b – Cell Performance Comparison with Various GDLs with Medium Anode Metal Catalyst Loadings

75°C, 40 psi, 2 mL/min 4M MeOH, Cathode: 0.4 mg/cm^2 Pt

5.2.5 - Effect of Methanol Concentration on DMFC Performance

A commercially available MEA [88], consisting of the previously mentioned CCM and GDL E (fabric) on both the anode and cathode sides, is used in this

evaluation. These data are taken at a cell temperature of 75°C, with dry air at 40-psi backpressure and a feed rate of 2 mL/min of varying molar concentrations of MeOH solution. The MEA has a catalyst loading of 4 mg/cm^2 Pt-Ru on the anode electrode and 4 mg/cm^2 Pt on the cathode electrode of the Nafion® N117 membrane. The results, presented in Figure 5.8, show that the optimum methanol concentration is between 2- 4 molar (6-12 wt%). At 1 molar (3 wt%) the power density reaches a maximum of 0.085 W/cm^2. At 2 molar (6 wt%) it attains a maximum of 0.119 mW/cm^2, a 29% increase in performance. At 4 molar (12 wt%) the cell reaches a maximum power density of 0.121W/cm^2, which is very similar to the 2 molar performance. However, the cell maintains this performance up to a current density of 0.4 A/cm^2 at 4 molar, whereas for 2 molar the maximum power output occurs at 0.3 A/cm^2. At 6 molar (20 wt%) and 8 molar (27.5 wt%) the power densities reach a maximum of 0.079 and 0.059 W/cm^2, respectively, showing a 33% and 50% drop from the maximum of 0.121 W/cm^2 at 4 molar concentration.

It is generally accepted that the optimum concentration of MeOH is somewhere in the range of 1-2 molar [11,85] because of increased methanol crossover with higher concentrations, so these results are somewhat surprising. The reason that the optimum methanol concentration obtained in this system is higher (nearly double) than the commonly reported values may be due to the relatively high cathode pressure of 40 psi used in this study. This high-pressure differential between the cathode and anode helps to limit the electro-osmotic drag and thus the methanol crossover, as discussed in Section 5.2.1. This

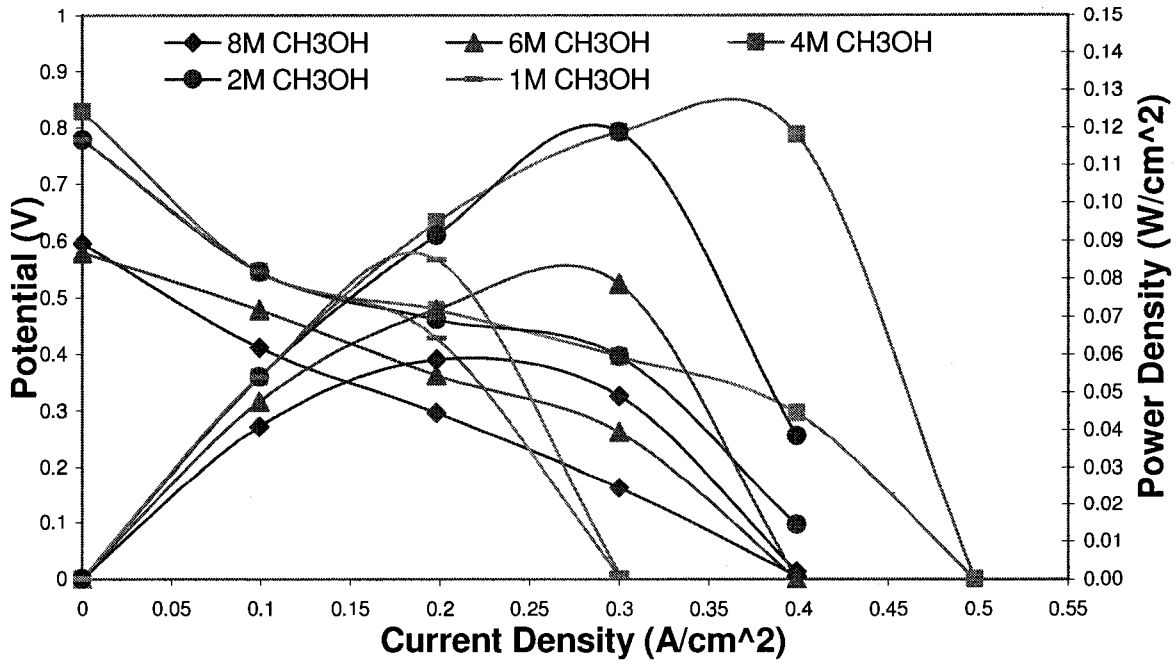

Figure 5.8 – Effect of MeOH Solution Concentration on DMFC Performance

75°C, 40 psi, 2 mL/min MeOH, Anode: 4mg/cm^2 Pt-Ru, Cathode: 0.4 mg/cm^2 Pt, GDL E

allows us to operate the cell with more concentrated methanol solutions without losing much performance due to crossover effects.

5.2.6 - Effect of Methanol Flow Rate on DMFC Performance

The flow rate of methanol can also have a large impact on the performance of a DMFC. If the flow rate is too high then the methanol crossover will increase and if it is too low then there will not be enough methanol present at the catalyst sites to produce energy, resulting in poor performance. The optimum flow rate has been shown to be related to the methanol concentration being used [86], which indicates that this analysis is only relevant to these specific operating conditions.

The data for this evaluation are taken at a cell temperature of 75°C, using 40 psi-air backpressure and with varying flow rates of 4M MeOH solution. The MEA used in these experiments consists of a commercial Nafion® N117 membrane (CCM) coated with 4 mg/cm^2 Pt on the cathode side and 4 mg/cm^2 Pt-Ru on the anode side. GDL A (paper) is used as the GDL on both the anode and cathode sides, with the CCM between them.

The methanol flow rates range from 1.5 mL/min (syringe setting 20) to 7.5 mL/min (syringe setting 100) at 1.5 mL/min increments. The results, presented in Figure 5.9, show that the optimum MeOH flow rate for the DMFC system is about 3 mL/min (syringe setting 40). At the 1.5 mL/min flow rate, the cell achieved a maximum power density of 0.075 W/cm^2. At the 3 mL/min flow rate the cell reached a maximum of 0.095 W/cm^2, a 21% increase. As the flow rate is increased further the maximum power density decreased to 0.091 (-4%), 0.081 (-14%) and 0.056 (-41%) W/cm^2 for flow rates of 4.5, 6 and 7.5 mL/min, respectively. From these results it can be concluded that at low flow rates (1.5 mL/min and lower) there is not enough methanol present at the anode to reach the maximum cell performance. On the other hand, above the optimum methanol flow rate of 3 mL/min, the cell performance begins to drop possibly due to increased methanol crossover or flooding. For all subsequent experiments the flow rate is held at 3 mL/min unless otherwise specified.

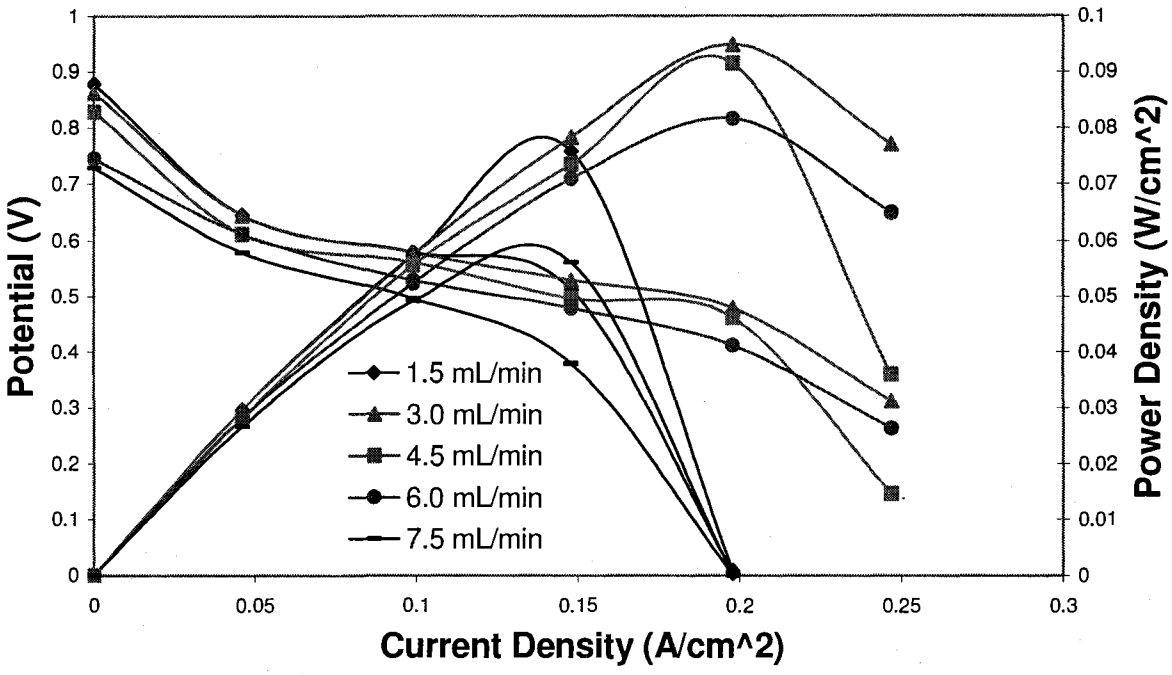

Figure 5.9 – Effect of MeOH Solution Flow Rate on DMFC Performance
75°C, 40 psi, 4M MeOH, Anode: 4mg/cm^2 Pt-Ru, Cathode: 0.4 mg/cm^2 Pt, GDL A

5.3 – Development of an Anode GDL Specifically for DMFCs

The DMFC shows promise in its use in the portable electronic industry. The high energy density of approximately 6000 Wh/kg for methanol compared to the approximately 200 Wh/kg for lithium ion batteries make it the ideal choice for electricity generation as the power requirements for portable electronics increase. Additional benefits include the elimination of down time due to recharging, increased run time, and decreased weight. There are also many environmental benefits, such as reduced pollutant emissions and wastes. As we have seen in Chapter 2, there has been significant progress made in membrane and catalyst technology in the last few years, but little work has been done on the GDL development.

The functions of the cathode GDL, removing excess water and allowing oxygen to reach the catalyst sites, are similar as in the PEMFC. These have been studied carefully over the past 5 years and much progress has been made. The demands on the anode GDL for a DMFC, however, are very different from that of the PEMFC. In the DMFC the anode GDL must transport methanol to the catalyst sites and water to the membrane. It must also help to remove excess water, to prevent flooding, especially with solutions consisting of lower concentrations of methanol. It must also be able to remove waste gases, CO and CO_2 that are formed during the breakdown of methanol.

The focus of this part of the study is an attempt to improve the anode GDL performance for the DMFC. As we previously discussed in Chapter 2, a GDL is comprised of a base substrate, which is typically either carbon fabric or carbon paper. This base paper may be hydrophobic or hydrophilic, depending on the application. A mixture of carbon particles and aqueous PTFE (Teflon®) solution, known as a microporous layer or MPL, may be coated on this base substrate to improve performance.

The PTFE content in the substrate itself should help with the rejection of excess water, due to increased hydrophobicity, which helps to prevent flooding. The MPL weight, or loading, changes the thickness and the pore size distribution of the GDL, which helps in the removal of CO/CO_2 gas and prevents flooding. The PTFE content in the MPL helps manage the water content near the membrane surface in order to keep it fully hydrated.

This part of our study is focused towards the modification of a GDL, which will improve the DMFC performance. This is done by first determining how each of the previously discussed parameters, namely PTFE content and microporous layers, impact GDL performance in the DMFC. Once the impact is understood, it will be possible to optimize the characteristics of the GDL, thereby improving the cell performance.

5.3.1 – Development of an Anode GDL

As has been previously discussed, GDLs play an intricate role in cell performance by controlling gas and liquid transport through and out of the cell. As an obvious extension of our work, the following investigation is in the area of development of a new GDL material for the anode. This work has been sponsored by Ballard Material Products (Lowell, MA). A test matrix for the development of this new GDL has been presented in Table 5.3, which focuses on the three main areas of anode GDL improvement previously discussed. A 3X3 design matrix is developed to analyze the effect of 1) substrate PTFE content, 2) microporous sublayer weight and 3) MPL PTFE content. The PTFE contents of the substrate and sublayer are examined in low (0-10%), medium (10-25%) and high (25-50%) ranges, represented by -, 0, +, respectively in Table 5.3. The sublayer weights are also set in a low (0-20g/m^2), medium (20-60 g/m^2), and high range (60-100 g/m^2), again represented by the same symbols (Table 5.3).

Table 5.3 – Design of Experiments for Anode GDL Development

Sample #	Substrate PTFE Loading Level	MPL Weight	MPL PTFE Loading Level
1	-	-	-
2	-	0	0
3	-	+	+
4	0	0	-
5	0	+	0
6	0	-	+
7	+	+	-
8	+	-	0
9	+	0	+

These samples are prepared using GDL F (paper) as the substrate material with the appropriate substrate PTFE content. The various MPLs, which are primarily composed of uniform sized graphite particles and PTFE solution, are applied to the GDL by hand using a gap adjustable knife-blade. The GDL is then dried and sintered at high temperature (~700°F) for approximately 20 minutes. The modified GDL samples are provided to us by Ballard Material Products. Each of the individual samples (1 through 9) is studied under the optimized conditions (Section 5.2) of 75°C, 3 mL/min of a 4M MeOH feed, 40 psi backpressure. A commercially available CCM, composed of 4 mg/cm^2 Pt-Ru on

the anode, 4 mg/cm^2 Pt black on the cathode side of a Nafion® 117 membrane, is used for all experiments for consistency reasons.

5.3.2 – Effect of Microporous Layer Weight on DMFC Performance

The results are grouped at constant substrate PTFE loadings to study the effect of MPL weight and PTFE loading on the cell performance. Figure 5.10a shows the performance results for samples 1 through 3, Figure 5.10b for samples 4 through 6 and Figure 5.10c for samples 7 through 9 (Table 5.3).

Figure 5.10a shows that sample 3 (high sublayer MPL weight) performs the best, providing a power output of 0.058 W/cm^2. This is followed by sample 2 (medium sublayer weight) giving a power output of 0.043 W/cm^2 and then sample 1 (low sublayer weight) with a power output of 0.032 W/cm^2. This shows that the MPL weight should be high for good performance with low substrate PTFE loadings.

Figure 5.10b shows that sample 5 (high sublayer weight) performs the best with a maximum power output of 0.068 W/cm^2. This is followed by sample 4 (medium sublayer weight) with a power output of 0.058 W/cm^2 and sample 6 (low sublayer weight) with a power output of 0.017 W/cm^2. Again the high sublayer MPL weight gives the maximum power of the three samples evaluated. Also sample 5 performs adequately with a current density of 0.35 A/cm^2, while all other samples, 1 through 4 and 6, have shown that performance starts to decline at 0.15 A/cm^2. This increase in sample 5 performance indicates a reduction in mass transport losses, possibly due to improved water management.

Figure 5.10c shows that sample 7 (high sublayer weight) performs the best with a power density of 0.078 W/cm^2. This is followed by sample 8 (low sublayer weight) with a power output of 0.039 W/cm^2 and sample 9 (medium sublayer weight) with a power output of 0.032 W/cm^2. Also sample 7, like sample 5, performs at a much higher current density (0.4 A/cm^2) than the other two samples.

It is clear from the three data sets that high sublayer MPL weight samples perform the best regardless of PTFE content. It is also seen that samples with high MPL weights do not have the sharp drop in performance associated with mass transport losses. This may be due to improvements in water management, a decrease in methanol crossover, better management of CO/CO_2, or some combination of these effects.

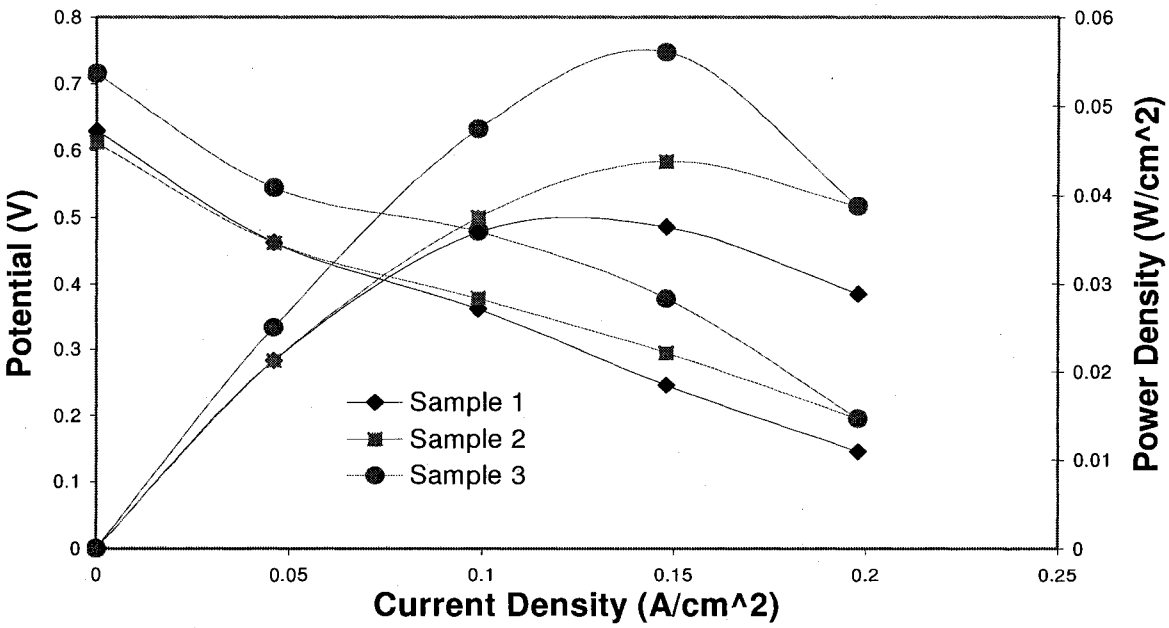

Figure 5.10a – Cell Performance Evaluation of GDLs with Low Substrate PTFE Content

75°C, 40 psi, 3 mL/min 4M MeOH, CCM

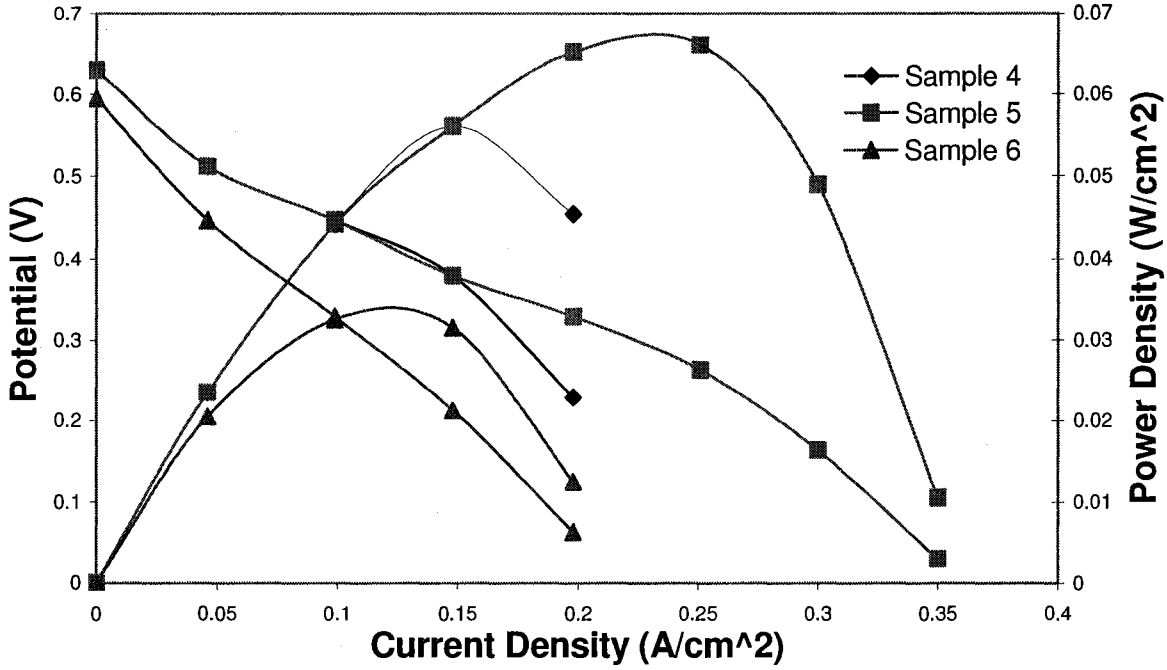

Figure 5.10b – Cell Performance Evaluation of GDLs with Medium Substrate PTFE Content

75°C, 40 psi, 3 mL/min 4M MeOH, CCM

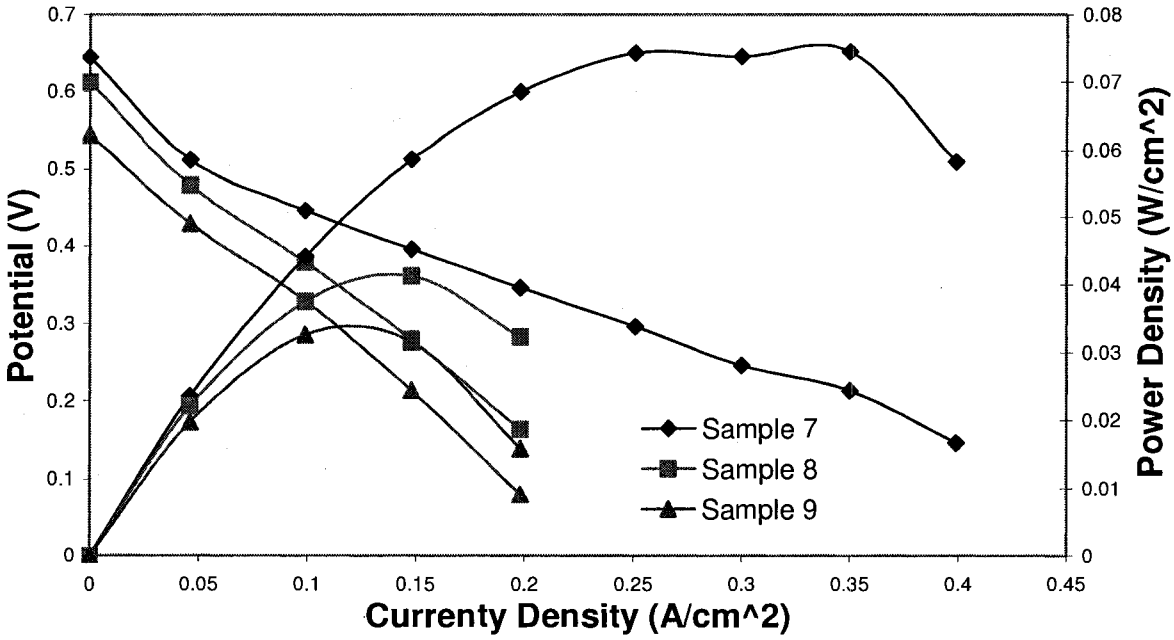

Figure 5.10c – Cell Performance Evaluation of GDLs with High Substrate PTFE Content

75°C, 40 psi, 3 mL/min 4M MeOH, CCM

5.3.3 – Effect of GDL Substrate PTFE Content on DMFC Performance

The effect of PTFE loading in the GDL substrate is examined by regrouping the results of our previous experiments at constant MPL weights. Figure 5.11a shows the performance results for samples 1, 6 and 8 (low sublayer weight), while Figure 5.11b shows performance for samples 2, 4 and 9 (medium sublayer weight) and Figure 5.11c shows performance for samples 3, 5 and 7 (high sublayer weight), as presented in Table 5.3.

It is seen from Figure 5.11a that sample 8 (high PTFE in the substrate) provides the highest power output of 0.041 W/cm^2. Sample 1 (low PTFE in the substrate) has the second best power output with 0.035 W/cm^2 and finally sample 6 (medium PTFE in the substrate) with a power output of 0.030 W/cm^2. Since there is no discernible pattern to the results, the effect of PTFE content in the GDL substrate on DMFC performance is inconclusive for low sublayer weights.

Figure 5.11b shows that sample 4 (medium PTFE in the substrate) has the highest power output of 0.058 W/cm^2. Sample 2 (low PTFE in the substrate) is next with a power output of 0.043 W/cm^2 and sample 9 (high PTFE in the substrate) achieves a power output of 0.032 W/cm^2. Since there is no clear pattern to these results, the effect of PTFE content in the substrate on DMFC performance is inconclusive for medium MPL loadings.

It is seen in Figure 5.11c that sample 7 (high PTFE in the substrate) achieves the maximum power output, 0.078 W/cm^2, followed by sample 5 (medium PTFE in the substrate) with a power output of 0.068 W/cm^2 and then

sample 3 (low PTFE in the substrate) with a power output of 0.058 W/cm^2. These results show that higher PTFE loadings in the substrate of a GDL improve performance for high MPL loadings. This may be due to an improvement in the GDL's ability to remove excess water from the anode and thus prevent flooding. It may be assumed that this influence is present for all samples, but is hidden by the effect of the sublayer weight and sublayer PTFE content.

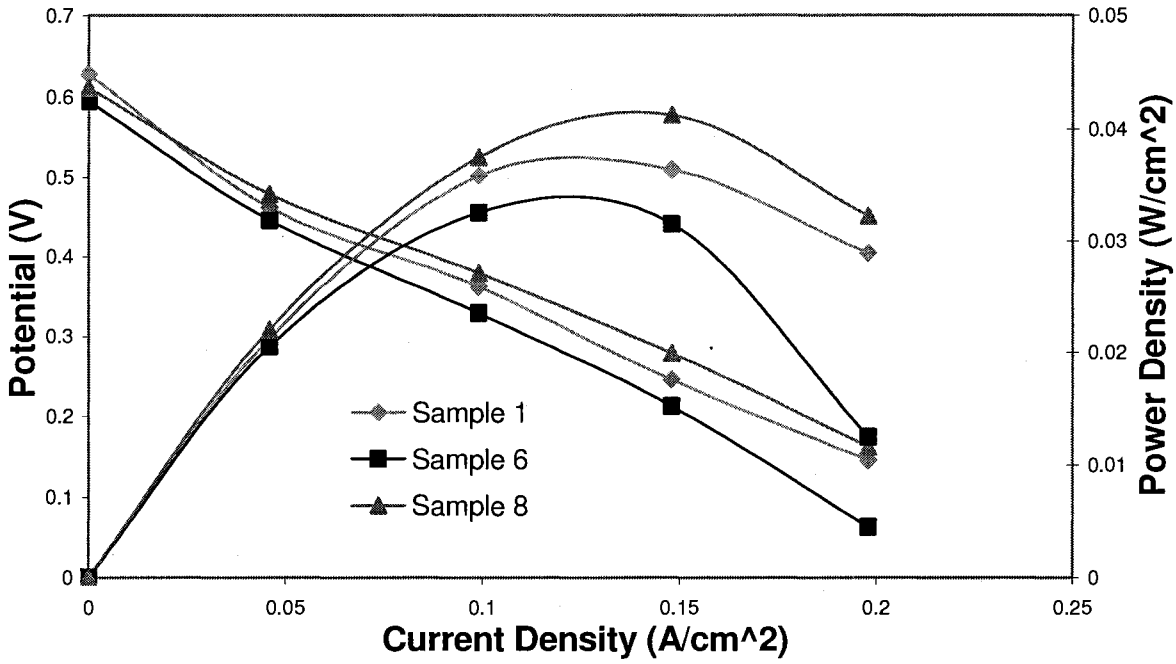

Figure 5.11a – Cell Performance Evaluation of GDLs at Constant Low Sublayer Loadings
75°C, 40 psi, 3 mL/min 4M MeOH, CCM

5.3.4 – Effect of PTFE Content in the MPL on DMFC Performance

We examine the effect of PTFE content in the MPL on cell performance by grouping the samples by MPL weight. From Figure 5.11a, it is clear that sample 8 (medium sublayer PTFE) performs the best reaching a maximum power output of 0.041 W/cm^2, followed by sample 1 (low sublayer PTFE) with a power output

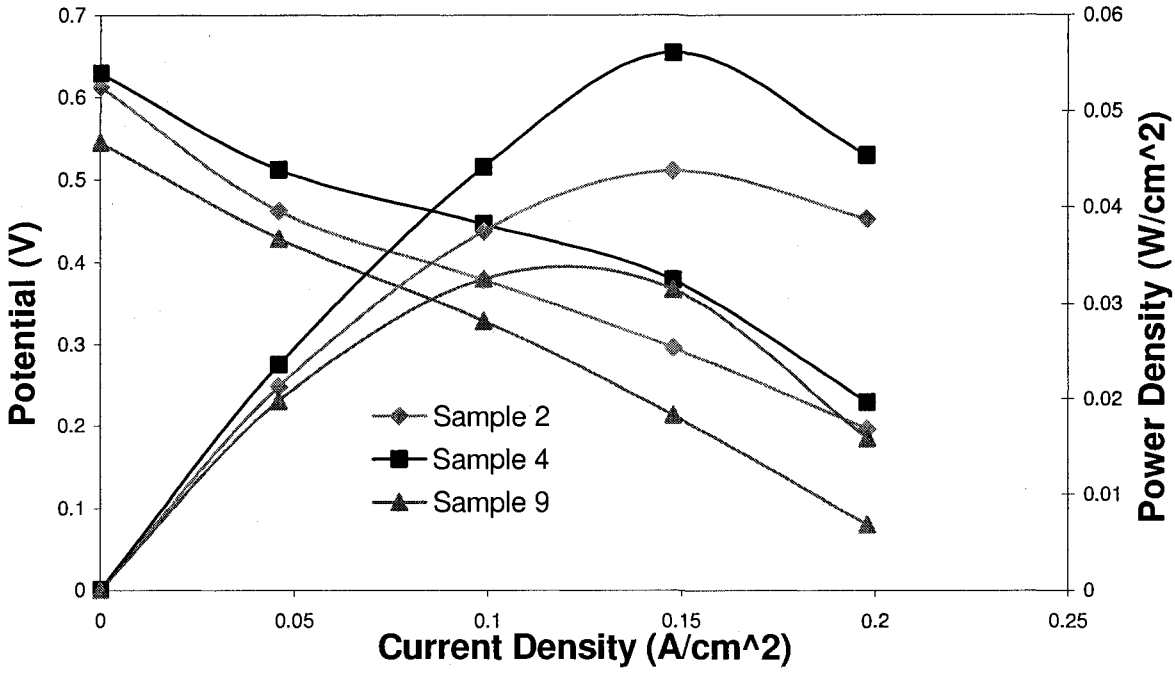

Figure 5.11b – Cell Performance Evaluation of GDLs at Constant Medium Sublayer Loadings

75°C, 40 psi, 3 mL/min 4M MeOH, CCM

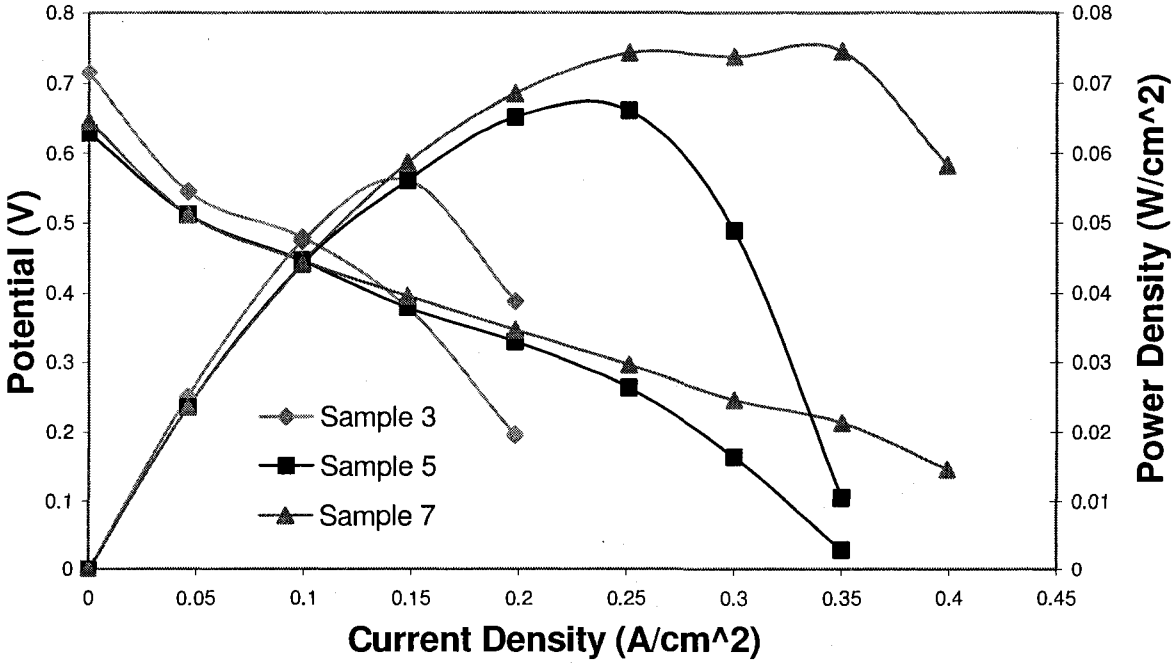

Figure 5.11c – Cell Performance Evaluation of GDLs at Constant High Sublayer Loadings

75°C, 40 psi, 3 mL/min 4M MeOH, CCM

of 0.035 W/cm^2 and finally sample 6 (high sublayer PTFE) with a power output of 0.030 W/cm^2. There is no clear pattern to these results and thus the effect of PTFE content in the MPL for GDLs with low MPL loadings is inconclusive.

Figure 5.11b, shows that the maximum power output, 0.058 W/cm^2 is achieved with sample 4 (low sublayer PTFE), followed by sample 2 (medium sublayer PTFE) with a power output of 0.043 W/cm^2 and then sample 9 (high sublayer PTFE) with a power output of 0.032 W/cm^2. These results show that cell performance increases as the PTFE content in the MPL decreases for GDLs with medium MPL loadings.

Figure 5.11c shows that the maximum power output of 0.078 W/cm^2 is achieved with sample 7 (low sublayer PTFE), followed by sample 5 (medium sublayer PTFE) with a power output of 0.068 W/cm^2 and then sample 3 (high sublayer PTFE) with a power output of 0.058 W/cm^2. These results indicate that lower PTFE loadings in the MPL improve performance of GDLs with high MPL loadings. This may be due to an improvement in the water management near the membrane surface, allowing the membrane to remain fully hydrated. When the membrane is fully hydrated, proton conductivity is improved resulting in better cell performance.

From the experimental results from sections 5.3.2 through 5.3.4 some important conclusions can be made. First, an increase in MPL weight (Section 5.3.2) and decrease in MPL PTFE content (Section 5.3.4) improves cell performance. In addition, for GDLs with high MPL loadings, an increase in PTFE content (Section 5.3.3) in the substrate will improve performance. **For these**

reasons the best anode GDL is found to be sample 7, which is modified GDL F, with high MPL weight, low MPL PTFE loading, and high substrate PTFE loading.

The following are the several reasons to expect the results that we have observed. The increase in MPL weight increases the thickness of the GDL. This increased thickness may retard the flow of methanol, which leads to improvements in methanol utilization and reduced methanol crossover. The MPL also changes the pore size distribution [87], which helps remove the excess water and allows the methanol to reach the catalyst sites. This change in pore size distribution may also improve the ability of the GDL to effectively remove CO/CO_2 from the cell, reducing catalyst poisoning and improving mass transport of methanol.

The total increase in GDL thickness may be the key reason for the decline in performance as the MPL PTFE content is increased. As the GDL becomes thicker, there is more electrical resistance. Since PTFE is a poor electrical conductor, there may be high electrical resistivity, leading to a drop in performance. Another possible reason for this behavior may be related to membrane hydration. Since the MPL is close to the membrane, a high level of hydrophobicity would drive water away, which may dry out the membrane. This would lower proton conductivity and thus decrease performance. It is believed that a combination of these two factors leads to the improvement with lower MPL PTFE loadings in the GDLs.

The improvement in DMFC performance with an increase in substrate PTFE loading may be related to the ability of the GDL to reject excess water. This effect is consistent for the samples with high MPL loadings, but obscured for the low and medium MPL loadings in GDLs. The MPL weight and PTFE content effects are difficult to separate from the substrate PTFE effects in this study, due to the matrix design (Table 5.3).

Samples of this modified GDL G combination were sent to independent outside lab facilities to verify the results of this work. The data confirmed lowered water transport through the membrane and increased methanol utilization, which strongly supports reduced methanol crossover effects. **This supports the concept that methanol crossover can be reduced by the GDL itself.** This finding should prove very useful in developing high performance DMFCs that allow high concentrations of methanol to be fed directly to the cell. This will help to increase the methanol throughput and thus reduce the overall size of the fuel storage system and simplify the stack design.

5.3.5 – Effect of Cathode GDL Properties on DMFC Performance

Further work has been done in an attempt to improve cell performance by investigating the cathode GDL material. The anode GDL for this study is held constant as GDL F (Table 5.2) modified with the sample 7 configuration (Table 5.3 and Section 5.3.4). Three different paper GDL samples (F, G and H) are used on the cathode side without any modification with MPL. Ballard Material Products provided these samples for our investigation. Detailed ex-situ

properties of these unmodified GDLs are provided in Table 5.4 and the results of the experiments are presented in Figure 5.13.

Table 5.4 – Detailed Properties of Unmodified GDLs F through H

Properties	GDL F	GDL G	GDL H
Thickness (μm)	169	254	198
Basis Weight (g/m^2)	62	88	49
Air Permeability (Gurley)	47	7	30.6
Taber Stiffness (Taber units)	8.8	23.5	9.8
Tensile Strength (lbf)	15.2	20	14.5
Electrical Resistivity ($m\Omega*cm^2$)	11.7	13.4	12.8

It is seen that the cell performs the best with the GDL combination of cathode GDL G and anode with modified GDL F, under our test conditions, providing a maximum power output of 0.167 W/cm^2. GDL F and GDL H both performed well below cathode GDL G, reaching maximum power outputs of only 0.083 and 0.062 W/cm^2, respectively. In addition to this increased maximum power output, GDL G also provides significant performance up to 0.6 A/cm^2, while the performance for GDLs F and H drop quickly around 0.3 A/cm^2.

There appears to be a correlation between basis weight and cell performance. GDL G has a basis weight of 88 g/m^2, which is 33% higher than GDL F and 45% higher than GDL H. It provides a maximum power output that is 50% greater than GDL F and

63% greater than GDL H. This increase in basis weight may be caused by an increase in the fiber density and therefore, a smaller pore size distribution. This would help to remove excess water more efficiently by preventing water build-up in the pores, leading to an improvement in cell performance.

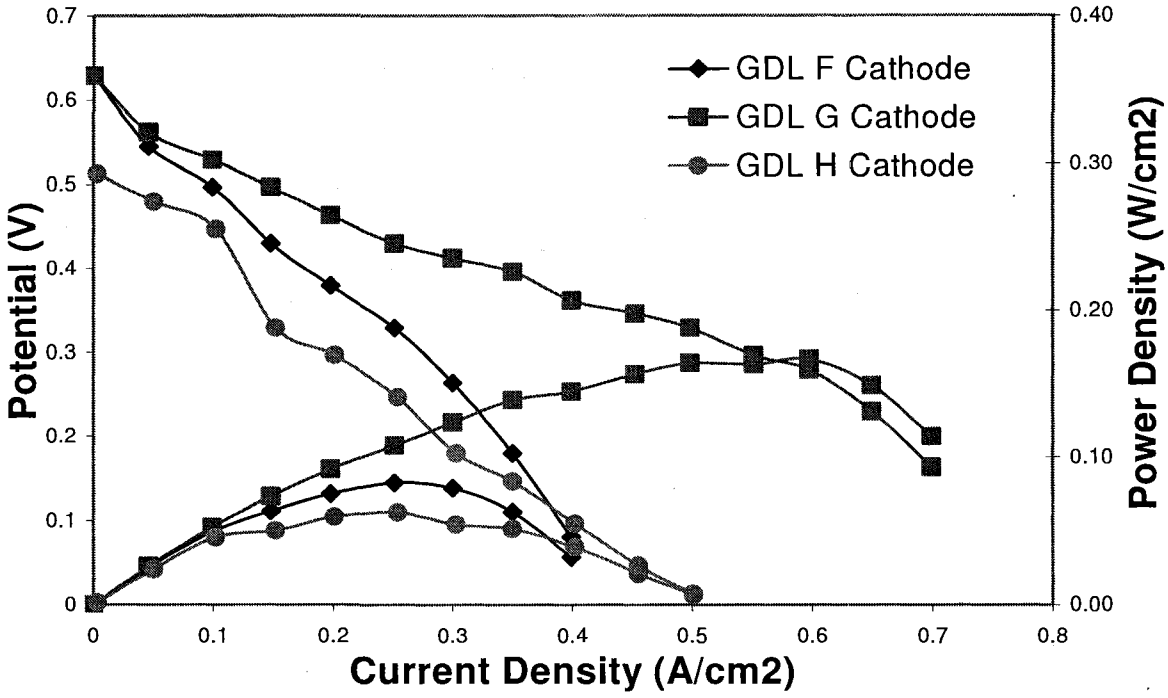

Figure 5.12 – Cell Performance Evaluation using Cathode GDLs F, G, H and Modified GDL F on the Anode
75°C, 40 psi, 3 mL/min 4M MeOH, CCM

5.3.6 – Effect of Anode GDL Characteristics on DMFC Performance

The effects of ex-situ properties of the anode GDL on DMFC performance are also studied. The anode GDLs evaluated are modified paper GDLs F, G and H. These are modified to have the optimum anode conditions (sample 7) as described in Table 5.3 and Section 5.3.4. For these experiments the cathode GDL is held constant as unmodified GDL G, which is found to perform the best in Section 5.3.5.

The results, presented in Figure 5.13, show that the MEA comprised of the modified GDL G as the anode and unmodified GDL G as the cathode performs the best, providing a maximum power output of 0.179 W/cm^2. The MEA with modified GDL F on the anode and unmodified GDL G on the cathode produces a maximum power output of 0.167 W/cm^2, a 6% decrease. The MEA with modified GDL H on the anode and unmodified GDL G on the cathode reaches a maximum power output of only 0.121 W/cm^2, a 32% decrease.

There does not appear to be any noticeable correlation between the measured ex-situ anode GDL properties and the cell performance. Increasing the basis weight of the anode substrate does appear to improve cell performance, as was seen for the cathode (Section 5.3.5). The cell performance increase between modified GDLs G and F is not large enough, however, to be related to the 33% reduction in basis weight. In addition, the large disparity between the cell performance with modified GDLs F and H, does not correlate to the relatively small change in basis weight. The MEA with modified GDL G as the anode and unmodified GDL G on the cathode does provide the best DMFC performance, however.

The results of the MEA fitted with modified GDL G as the anode and unmodified GDL G on the cathode are more closely examined against the results of the MEA fitted with commercially available GDL I as both the anode and cathode electrodes. These experiments are conducted under two different sets of conditions. The first set of conditions is the optimized conditions previously explored focusing only on these GDL combinations. The second set of

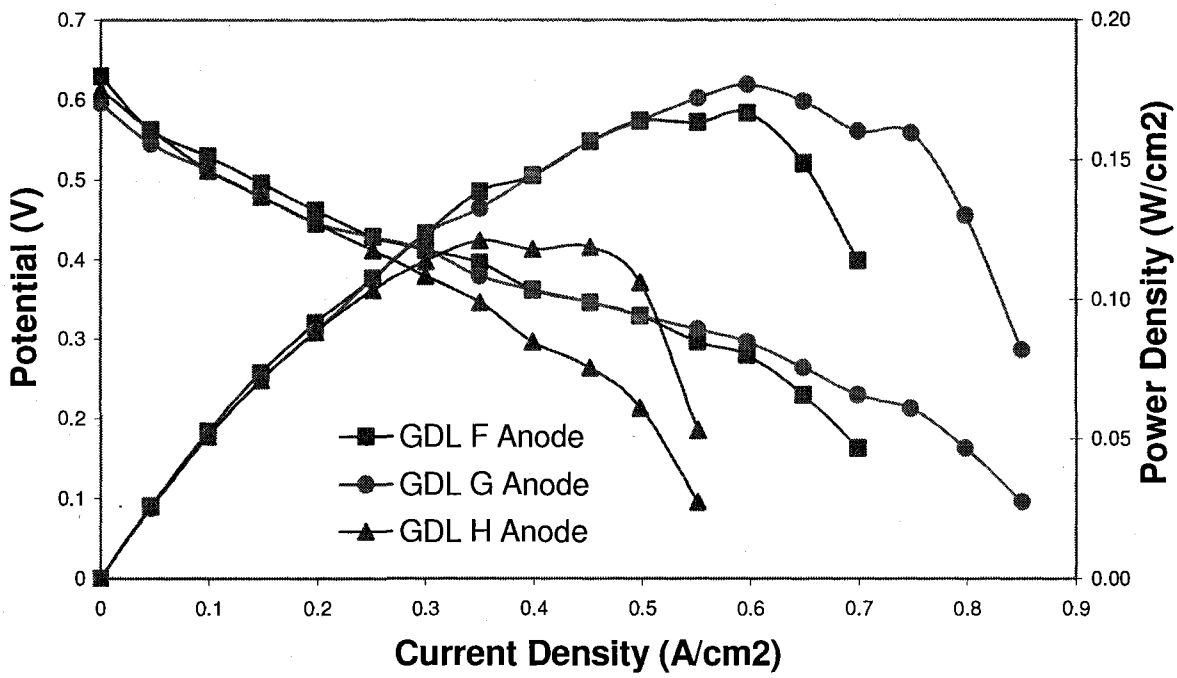

Figure 5.13 – Cell Performance Evaluation using Modified Anode GDLs F, G, H and Unmodified GDL G on the Cathode

75°C, 40 psi, 3 mL/min 4M MeOH, CCM

conditions are ambient temperature and pressure and more closely mimics actual operating conditions for DMFC products. The flow rate of methanol and air are increased to help drive the reactions under these conditions because such low temperature and pressure tends to give poor performance. The results of this investigation are presented in Figures 5.14 and 5.15.

Figure 5.14 shows that the MEA with modified GDL G combination produces a maximum power output of 0.180 W/cm^2 at 0.6 A/cm^2, while the GDL I combination provides a maximum power output of 0.162 W/cm^2 at 0.65 A/cm^2. The MEA fitted with modified GDL G combination provides improved performance in both the ohmic loss range (0.4-0.6 A/cm^2) and the mass transport loss range (>0.6 A/cm^2) compared to the MEA made with GDL I.

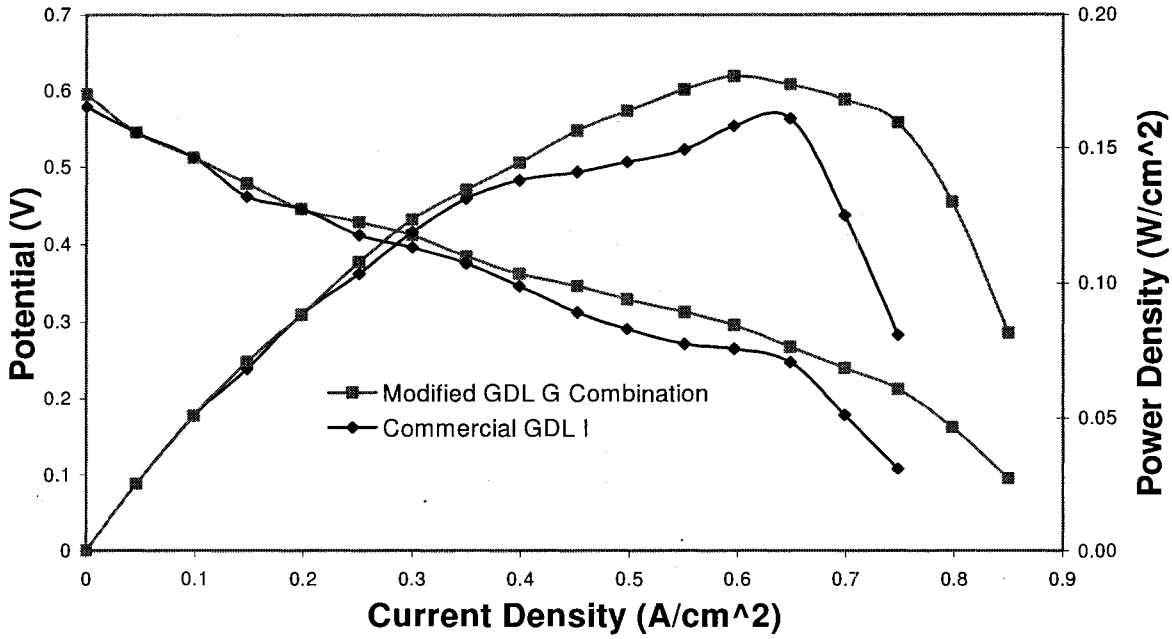

Figure 5.14 – Cell Performance Evaluation at High Temperature and Pressure using Modified GDL G Combination and GDL I Combination

75°C, 40 psi, 3 mL/min 4M MeOH, CCM

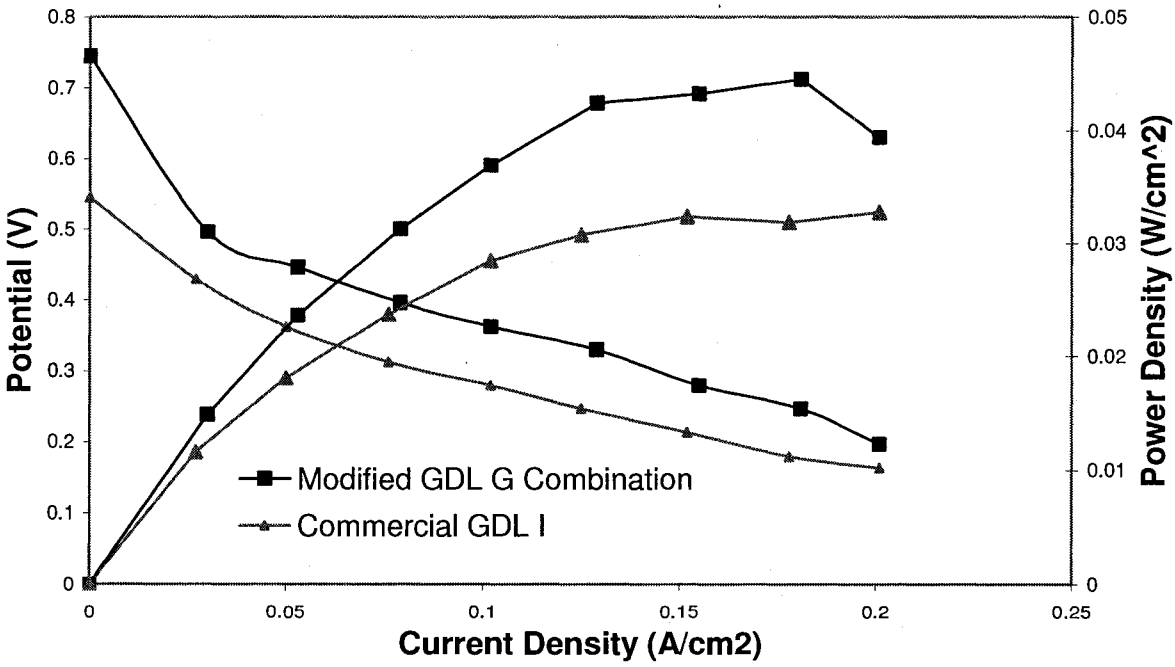

Figure 5.15 – Cell Performance Evaluation at Ambient Temperature and Pressure using Modified GDL G Combination and GDL I Combination

25°C, 1atm, 10 mL/min 4M MeOH, CCM

Figure 5.15 gives the performance of both the MEA fitted with modified GDL G combination and the MEA with the GDL I combination under ambient conditions. The modified GDL G combination achieves a maximum power output of 0.046 W/cm^2 at 0.175 A/cm^2, while the MEA with GDL I achieves a maximum power output of only 0.033 W/cm^2 at 0.175 A/cm^2. The improved performance of the GDL G combination can be seen as early as 0.05 A/cm^2 and lasts for the rest of the curve, showing improved design characteristics compared to the GDL I combination.

Under both sets of conditions the modified GDL G combination outperforms the MEA fitted with GDL I. The 20% increase in performance in the ohmic loss portion of the curve (0.05-0.15 A/cm^2) is believed to be due to improved electrical conductivity in the MPL leading to lower internal electrical resistance. The 25% improvement in the mass transport range (0.15-0.2 A/cm^2) are believed to be due to improved methanol / water management, which helps to decrease methanol crossover effects.

This modified GDL G combination has shown improved electrical properties, as well as the ability to reduce water transport through the membrane, which helps to reduce methanol crossover effects. This combination has been shown to outperform numerous commercially available GDLs under the optimized conditions found in this study. In addition it has shown improved performance under ambient conditions compared to the highest performing commercially available GDL. **Several independent laboratories have also verified the improved performance of MEAs made with the modified GDL G**

combination. Ballard Material Products is planning to manufacture the modified GDL G on a commercial scale using a continuous process.

CHAPTER VI

CONCLUSIONS

The following conclusions can be drawn from this investigation:

6.1 - Validation of the Apparatus for Accuracy and Reproducible Results

1) An experimental fuel cell apparatus has been designed, fabricated, and operated satisfactorily with both hydrogen and methanol fuels.
2) The accuracy of the apparatus has been validated against the results of previous work done at the University of New Hampshire using hydrogen as the fuel.
3) The apparatus is further validated against published data and the results show that the apparatus provides comparable results when hydrogen or methanol is used as the fuel.

6.2 - Optimization of Experimental Variables in a DMFC

4) The cell temperature is optimized for best performance in a DMFC by varying it in the range of 40°C-80°C. The optimum temperature is found to be 80°C providing a maximum power output of 0.060 W/cm^2. Due to concerns about membrane degradation, the cell is operated at 75°C for all experiments in this study.
5) The effect of catalyst loading on fabric GDLs is investigated and the optimum is found to be 2.5 mg/cm^2 generating a maximum power output of 0.100 W/cm^2.
6) The effect of catalyst loading on paper GDLs has been investigated and the best performance is found with approximately 2 mg/cm^2, giving a maximum power output of 0.039 W/cm^2.
7) The performance of two fabric GDLs and one paper GDL are compared under catalyst loadings of about 0.5 mg/cm^2 and 1 mg/cm^2. The fabric GDLs performance is similar under both loadings, giving a maximum power output of approximately 0.049 W/cm^2 with the 1 mg/cm^2 catalyst loading. The paper GDL provides maximum power outputs of 0.039 W/cm^2, well below that of the two fabric GDLs at the same loading.
8) The methanol feed solution concentration is optimized for the DMFC by varying it from 1 molar (3%) through 8 molar

(27%). The optimum is found to be between 2 and 4 molar (6-12%). The high concentration for this fuel cell system, as opposed to the literature reported values, is believed to be due to reduced electro-osmotic drag. This reduction helps to lower methanol crossover and improve cell performance at higher methanol concentrations.

9) The methanol flow rate is optimized by varying it from 1.5 mL/min to 7.5 mL/min and the optimum for the system is found to be 3 mL/min. This optimum is greatly influenced by operating parameters, such as temperature, pressure, air flow rate, and cell characteristics.

6.3 - Microporous Sublayer Study with DMFC

10) A study into the effect of microporous sublayers (MPLs) on anode GDL performance is conducted. It is found that performance is improved with high substrate PTFE content (30%), high MPL loading (80 g/m^2) and low MPL PTFE content (5%).

11) A study into the effect of ex-situ properties of both cathode GDL (with no MPL) and anode GDL (with MPL) on cell performance is conducted. The results show that increases in basis weight, for both the anode and cathode GDLs, improve cell performance.

12) The DMFC performance using an MEA made with the modified (with MPL) GDL G and unmodified (without MPL) GDL G as the anode and cathode, respectively, is compared with DMFC MEAs comprised of various commercially available GDLs. Under the optimized conditions from this study (Section 5.3.3) the MEAs made with the modified combination show improvements in the ohmic and mass transport loss regions of the performance curve as compared with the data obtained using commercially available GDLs.

13) The performance of an MEA made with commercially available GDL I, which is shown to give the best performance of the commercially available GDLs (5.4.6), is compared with the performance of an MEA comprised of the modified GDL G combination under ambient temperature and pressure conditions. The modified GDL G combination provides a maximum power output of 0.046 W/cm^2 compared to 0.033 W/cm^2 for GDL I.

14) The modified GDL G combination, developed in this study, is evaluated at several outside laboratories. Performance data reported by these labs confirm our results, giving us great confidence in our DMFC system and evaluation methodology. The anode GDL developed in this study

allows commercially available membranes, such as Nafion®, to be used with high (>2M) methanol concentrations with no performance loss due to methanol crossover. In addition, this GDL may be manufactured continuously, at a low cost, to help with the commercialization of DMFCs in the future.

CHAPTER VII

RECOMMENDATIONS

The following recommendations are made for the improvement of DMFC performance with particular reference to research and development for gas diffusion layers (GDLs).

7.1 - GDL and MPL Modifications

1) Since this study has shown that increasing the sublayer loading leads to improved cell performance, it would be helpful to explore increasing the loading further. At some point the increased thickness and reduced conductivity will lead to a drop in performance and allow us to determine an optimum loading.
2) In this investigation we are unable to determine the effect of PTFE loading in the substrate because the effects of sublayer loading and sublayer PTFE loading have a dominant influence. Additional samples should be made specifically to study the effect of PTFE content in the GDL in order to understand how to further improve performance.

3) All of the microporous layers applied to the anode GDL consisted of graphite particles of just one size. Changing the size of the particle could influence GDL parameters, such as pore size distribution or permeability, which may lead to improved cell performance. Different particle sizes should be used in the MPL so that this effect can be understood.
4) This investigation is limited to only the effect of a microporous layer on the anode GDL. A similar study should be performed focusing on the effect of a microporous layer on the cathode GDL. It would be helpful to understand the effect of PTFE content in both the sublayer and the substrate and the effect of sublayer loadings on the cathode GDL. This may lead to improved water management and improved performance.
5) The microporous layers applied to the anode GDLs in this study consisted of only one layer. Applying multiple layers of varying particle sizes and PTFE contents may lead to improved performance. The number of additional layers should be determined by balancing the benefit of the performance improvement against the added difficulty and cost in manufacturing to find an optimum number of MPLs.
6) All of the experiments conducted in this investigation were run for only a short period of time. These materials should be studied more in-depth in order to understand the degradation effects of methanol on

the MPL/GDL. It is important to ascertain that these materials can be run for a significant amount of time without decreased performance, such that they are useful in commercial applications.

7.2 - Apparatus Modifications

7) All of the experiments performed in this investigation were done using serpentine flow channels. Serpentine channels are known to have high pressure drop, which may lead to an increase in parasitic losses due to increased pumping costs. In addition CO_2 generated at the anode tends to block flow as the gas tries to rise until the liquid pressure is high enough to force it out of the cell. The use of parallel flow channels at the anode side could decrease the pressure drop and prevent the flow from being blocked.
8) In these experiments the compression of the cell was not measured for each trial. It was assumed that the torque applied was similar for all experiments and that the compression was similar. The compressibility of the GDL can impact the cell performance and should be studied in greater detail to understand the effect of compression on the cell and how it impacts methanol and CO_2 flow through the channels.
9) From our performance data and from feedback received from independent labs we can postulate that the modified DMFC GDL combination developed in this study may be helping reduce methanol

crossover. In order to more accurately investigate this effect the methanol crossover for different GDL designs should be measured. This will lead to a better understanding of the effect of GDL parameters on methanol permeation and methanol crossover.

7.3 - Membrane and Catalyst Improvements

10) For this investigation only Nafion® membranes were used in all experiments. Nafion® membranes, although known to have very high proton conductivities, have high methanol crossover effects. GDLs should be investigated with other membranes (Gore®, PolyFuel®, etc.) to help further limit methanol crossover and improve cell performance.
11) All of the experiments in this investigation were done with Pt-Ru catalyst in a 50:50 ratio. This ratio might not be ideal if the mechanism for breaking down the methanol to hydrogen requires more Pt than Ru or vice-versa. The effect of different ratios of Pt:Ru on DMFC cell performance should be investigated to determine if there is an optimum.
12) The commercial CCMs used in most of this study all reported the same amount of catalyst on the anode (4mg/cm^2 Pt-Ru) and the cathode (4mg/cm^2 Pt). Different catalyst loadings on the membrane may enhance performance and lower the cost, leading to an improved product that is more cost efficient.

LITERATURE CITED

[1] Hoogers G, "Fuel Cell Technology Handbook", CRC, NY, USA, 2003.

[2] Larminie J, Dicks A, "Fuel Cell Systems Explained", John Wiley and Sons, NY, USA, 1999.

[3] Zaidi S.M.J., Mikhailenko S.D., Robertson G.P., Guiver M.D., Kaliaguine S, "Proton conducting composite membranes from polyether ketone and heteroplyacids for fuel cell applications", Journal of Membrane Science, Vol. 173, 17-34, 2000.

[4] Smitha B, Sridhar S, Khan A.A., "Synthesis and Characterization of Poly(vinyl alcohol)-Based Membranes for Direct Methanol Fuel Cell", Journal of Applied Polymer Science, Vol. 95, 1154-1163, 2005.

[5] Xie X, Mao Z, Xu J, "A Hybride Membrane of Modified Polybenzimidazole and Heteropoly Acid for Direct Methanol Fuel Cell", Power System Technology, Vol. 1, 13-17, Oct 2002.

[6] Wakizoe M, Velev O.A., Srinivasan S, "Analysis of Proton Exchange Membrane Fuel Cell Performance With Alternate Membranes", Electrochimica Acta, Vol. 40, 335-344, 1995.

[7] Shen M, Roy S, Scott K, "Preparation and characterization of Pt deposition on ion conducting membrane for direct methanol fuel cell electrodes" Journal of Applied Electrochemistry, Vol. 35, 1103-1109, 2005.

[8] Toda T, Igarashi H, Uchida H, Watanabe M, "Enhancement of the Electroreduction of Oxygen on Pt Alloys with Fe, Ni, and Co", Journal of the Electrochemical Society, Vol. 146, No. 10, 3750-3756, 1999.

[9] Gupta S, TryK D, Zecevic S.K., Aldred W, Guo D, Savinell R.F., "Methanol-tolerant electrocatalysts for oxygen reduction in a polymer electrolyte membrane fuel cell", Chapman & Hall, 673-682, 1998.

[10] Wang C.Y., "Two-phase flow and Transport", Handbook of Fuel Cells – Fundamentals, Technology and Applications, Vol. 3 – part 3, 337-347, 2003.

[11] Lu G.Q., Liu F.Q., Wang C.Y., "Water Transport Through Nafion 112 Membrane in DMFCs", Electrochemical and Solid-State Letters, Vol. 8, A1-A4, 2005.

[12] Lim C, Wang C.Y., "Development of high-power electrodes for a liquid-feed direct methanol fuel cell", Journal of Power Sources, Vol. 113, 145-150, 2003.

[13] Liu F, Lu G, Wang C.Y., "Low Crossover of Methanol and Water Through Thin Membranes in Direct Methanol Fuel Cells", Journal of the Electrochemical Society, Vol. 153, A543-A553, 2006.

[14] Costmanga P, Srinivasan S, "Quantum jumps in the PEMFC science and technology from the 1960s to the year 2000: Part I Fundamental scientific aspects", Journal of Power Sources, Vol. 102, 242-252, 2001.

[15] Gamburzev S, John Appleby A, "Recent progress in performance improvement of the proton exchange membrane fuel cell (PEMFC)", Journal of Power Sources, Vol. 107, 5-12, 2002.

[16] Prater, K, "The Renaissance of the Solid Polymer Fuel Cell", Journal of Power Sources, Vol. 29, 239-250, 1990.

[17] Yeom J, Mozsgai G.Z., Flachsbart B.R., Choban E.R., Asthana A, Shannon M.A., Kenis P.J.A., "Microfabrication and characterization of a silicon-based millimeter scale, PEM fuel cell operating with hydrogen, methanol or formic acid", Sensors and Actuators, B 107, 882-891, 2005.

[18] Lee H, Park J, Kim D, Lee T, "A study on the characteristics of the diffusion layer thickness and porosity of the PEMFC", Journal of Power Sources, Vol. 131, 200-206, 2004.

[19] Frey T, Friedrich K.A., Jorissen L, Garche J, "Preparation of Direct Methanol Fuel Cells by Defined Multilayer Structures", Journal of The Electrochemical Society, Vol. 152, A545-A551, 2005.

[20] Kim S, Shimpalee S, Van Zee J.W., "The effect of reservoirs and fuel dilution on the dynamic behavior of a PEMFC", Journal of Power Sources, Vol. 137, 43-52, 2004.

[21] http://www.energy.ca.gov/2006publications/CEC-500-2006-025/CEC-500-2006-025.PDF

[22] Barragan V.M., Ruiz-Bauza C, Villaluenga J.P.G., Seoane B, "Transport of methanol and water through Nafion membranes", Journal of Power Sources, Vol. 130, 22-29, 2004.

[23] Guo Q, Pintauro P.N., Tang H, O'Connor S, "Sulfonated and crosslinked polyphospazene-based proton-exchange membranes", Journal of Membrane Science, Vol. 154, 175-181, 1999.

[24] Chen S, Krishnan L, Srinivasan S, Benziger J, Bocarsly A.B., "Ion exchange resin/polystyrene sulfonate composite membranes for PEM fuel cells", Journal of Membrane Science, Vol. 243, 327-333, 2004.

[25] Park Y, Nagai M, "Proton exchange nanocomposite membranes based on 3-glycidoxypropyltrimethoxysilane, silicotungstic acid and α-zirconium phosphate hydrate", Solid State Ionics, Vol. 145, 149-160, 2001.

[26] Jalani N.H., Dunn K, Datta R, "Synthesis and characterization of Nafion®-MO_2 (M=Zr, Si, Ti) nanocomposite membranes for higher temperature PEM fuel cells", Electrochimica Acta, Vol. 51, 553-560, 2005.

[27] Adjemian K.T., Srinivasan S, Benziger J, Bocarsly A.B., "Investigation of PEMFC operation above 100ºC employing perfluorosulfonic acid silicon oxide composite membranes", Journal of Power Sources, Vol. 109, 356-364, 2002.

[28] Hogarth W.H.J., Diniz da Costa J.C., Lu G.Q.(Max), "Solid Acid Membranes for High Temperature (>140ºC) Proton Exchange Membrane Fuel Cells", Journal of Power Sources, Vol. 142, 223-237, 2005.

[29] Beattie P.D., Orfino F.P., Basuar V.I., Zychowska K, Din J, Chuy C, Schmeisser J, Holdcroft S, "Ionic conductivity of proton exchange membranes", Journal of Electroanalytical Chemistry, Vol. 503, 45-56, 2001.

[30] Okada T, Xie G, Gorseth O, Kjelstrup S, Nakamura N, Arimuar T, "Ion and water transport characteristics of Nafion membranes as electrolytes", Electrochimica Acta, Vol. 43, No. 24, 3741-3747, 1998.

[31] Gardner C.L., Anantaraman A.V., "Measurement of membrane conductivities using an open-ended coaxial probe", Journal of Electroanalytical Chemistry, Vol. 395, 67-73, 1995.

[32] Francesco M.D., Arato E, Costa P, "Transport phenomena in membranes for PEMFC applications: an analytical approach to the calculation of membrane resistance", Journal of Power Sources, Vol. 132, 127-134, 2004.

[33] Park G, Sohn Y, Yang T, Yoon Y, Lee W, Kim C, "Effect of PTFE contents in the gas diffusion media on the performance of PEMFC", Journal of Power Sources, Vol. 131, 182-187, 2004.

[34] Giorgi L, Antolini E, Pozio A, Passalacqua E, "Influence of the PTFE content in the diffusion layer of low-Pt loading electrodes for polymer electrolyte fuel cells", Electrochimica Acta, Vol. 43, No. 24, 3765-3680, 1998.

[35] Sasikumar G, Ihm J.W., Ryu H, "Dependence of optimum Nafion content in catalyst layer on platinum loading", Journal of Power Sources, Vol. 132, 11-17, 2004.

[36] Lee S.J., Mukerjee S, McBreen J, Rho Y.W., Kho Y.T., Lee T.H., "Effects of Nafion impregnation on performances of PEMFC electrodes", Electrochimica Acta, Vol. 43, No. 24, 3693-3701, 1998.

[37] Prasanna M, Ha H.Y., Cho E.A., Hong S.-A., Oh I.-H., "Influence of cathode gas diffusion media on the performance of the PEMFCs" Journal of Power Sources, Vol. 131, 147-154, 2004.

[38] Kong C, Kim D, Lee H, Shul Y, Lee T, "Influence of pore-size distribution of diffusion layer on mass-transport problems of proton exchange membrane fuel cells", Journal of Power Sources, Vol. 108, 185-191, 2002.

[39] Chu H, Yeh C, Chen F, "Effects of porosity change of gas diffuser on performance of proton exchange membrane fuel cell", Journal of Power Sources, Vol. 123, 1-9, 2003.

[40] Koppula K, "Study of Gas Diffusion Layers in PEM Fuel Cells", Masters Thesis, University of New Hampshire, 2004.

[41] Mathur V.K., Crawford J, "Fundamentals of Gas Diffusion Layers in PEM Fuel Cells", Recent Trends in Fuel Cell Science and Technology, Anamaya Publishers, New Delhi, 116-128, 2007.

[42] Qi Z, Kaufman A, "Low Pt Loading High Performance Cathodes for PEM Fuel Cells", Journal of Power Sources, Vol. 113, 37-43, 2003.

[43] Passalacqua E, Lufrano F, Squadrito G, Patti A, Giorgi L, "Influence of the structure in low-Pt loading electrodes for polymer electrolyte fuel cells", Electrochimica Acta, Vol 43, No. 24, 3665-3673, 1998.

[44] Moreira J, Sebastian P.J., Ocampo A. L., Castellans R. H., Cano U, Salazar M.D., "Dependence of PEM Fuel Cell Performance on the Configuration of the Gas Diffusion Electrodes", Journal of New Materials for Electrochemical Systems, Vol. 5, 173-175, 2002.

[45] Song J.M., Cha S. Y., Lee W.M., "Optimal Composition of Polymer Electrolyte Fuel cell Electrodes Determined by the AC impedance Method", journal of Power Sources, Vol. 94, 78-84, 2001.

[46] Glora M, Wiener M, Petricevic R, Probstle H, Fricke J, "Integration of carbon aerogels in PEM fuel cells", Journal of Non-Crystalline Solids, Vol. 285, 283-287, 2001.

[47] Qi, Z. and Kaufman, A., "Improvement of water management by a microporous sublayer for PEM fuel cells", Journal of Power Sources, Vol. 109, 38-46, 2002.

[48] Shin S.J., Lee J.K., Ha H.Y., Hong S.A., Chun H.S., Oh I.H., "Effect of the catalytic ink preparation method on the performance of polymer electrolyte membrane fuel cells", Journal of Power Sources, Vol. 4679, 1-7, 2002.

[49] Liu L, Pu C, Viswanathan R, Fan Q, Liu R, Smotkin E.S., "Carbon supported and unsupported Pt-Ru anodes for liquid feed direct methanol fuel cells", Electrochimica Acta, Vol. 43, No. 24, 3657-3663, 1998.

[50] Tian J.H., Wang F.B., Shan ZH.Q., Wang R.J., Zhang J.Y., "Effect of preparation conditions of Pt/C catalysts on oxygen electrode performance in proton exchange membrane fuel cells", Journal of Applied Electrochemistry, Vol. 34, 461-467, 2004.

[51] Maruyama J, Abe I, "Application of conventional activated carbon loaded with dispersed Pt to PEFC catalyst layer", Electrochimica Acta, Vol. 48, 1443-1450, 2003.

[52] Gasteiger H.A., Panels J.E., Yan S.G., "Dependence of PEM fuel cell performance on catalyst loading", Journal of Power Sources, Vol. 127, 162-171, 2004.

[53] Antoine O, Bultel Y, Durand R, Ozil P, "Electrocatalysis, diffusion and ohmic drop in PEMFC: Particle size and spatial discrete distribution effects", Electrochimica Acta, Vol. 43, No. 24, 3681-3691, 1998.

[54] Darling R, Meyers J, "Kinetic Model of Platinum Dissolution in PEMCs", Journal of The Electrochemical Society, Vol. 150, A1523-A1527, 2003.

[55] Cha S.Y., Song J.M., Lee W.M., "Electrochemical behavior of a hydrogen/oxygen gas mixture at a solid polymer electrolyte interface", Journal of Applied Electrochemistry, Vol. 28, 1413-1418, 1998.

[56] Gloaguen F, Andolfatto F, Durand R, Ozil P, "Kinetic study of electrochemical reactions at catalyst-recast ionomer interfaces from thin active layer modeling", Chapman & Hall, 863-869, 1994.

[57] Grgur B.N., Markovic N.M., Ross P.N., "Electrooxidation of H_2, CO and H_2/CO mixtures on a well-characterized Pt-Re bulk alloy electrode and comparison with other Pt binary alloys", Electrochimica Acta, Vol. 43, No. 24, 3631-3635, 1998.

[58] Pozio A, Giorgi L, Antolini E, Passalacqua E, "Electroxidation of H_2 on Pt/C Pt-Ru/C and Pt-Mo/C anodes for polymer electrolyte fuel cell", Electrochimica Acta, Vol. 46, 555-561, 2000.

[59] Ye Q, Zhao T.S., Liu J.G., "Effect of Transient Hydrogen Evolution/Oxidation Reactions on the OCV of Direct Methanol Fuel Cells", Electrochemical and Solid-State Letters, Vol. 8, No. 10, A549-A553, 2005.

[60] Jeng K.T., Kuo C.P., Lee S.F., "Modeling the catalyst layer of a PEM fuel cell cathode using a dimensionless approach", Journal of Power Sources, Vol. 128, 145-151, 2004.

[61] Song D, Wang Q, Liu Z, Navessin T, Eikerling M, Holdcroft S, "Numerical Optimization study of the catalyst layer of PEM fuel cell cathode", Journal of Power Sources, Vol. 126, 104-111, 2004.

[62] Haug A.T., White R.E., Weidner J.W., Huang W, Shi S, Stoner T, Rana N, "Increasing Proton Exchange Membrane Fuel Cell Catalyst Effectiveness Through Sputter Deposition", Journal of The Electrochemical Society, Vol. 149, No. 3, A280-A287, 2002.

[63] Hirano S, Kim J, Srinivasan S, "High performance proton exchange membrane fuel cells with sputter-deposited Pt layer electrodes", Electrochimica Acta, Vol. 42, No. 10, 1587-1593, 1997.

[64] Choi K.H., Kim H.S., Lee T.H., "Electrode fabrication for proton exchange membrane fuel cells by pulse electrodeposition", Journal of Power Sources, Vol. 75, 230-235, 1998.

[65] Zhang J, Zou Y, He J, "Influence of graphite particle size and its shape on performance of carbon composite bipolar plate", Journal of Zhejiang University Science, Vol. 6a, No. 10, 1080-1083, 2005.

[66] Arico A.S., Creti P, Baglio V, Modica E, Antonucci V, "Influence of flow field design on the performance of a direct methanol fuel cell", Journal of Power Sources, Vol. 91, 202-209, 2000.

[67] Yang H, Zhao T.S., "Effect of anode flow field design on the performance of liquid feed direct methanol fuel cells", Electrochimica Acta, Vol. 50, 3243-3252, 2004.

[68] Jung G.B, Su A, Tu C.H., Weng F.B., Chan S.H., "Innovative flow field combination design on direct methanol fuel cell performance", Proceedings of the 3rd International Conference on Fuel Cell Science, Engineering and Technology, May 23-25, 2005.

[69] Yang H, Zhao T.S., Ye Q, "In situ visualization study of CO_2 gas bubble behavior in DMFC anode flow fields", Journal of Power Sources, Vol. 139, 79-90, 2005.

[70] Yang H, Zhao T.S., Ye Q, "Pressure drop behavior in the anode flow field of liquid feed direct methanol fuel cells", Journal of Power Sources, Vol. 142, 117-124, 2004.

[71] Senn, S.M., Poulikakos D, "Multiphase Transport Phenomena in the Diffusion Zone of a PEM Fuel Cell", Journal of Heat Transfer, Vol. 127, 1245-1259, 2005.

[72] Berning T, Djilali N, "Three-dimensional computational analysis of transport phenomena in a PEM fuel cell – a parametric study", Journal of Power Sources, Vol. 124, 440-452, 2003.

[73] Roh Y.W, Srinivasan S, "Mass Transport Phenomena in Proton Exchange Membrane Fuel Cells Using O_2/He, O_2/Ar, and O_2/N_2 mixtures", Journal of Electrochemical Society", Vol. 141, 2089-2096, 1994.

[74] Baschuk J.J., Xiangua L, "Modeling of polymer electrolyte membrane fuel cells with variable degrees of water flooding", Journal of Power Sources, Vol. 86, 181-196, 2000.

[75] Natarajan D, Nguyen T.V., "Three-dimensional effects of liquid water flooding in the cathode of a PEM fuel cell", Journal of Power Sources, Vol. 115, 66-80, 2003.

[76] Yan W.M, Chen F, Wu H.Y., Soong C.Y., Chu H.S., "Analysis of thermal and water management with temperature-dependent diffusion effects in membrane of proton exchange membrane fuel cells", Journal of Power Sources, Vol. 129, 127-137, 2004.

[77] Tuber K, Pocza D, Hebline C, "Visualization of water buildup in the cathode of a transparent PEM fuel cell", Journal of Power Sources, Vol. 124, 403-414, 2003.

[78] Satija R, Jacobson D.L., Arif M, Werner S.A., "In situ neutron imaging technique for evaluation of water management systems in operating PEM fuel cells", Journal of Power Sources, Vol. 129, 238-245, 2004.

[79] Nguyen T.V., Knobbe M.W., "A liquid water management strategy for PEM fuel cell stacks", Journal of Power Sources, Vol. 114, 70-79, 2003.

[80] Jiang W, Mingheng S, "Study on two-phase countercurrent flow and transport phenomenon in PEM of a direct methanol fuel cell", Science in China: Series E Technological Sciences, Vol. 49, 102-114, 2006.

[81] Um S, Wang C.Y., "Three-dimensional analysis of transport and electrochemical reactions in polymer electrolyte fuel cells", Journal of Power Sources, Vol. 125, 40-51, 2004.

[82] Arico A.S., Creti P, Antonucci P.L., Cho J, Kim H, Antonucci V, "Optimization of operating parameters of a direct methanol fuel cell and physico-chemical investigation of catalyst-electrolyte interface", Electrochimica Acta, Vol. 43, No. 24, 3719-3729, 1998.

[83] Xie X, Tsinghua University, Beijing, China, Private Communication, April 2005.

[84] Jinnouchi R, Yamada H, Morimoto Y, "Measurement of Electro-osmotic Drag Coefficient of Nafion Using a Concentration Cell", 14th International Conference on the Properties of Water and Steam, Kyoto, August 2004.

[85] Song S.Q., Zhou W.J., Li W.Z., Sun G, Xin Q, Kontou S, Tsiakaras P, "Methanol crossover and its influence on single DMFC performance" Ionics, Vol. 10, Numbers 5-6, 458-462, 2004.

[86] Lin J, Trivisonno A, Wycisk R, Pintauro P.N., "Optimized DMFC Performance Comparison for Modified and Unmodified Nafion® Membranes", Electrochemical Society, 210th Meeting, October 2006.

[87] Tucker M, Odgaard M, Lund P, Yde-Andersen S, Thomas J.O., "The Pore Structure of Direct Methanol Fuel Cell Electrodes", Journal of the Electrochemical Society, Vol. 152, A1844-A1850, 2005.

[88] www.fuelcellstore.com

APPENDICES

APPENDIX A

EXPERIMENTAL PROCEDURE FOR MAKING MEMBRANE ELECTRODE ASSEMBLIES (MEAs)

The membrane electrode assemblies (MEAs) used in this experimental work are prepared in house. Unless otherwise noted, the MEAs are composed of two catalyst- coated GDLs, with a Nafion® membrane in the middle, which are hot pressed at 175°F at 1500 psi for 90 seconds. The catalyst is hand-painted onto the GDL, layer by layer, using a very fine brush. The details of these procedures are included in the following sections.

A.1 - Membrane Preparation

The Nafion® membranes are carefully treated to remove any contaminates. They are next sulphonated for improved proton conductivity. The procedure is given below:

1) Cut squares of untreated Nafion® membrane 3" x 4" to be used in the fuel cell system.
2) Fill a beaker with 450 mL of 3% hydrogen peroxide and place it on the hot plate until it reaches a slow boil.

3) Submerge the membrane(s) completely in the hydrogen peroxide solution. Carefully place two magnetic stirrers on either side of the membrane(s).
4) Allow boiling for 1 hour, refilling the hydrogen peroxide as necessary to keep the membrane(s) submerged.
5) Fill another beaker with 450 mL of DI water, place it on a hot plate and allow it to come to a slow boil.
6) Carefully remove the membrane(s) from the hydrogen peroxide solution and submerge them completely in the boiling DI water.
7) Allow boiling for 1 hour, replenishing the DI water as necessary to keep the membrane(s) completely submerged.
8) Carefully measure out 25 mL of highly concentrated sulfuric acid and slowly add it to 475 mL of DI water to make 500 mL of 5% (vol.) sulfuric acid solution. Note: Be sure to add the acid to the water solution for safety.
9) Place the dilute sulfuric acid solution on a hot plate and allow it to come to a slow boil. Note: Be sure to have the fume hood on before boiling the acid.
10) Carefully transfer the membrane(s) from the DI water to the boiling sulfuric acid solution.

11) Keep the membrane(s) submerged in the sulfuric acid solution for 1 hour. Do not add any DI water to the solution unless the level is too low to keep the membrane submerged.

12) Fill a container with 450 mL of DI water, place it on a hot plate and allow the water to come to a slow boil.

13) Carefully transfer the membrane(s) from the sulfuric acid solution to the boiling DI water and keep them submerged, replenishing the DI water as necessary, for 1 hour.

14) Clean and rinse a jar with DI water then fill the jar ¾ full with DI water. Affix a label with the name, date and type of membrane to the front of the jar.

15) Carefully remove the membrane(s) from the boiling DI water, remove the magnetic stirrers and place the membrane(s) in the above-mentioned labeled jar and seal it. The membrane(s) are now cleaned and ready for use and should be kept submerged to avoid exposure to any contaminants.

A.2 - Catalyst Ink and GDL Preparation

The catalyst, purchased from Ion power, is mixed with n-propanol, DI water and 15% Nafion® solution to form an ink, which is painted onto the GDL. The catalysts may be different for anode and cathode electrodes. The preparation of the ink is as follows:

1) Carefully tare out a small plastic dish

2) Slowly add catalyst powder to the dish until the proper amount is transferred for the correct Pt loading on the GDL. (e.g. for a 0.4 mg/cm^2 Pt loading, using 20% Pt carbon catalyst, the proper catalyst amount is 10 mg of catalyst.)

3) Carefully crush the catalyst particles using the flat end of a feeding spoon to prevent the large particles from settling out of the solution.

4) Transfer the catalyst to a jar and place it on the scale.

5) Carefully add 250 mg of DI water to the catalyst-containing jar.

6) Now carefully add 250 mg of n-propanol to the solution. Note it is important to add the n-propanol after the DI water to prevent possible ignition between the carbon particles and the n-propanol vapors.

7) Quickly add 100 mg of 15% Nafion® solution to the mixture and place a small magnetic stirrer into jar, cap the jar and place it on a stir plate inside a large bowl full of ice, to prevent n-propanol evaporation.

8) Repeat steps 1-7 for the cathode ink preparations if the catalyst used is different from the one used for the anode electrode. If both are the same then just use double the amounts of all components.

9) Place the jar with the catalyst solution on the stir plate and turn it on to setting 7. Allow the stirrer to mix the solution for an hour. Note: if after one hour the solution is not well mixed, allow the stir plate to

run longer checking every 20 minutes until the solution is well mixed.

10) Cut the appropriate number of GDL samples (2.5"x2.5") for 5 cm^2 samples. Weigh the uncoated GDL piece(s) and place them on a glass plate. Carefully coat the GDL(s) uniformly in one direction. Note: be very careful to make the first two layers very thin to prevent the solution from seeping through, as this leads to a non-uniform catalyst layer and poor cell performance.

11) Place the coated GDL into a vacuum dryer (60°C, -15 in.) for 15 minutes.

12) Repeat steps 10-11 until the entire solution is consumed. Note: be sure to alternate the direction, vertical and horizontal, while coating the GDL to ensure uniform catalyst distribution.

13) Completely dry the GDL piece(s) and re-weigh them to determine the catalyst loading.

14) Fill a new jar with 50 mg of 15% Nafion® solution and 100 mg of DI water and carefully apply one coat to the surface of the GDLs.

15) Dry the GDLs completely and re-weigh to determine the total Nafion® loading.

A.3 - MEA Preparation

1) Place Teflon paper over a flat metal base and carefully lay the catalyst-coated anode GDL (with the catalyst layer facing up) on top of the paper.
2) Carefully transfer a piece of treated Nafion® membrane (see Section 4.3.1) from the DI water and lay it over the anode GDL (catalyst coated surface facing up), making sure that the GDL is in the center of the membrane.
3) Very carefully place the catalyst-coated cathode GDL (with the catalyst layer facing down) on top of the membrane such that it completely lines up with the anode GDL.
4) Place another piece of Teflon paper over the MEA and place a metal sheet on top of the Teflon paper, being sure not to allow the GDLs/membrane to slide out of place.
5) Carefully lift the two metal pieces, holding them together to prevent the GDL/membrane from sliding and place them into the heated (250°F) mechanical press.
6) Raise the pressure to 1500 psi and allow the MEA to be pressed for 90 seconds.
7) Carefully remove the plates from the press (be careful as the plates will be hot) and allow them to slowly cool to room temperature.

8) Very carefully peel back the top layer of Teflon paper. Note: If not done properly it can remove part of the GDL paper and render the MEA useless.

9) Carefully pull the membrane/GDL away from the bottom layer of Teflon paper, again being careful not to damage the system.

10) If using a methanol MEA place a dot in the upper left hand corner of the MEA (when the anode side is under the membrane) so that the user can identify the anode/cathode side.

APPENDIX B

LIST OF VENDORS

Table B.1 – List of Vendors

List of Purchases	Vendors	Contact Telephone No.
Thermocouples Thermocouple connectors Thermocouple wires Solid-state relays Heat sinks Pressure transducers Power supply Twist lock connector Pressure snubber Heat tapes Mass flow controllers Mass flow controller cables	Omega	203-359-1660
Teflon tape Wiring Fan/fan screen	McMaster-Carr	330-342-330
Piping Tubing Unions Fittings Humidification cylinders Cylinder rings Tees Pressure gauges Filters Check valves	Swagelok (Maine Valve and Fitting)	207-947-3353
Regulators	Harris Calorific	513-754-2000
Solenoids Backpressure gauge	Washburn-Garfield	508-753-7225
PCI GPIB Shielded cabling Shielded connector block PCI-6071 DAQ Card LabVIEW	National Instruments	800-531-5066

List of Purchases	Vendors	Contact Telephone No.
Electronic load Mainframe	Agilent Technologies	800-452-4844
Power Supply	Radio Shack	800-843-7422
NFB DC Power Supply	Epsco Incorporated	800-294-8585
Fuse box Grommets Electrical supplies	Home Depot	800-553-3199
Gases	Airgas Incorporated	610-687-5253
Nafion membrane 15 % wt Nafion solution	Ion Power	302-832-9550
CCM GDL samples	Fuel Cell Store	303-237-3834
60% PTFE Methanol	Aldrich Chemical Company	800-521-8956
Pt catalyst – 20% Pt/C Pt catalyst – 40% Pt/C Pt-Ru catalyst: 50-50 Pt-Ru catalyst: 30-15 Pt-Ru catalyst: 20-10	Alfa Aesar	800-343-0660
Syringe Pump	Sage Instruments	831-786-3304
Fuel cell hardware	Fuel Cell Technologies	505-821-4672

APPENDIX C

STOICHIOMETRIC VALUES

Table C.1 – Stoichiometric Values for Anode/Cathode Feeds

Total Current (A)	Current Density (A/cm^2)	H2 Flow (1x Stoich) cm^3/min	Air Flow (1x Stoich) cm^3/min	MeOH Flow (3M, 1x Stoich) µL/min
0.5	0.1	3.5	8.3	17.3
1	0.2	7	16.7	34.5
1.5	0.3	10.5	24.7	51.8
2	0.4	14	33.0	69.1
2.5	0.5	17.5	41.3	86.4
3	0.6	21	49.7	103.7
3.5	0.7	24.5	57.7	121
4	0.8	28	66.0	138.3
4.5	0.9	31.5	74.3	155.6
5	1	35	82.7	172.9
5.5	1.1	38.5	91.0	190.2
6	1.2	42	99.3	207.5

APPENDIX D

Performance Comparison of Modified GDL G and Commercial References

No product development is complete unless the performance of the product is satisfactorily compared against the performance of other similar products that are commercially available. For this part of the study an MEA is prepared with modified GDL G as the anode and unmodified GDL G as the cathode. The performance of this MEA is compared against the performance of six similar MEAs consisting of GDLs A, B, C, D, E and I as both the anode and cathode sides of a commercially available CCM. In addition two MEAs fitted with modified GDLs F and H on the anode and unmodified GDL G on the cathode are also evaluated. The results are presented in Appendix D Figures D.1 (Potential vs. Current Density) and D.2 (Power Density vs. Current Density).

Figure D.1 presents the V-I performance curves of each of the MEAs studied under the optimized operating conditions found in Section 5.2. From these results it is clear that the GDL combination (modified GDL G as the anode and unmodified GDL G as the cathode) developed in this study performs the best, giving a voltage of approximately 0.2V at 0.7 A/cm^2. The only other MEA that compares well is made with commercially available GDL I, which achieves 0.17V at 0.65 A/cm^2. GDLs A and E start off very strongly, but their performance

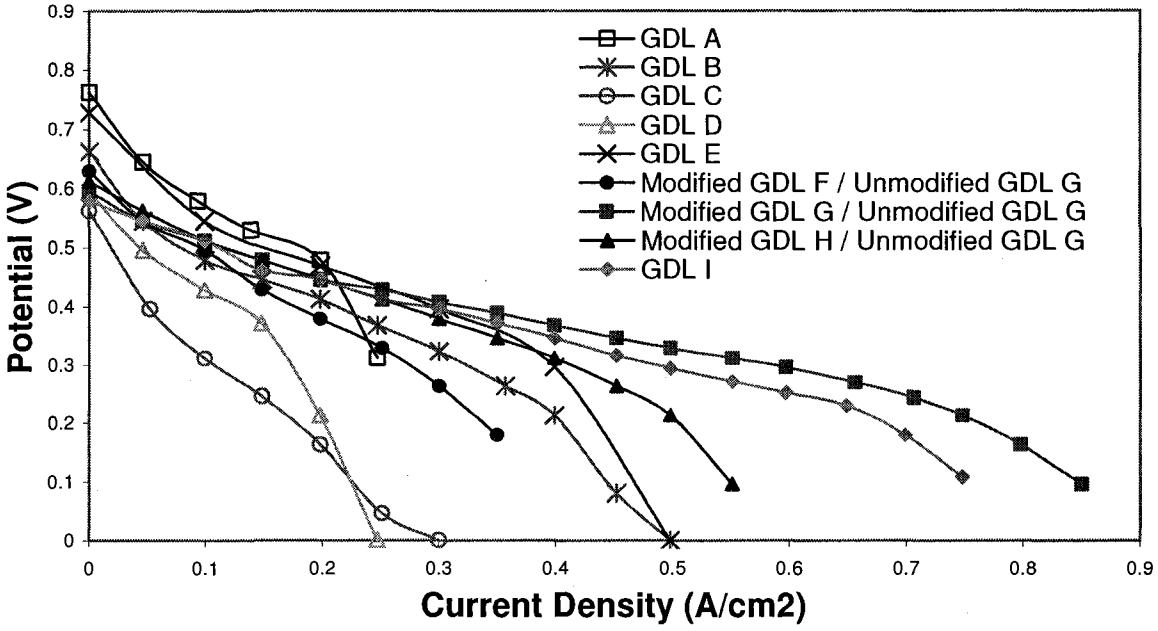

Figure D.1 – Voltage Comparison of GDL Combination with Commercially Available GDLs (Potential vs. Current Density)

75°C, 40 psi, 3 mL/min 4M MeOH, CCM

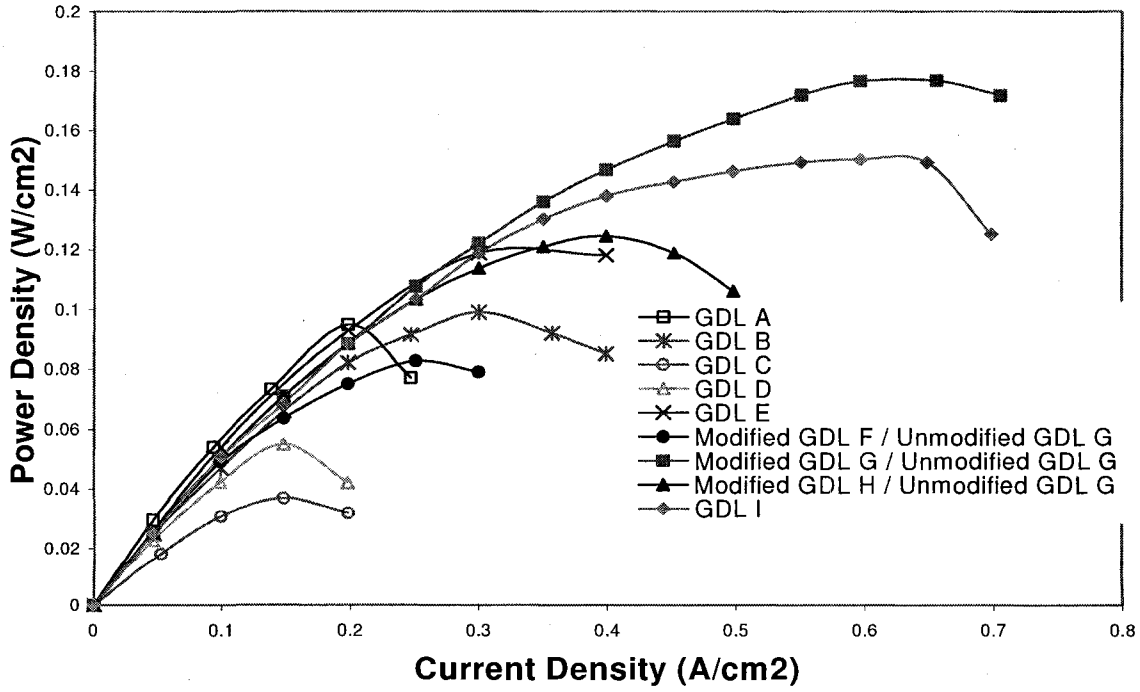

Figure D.2 – Power Density Comparison of GDL Combination with Commercially Available GDLs (Power Density vs. Current Density)

75°C, 40 psi, 3 mL/min 4M MeOH, CCM

quickly declines due to mass transport limitations, indicating that they cannot effectively remove the water from the cell. Modified GDLs F and H perform well compared with most of the other commercially available GDLs (A through D) producing 0.2V at 0.35 A/cm^2 and 0.5 A/cm^2, respectively. In order to better understand the differences in these GDL performances, we evaluated the power densities, as shown in Figure 5.15.

Figure D.2 shows the power densities for each of the MEAs studied under the optimized operating conditions. It is clear that the GDL combination developed in this study performs the best, achieving a maximum power output of 0.18 W/cm^2. The MEA with GDL I on both the anode and cathode sides produces the closest results with a maximum power output of 0.151 W/cm^2, 16% less. These are the only two MEAs that produce significant power above the current density of 0.4 A/cm^2.

The MEA with GDL E on both sides and the MEA with the combination of modified GDL H and unmodified GDL G perform similarly, reaching maximum power densities of approximately 0.12 W/cm^2. The MEA with a combination of modified GDL H and unmodified GDL G performs at a higher current density (0.4 A/cm^2) than the MEA with GDL E (0.3 A/cm^2). The MEAs made with GDLs A and B on both sides and the MEA combination with modified GDL F and unmodified GDL G provides the third best performance group, each reaching maximum power densities of approximately 0.1 W/cm^2. The MEA with GDL B (0.3 A/cm^2) reaches higher current densities than the MEA with GDL A (0.2 A/cm^2) or the

MEA with modified GDL F (0.25 A/cm^2). Finally the MEAs composed of GDLs C and D perform very poorly compared to the others and may be considered unsuitable for DMFC use under the specific experimental conditions.